Supporting information

Synthesis routes to carbon substituted cobalt bis(dicarbollide) alkyl halides and aromatic amines along with closely related irregular pathways

Jan Nekvinda,[a,*] Dmytro Bavol,[a] Miroslava Litecká,[a] Ece Tüzün,[a] Michal Dušek[b] and Bohumír Grüner[a]

[a]Institute of Inorganic Chemistry of the Czech Academy of Sciences, Hlavní 1001, Husinec-Řež 25068, Czech Republic

[b] Institute of Physics of the Czech Academy of Sciences, Na Slovance 1999/2, Prague 8, 182 21, Czech Republic

*e-mail: nekvinda@iic.cas.cz

Table of Contents

Instrumental Techniques:

NMR

^{1}H, ^{11}B NMR, $^{1}H\{^{11}B_{selective}\}$ and ^{13}C spectra were measured on a JEOL 600 MHz Instrument. The spectra of all the compounds were measured immediately after dissolution in a deuterated solvent, usually acetonitrile-d_3 or acetone-d_6. ^{11}B NMR (193 MHz) chemical shifts are given in ppm to high-frequency (low field) to $F_3B{\cdot}OEt_2$ as the external reference. Residual solvent ^{1}H resonances were used as internal secondary standards. Coupling constants $^{1}J(^{11}B–^{1}H)$ were taken from resolution-enhanced ^{11}B spectra with a digital resolution of 2 Hz. ^{1}H NMR (600 MHz) and ^{13}C NMR (151 MHz): chemical shifts δ in ppm relative to Me_4Si (0 ppm) as the external standard, coupling constants $J(H, H)$ in Hz. The chemical shifts corresponding to B–H resonances were obtained from $^{1}H\{^{11}B_{selective}\}$ NMR spectra. In $^{1}H\{^{11}B\}$ spectra the $\delta_{B\text{-}H}$ values and peak assignments were analyzed from $^{1}H\{^{11}B_{selective}\}$ experiments.

(HR)MS

Mass Spectrometry measurements were performed on a Thermo-Finnigan LCQ-Fleet Ion Trap instrument using electrospray ionization (ESI) with the detection of negative ions. For ESI, samples dissolved in acetonitrile (concentrations of approximately 100 $\mu g{\cdot}mL^{-1}$) were introduced to the ion source by infusion. Molecular ions $[M]^-$ were detected for all univalent anions as base peaks in the spectra. The experimental and calculated isotopic distribution patterns were fully agreed upon for all isolated compounds. The isotopic distribution in the boron plot of all peaks was in complete agreement with the calculated spectral pattern. The data are presented for the most abundant mass in the boron distribution plot (100%) and for the peak on the right side of the boron plot corresponding to the *m/z* value.

High-Resolution Mass spectrometry (HRMS) spectra were recorded by an Orbitrap Exploris™ 120 spectrometer equipped with heated electrospray ionization (HESI) in negative mode using nitrogen (5.0 Messer) as a collision gas. For HESI-MS, solutions of concentration approximately 100 $ng{\cdot}mL^{-1}$ in acetonitrile were introduced by infusion into the ion source from a syringe. Molecular ions $[M]^-$ were detected for all univalent anions as base peaks in the spectra. By comparison, the experimental isotopic distribution in the boron plot of the peaks in the measured spectra corresponded fully to the calculated spectral pattern. The data are presented for the most abundant mass in the boron distribution plot (100%) and for the signal corresponding to the *m/z* value. Conditions used for the HESI interface: vaporizer temperature 50 °C; N_2 (isolated from air in Genius XE35, Peak Scientific) as a nebulizing sheath gas and auxiliary gas, flow 3.22 $L{\cdot}min^{-1}$ and 6.12 $L{\cdot}min^{-1}$, respectively; ion spray voltage 3500 V; capillary temperature 280 °C and mass range from 100 to 1200.

Synthetic procedures

The starting cesium salt of cobalt bis(dicarbollide) was purchased from Katchem Ltd., Czech Republic. Other standard chemicals were purchased from commercial sources. Solvents were dried prior to use using standard techniques. TLC analyses were performed using aluminum-backed silica gel Merck Silica gel 60 F_{254} plates and visualized by UV light. Column chromatography was performed on a high-purity silica gel (Merck Grade, Type 7754, 70-230 mesh, 60 Å). All reactions were performed using standard Schlenk-type vacuum or inert-atmosphere techniques, although some operations, such as column chromatography and crystallization were carried out in the air.

General procedure **A** for preparation of bromo derivatives **3a-c**$^-$:

Respective cobalt bis(dicarbollide) hydroxy derivative (**1a-c**, 1.0 equiv.) was dissolved in dry MeCN (10 mL per 1.0 mmol of cobalt bis(dicarbollide) hydroxy derivative) and the PBr_3 (1M solution in DCM, 1.5 equiv.) was added under an inert atmosphere (argon). The reaction mixture was stirred at room temperature (25 °C) overnight (12 h) and the flask was equipped with the argon source (balloon). Progress of the reaction was monitored by the ESI-MS and the reaction was carried out until all of the starting material was consumed. After the completion of the reaction, the vapors were evaporated on a high vacuum line before the evaporation of the solvent using a rotary evaporator. The mixture was then dried on a high vacuum again, forming a foamy crude product applied on column silica-gel chromatography (gradient mixture of CH_2Cl_2:MeOH 0-5%). Collected fractions were evaporated with 2 mL of water and a saturated solution of Me_4NCl in water (1 mL) was then added to the aqueous solution. The precipitate was immediately collected and dried under a vacuum.

General procedure **B** for preparation of iodo derivatives **4a-c**$^-$:

Respective cobalt bis(dicarbollide) methanesulfonate ester (**5a-c**, 1.0 equiv.) and NaI (10.0 equiv) were dissolved in dry Me_2CO (20 mL per 0.1 mmol of cobalt bis(dicarbollide) ester) and the reaction mixture was stirred in a sealed tube at 40 °C. Progress of the reaction was monitored by the ESI-MS and the reaction was carried out until all of the starting material was consumed. After the completion of the reaction, the mixture was filtered out and the solvent was evaporated. The mixture was then dissolved in CH_2Cl_2 (double the volume of Me_2CO) and the precipitate was filtered again. Water (half the volume of Me_2CO) was added to the organic layer and the organic layer was evaporated so. A saturated solution of Me_4NCl in water (1 mL) was then added to the aqueous solution and the precipitate was immediately collected and dried under a vacuum. Note: The reaction time decreased significantly with the increasing length of the alkyl chain connecting cluster and amine.

General procedure **C** for preparation of alkyl aminium derivatives **7-11** from halide derivatives **3c**$^-$ or **4c**$^-$:

Note: This method is based on the screening results summarized in the Discussion and Table 1. Cobalt bis(dicarbollide) bromo derivative (**3c**$^-$, 1.0 equiv.) in a sealable tube was dissolved in dry PhMe (10 mL per 1.0 mmol of **3c**$^-$) and KO*t*Bu (2.0 equiv.) with respective aniline (2.0 equiv.) were added. The tube was sealed and the reaction mixture was heated at 100 °C overnight (14 hours). The reaction mixture was then concentrated and applied on the flash column chromatography using a gradient mixture of CH_2Cl_2:MeOH 0-5%.

Synthesis of [(1,7'-μ-CH_2CH_2)-(1,2-$C_2B_9H_{10}$)(1',2'-$C_2B_9H_{10}$)-3,3'-Co]$^-Me_4N^+$ (Me_4N**15a**) and [(1,8'-μ-CH_2CH_2)-(1,2-$C_2B_9H_{10}$))(1',2'-$C_2B_9H_{10}$)-3,3'-Co]$^-Me_4N^+$ (Me_4N**15b**)

Solid [(CH_3SO_2O-CH_2CH_2-1,2-$C_2B_9H_{10}$)(1',2'-$C_2B_9H_{11}$)-3,3'-Co]$^-Me_4N^+$ (150 mg), prepared according to Refs[1, 2] was dried in vaccum in a 8 mL glass vial with Teflon lined screw cap. The vial was filled with argon and then heated 16h at 105 ^oC and additional 24h at 95 ^oC in a temperature controlled drier. After cooling down the vial was opened, and the solid dissolved in CH_2Cl_2- acetonitrile solvent mixture (9: 1 b.v.), injected on a top of a silica gel column (250 x 15 mm I.D.) and eluted with the the mobile phase of the same composition and then by step gradient og CH_3CN up to 30%. Eluted fractions were checked by HPLC. The first three fractions containing mixtures of both isomers were combined and evaporated. The isomers were separated by flash chromatography on Bűchi RP column, 120 filled with irregular 12-25 µm C18-silica particles. Aqueous 50% MeOH was used for elution with gradual increase of its content to 75% over 50 min. The yellow-orange bands corresponding to individual isomers that were detected visually and in UV at 280 and 235 nm were collected and the colvent was evaporated in vaccum. The solids were dissolved in a minimum volume of MeOH and precipitated with an excess of aqueous solution of Me_4NCl and with water, and left to stand for 30 min. The precipitates were separated using syringe microfilter, washed with water (3x 1 ml) and dried in vacuum. Then, the samples were dissolved in CH_2Cl_2, overlayered carefuly with hexane and left to crystalize for 3 days. The crystals were collected. Yields: Me_4N**15a** 45 mg (37%); Me_4N**15a** 35 mg (29%). The reaction was also tested in DME or dioxane as solvents, however larger quantities of side products were observed that according to MS could be assigned to binding of the solvent or its fragments (DME) from its decomposition in the molecule.

Synthesis of [(1,7'-μ-CH_2CH_2-1,2-$C_2B_9H_{10}$)$_2$-3,3'-Co]$^-Me_4N^+$ (Me_4N20a) and [(1,8'-μ-CH_2CH_2-1,2-$C_2B_9H_{10}$)$_2$-3,3'-Co]$^-Me_4N^+$ **(Me_4N20b)**

Solid [(1,1'(CH_3SO_2O-CH_2CH_2-1,2-$C_2B_9H_{10}$)$_2$-3,3'-Co]$^-Me_4N^+$ (100 mg, pure *racemic* isomer), prepared according to Refs[1, 2] was dried in vaccum in a 8 mL glass vial with Teflon lined screw cap. The vial was filled with argon and then heated 60h at 95 ^oC in a temperature controlled drzing oven. After cooling down the vial was opened, and the solid dissolved in CH_2Cl_2- acetonitrile solvent mixture (95: 5 b.v.), injected on a top of a silica gel column (250 x 15 mm I.D.) and eluted with the the mobile phase of the same composition and then by step gradient og CH_3CN up to 40%. Eluted fractions were analzyed using HPLC. The first two fractions containing mixtures of both bridged isomers were combined and evaporated. The isomers were separated by repeated flash chromatography on Bűchi RP column, 120. Aqueous 55% MeOH was used for elution with gradual increase of its content to 75% over 65 min, flow rate 20 mL/min. The yellow bands corresponding to individual isomers that were detected visually and in UV at 280 and 235 nm were collected and the colvent was evaporated in vaccum. The solids were dissolved in a minimum volume of MeOH and precipitated with an excess of aqueous solution of Me_4NCl and with water, and left to stand for 30 min. The precipitates were separated using syringe microfilter, washed with water (3x 1 ml) and dried in vacuum. Then, the samples were dissolved in CH_2Cl_2, overlayered carefuly with hexane and left to crystalize for 3 days. The crystals were collected. Yields: Me_4N**20a** 30 mg (43%); Me_4N**20b** 25 mg (36%).

Crystallographic data

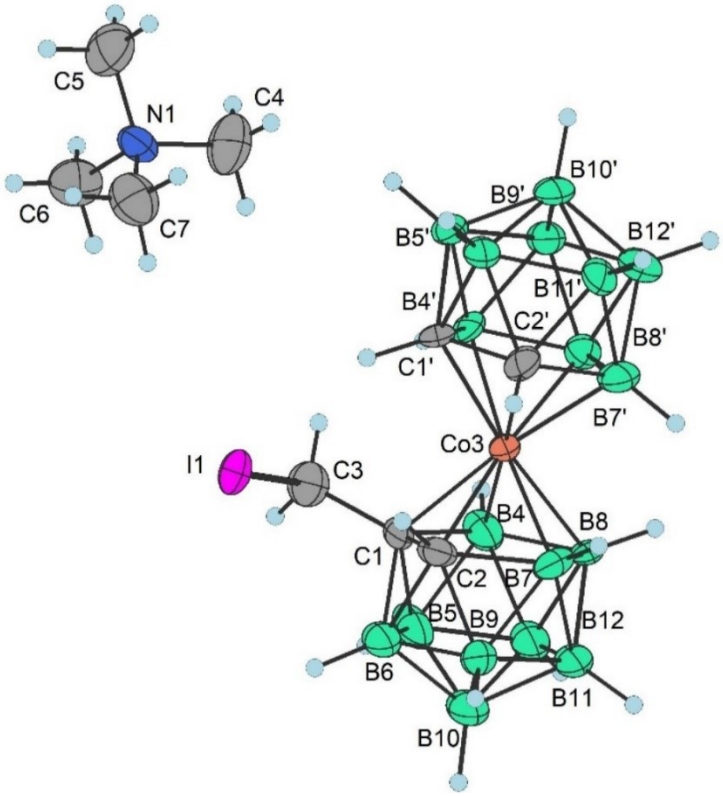

Figure S1. X-ray structure of ***4a***$^{-}$.

Crystallographic Data [(1-I-CH_2-1,2-$C_2B_9H_{10}$)(1′,2′-$C_2B_9H_{11}$)-3,3′-Co]$^{-}$ Me_4N^{+} (**4a**$^{-}$), $C_9H_{35}B_{18}CoIN$ (M =537.79 g/mol), **CCDC 2246096**: monoclinic, space group Pc (no. 7), a = 11.0665(2) Å, b = 10.5685(3) Å, c = 10.2132(2) Å, β = 95.816(2)°, V = 1188.35(5) Å^3, Z = 2, T = 100.00(10) K, μ(Cu Kα) = 15.795 mm^{-1}, D_{calc} = 1.503 g/cm^3, 20291 reflections measured (8.03° ≤ 2Θ ≤ 133.194°), 3565 unique (R_{int} = 0.0580, R_{sigma} = 0.0358) which were used in all calculations. The final R_1 was 0.0485 (I > 2σ(I)) and wR_2 was 0.1374 (all data).

Data were collected on the Rigaku XtaLAB Synergy S diffractometer equipped with micro-focus CuKα/MoKα radiation and a Hybrid Pixel Array Detector (HyPix-6000HE). An Oxford Cryosystems (Cryostream 800) cooling device was used for data collection and the crystals were kept at 100.00(10) K during data collection. CrysAlisPro software[3] was used for data collection, cell refinement, and data reduction. Data were corrected for absorption effects using empirical absorption correction (spherical harmonics), implemented in SCALE3 ABSPACK scaling algorithm and numerical absorption correction based on an analytical method using a multifaceted crystal model based on expressions derived by Clark & Reid.[4] Using Olex2[5], the structure was solved with the SHELXT[6] structure solution program using Intrinsic Phasing and refined with the SHELXL [7] refinement package using Least Squares minimization. Hydrogen atoms of **4a**$^{-}$ were placed in calculated positions. The iodide disorder model incorporates U_{ij} values similarity restraints (SIMU) and a thermal ellipsoid constraint (EADP). A molecular graphic for **4a**$^{-}$ was generated using DIAMOND software (Diamond, v4.6.3).[8]

(a)

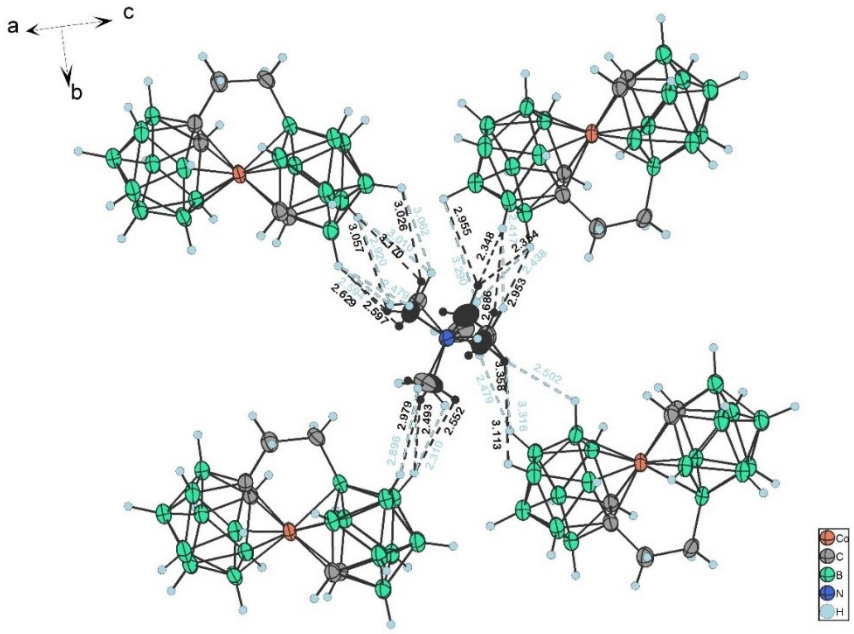

(b)

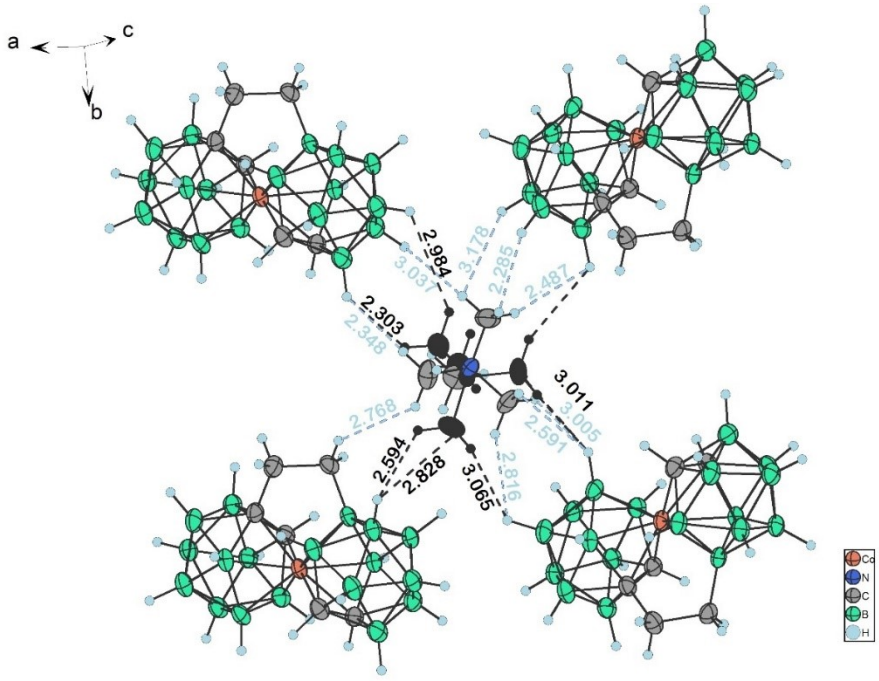

Figure *S2*. The TMA molecules surrounded by the nearest [1,8'-μ-CH_2CH_2-(1,2-$C_2B_9H_{10}$)$_2$-3,3'-Co]$^-$ molecules and highlighting the shortest H-H distances. The minor occupied positions of TMA are plotted in black. (a) The basic orientations of TMA for *t*=0, with refined occupancies 0.488(2) and 0.061(2); (b) The flipped orientations of TMA for *t*=0.5, with refined occupancies 0.4007(17) and 0.0503(17); **CCDC 2262251** (average structure).

The selected sample of Me_4N**15b** was measured on the Rigaku XtaLAB Synergy S diffractometer equipped with CuKα/MoKα radiation and a Hybrid Pixel Array Detector (HyPix-6000HE). An Oxford Cryosystems (Cryostream 800) cooling device was used for data collection and the crystals were kept at 100 K during data collection. CrysAlisPro software[3] was used for data collection, cell refinement, and data reduction. Data were corrected for absorption effects using empirical absorption correction (spherical harmonics), implemented in SCALE3 ABSPACK scaling algorithm. The diffraction pattern contained satellites, which could be indexed with q-vector (0, 0.4524(2), 0) up to the satellite order 2. The 2nd order satellites were close to the main reflections; however, the good quality of the sample and the properties of the hybrid photon counting detector allowed for their separation. The superspace symmetry was determined from systematic absences as $P2_1/n(0\beta0)00$ and confirmed by the program Superflip.[9] Superflip provided atomic positions and initial modulation functions. The structure was refined with the Jana2020 program.[10]

The [1,8'-μ-CH_2CH_2-(1,2-$C_2B_9H_{10})_2$-3,3'-Co]$^-$ molecule (Me_4N**15b**) could be solved easily because the atoms were harmonically modulated, although the modulation displacements were large – about 0.6 Å. We refined two independent rigid bodies $(C_2B_9H_{10})^{2-}$, where modulations of position were refined as rigid body modulations,[11] and displacement parameters were refined as TLS tensors[12] and their modulations. The other atoms, Co and the bridging C_2H_4, were refined as free atoms with constrained hydrogens.

The tricky part was the counterion tetramethylamine (TMA). The initial electron density provided by Superflip suggested crenel[13] modulation of carbon atoms of the width of approximately ½ (see Figures 4a and 4b in the main text). The crenel function describes that TMA exists in a basic orientation in one-half of cases and is flipped in the rest of the cases. The discontinuity point of the modulation function corresponds to the flipping of TMA. This behavior is demonstrated in the average structure as a disorder, which is resolved in the modulated structure as TMA's basic and flipped positions occur at different x_4. Our structure model described TMA as a rigid body in two positions corresponding to the basic and flipped TMA. We refined the center and width of the first position crenel modulation function, while for the second position, the width was calculated as a complementary value to 1, and the center was derived from the width. Modulations were calculated similarly to those for the cages: molecular modulations of positions, TLS tensors and their modulations for TLS tensors.

The resulting structure model still had unexpectedly large *R* values for main reflections and residual electron density located mainly around TMA. We found that the TMA's basic and flipped positions were accompanied by other weakly occupied rotated positions of TMA following the same crenel function, so – in our case – the modulated structure was still disordered. The occupation of the additional TMA positions was about 0.1, and their refinement required restrictions. The weakly occupied TMA positions were calculated like the additional positions of the TMA rigid body, which had now two pairs of positions: (1) the basic position and the weakly occupied position with the same crenel interval; (2) the flipped position, and the weakly occupied position with the same crenel interval. The positional and TLS modulations were kept identical for each pair, and the sum of occupations for each pair was kept one. Moreover, the occupancy of the major basic and flipped position was kept the same.

Refinement of this final structure model (see Figure S2) decreased *R* values to acceptable values, and the final difference Fourier map was without other strong extremes. We have to note that given the limitations of our refinement, the structure model is still an approximation, and the real disorder might be even more complex. An Indication of this fact is the unrealistic shape of the TMA molecule close to the discontinuity point of the crenel function.

Table S1. Crystal data of modulated structure Me4N**15b.**

Crystal data	
Chemical formula	$(C_2H_{10}B_9)_2(C_2H_4)Co$, $N(CH_3)_4$
M_r	423.9
Crystal system, space group	Monoclinic, $P2_1/n(0\beta0)00$†
Temperature (K)	100
Wave vectors	q = 0.458400b*
a, *b*, *c* (Å)	13.5941 (4), 10.4409 (3), 16.1919 (5)
β (°)	93.263 (2)
V (Å^3)	2294.47 (12)
Z	4
Radiation type	Cu Kα
μ (mm^{-1})	5.80
Crystal size (mm)	0.06 × 0.1 × 0.02
Data collection	
Diffractometer	XtaLAB Synergy, Dualflex, HyPix
Absorption correction	Multi-scan
CrysAlis PRO 1.171.42.76a (Rigaku Oxford Diffraction, 2022) Empirical absorption correction using spherical harmonics, implemented in SCALE3 ABSPACK scaling algorithm.	
T_{min}, T_{max}	0.604, 1
No. of measured, independent and observed [$I > 3\sigma(I)$] reflections	
all reflections	114516, 23744, 15902
main reflections	22485, 4749, 3638
1st order satellites	45606, 9500, 7237
2nd order satellites	46425, 9495, 5027
R_{int} (all, main, 1st order, 2nd order)	0.067, 0.045, 0.070, 0.190
$(\sin\theta/\lambda)_{max}$ (Å^{-1})	0.636
Refinement	
$R[F^2 > 3\sigma(F^2)]$, $wR(F^2)$, S	0.084, 0.222, 2.55*
$R[F^2 > 3\sigma(F^2)]$, $wR(F^2)$ for main reflections	0.062, 0.179
$R[F^2 > 3\sigma(F^2)]$, $wR(F^2)$ for 1st order satellites	0.078, 0.203
$R[F^2 > 3\sigma(F^2)]$, $wR(F^2)$ for 2nd order satellites	0.137, 0.310
No. of parameters	560
No. of restraints	16
H-atom treatment	H-atom parameters constrained for C atoms, which are not part of cages
$\Delta\rho_{max}$, $\Delta\rho_{min}$ (e Å^{-3})	0.98, −0.49

*Jana2020 does not refine the weighting scheme coefficients. The S is based on experimental weights and is usually above one.

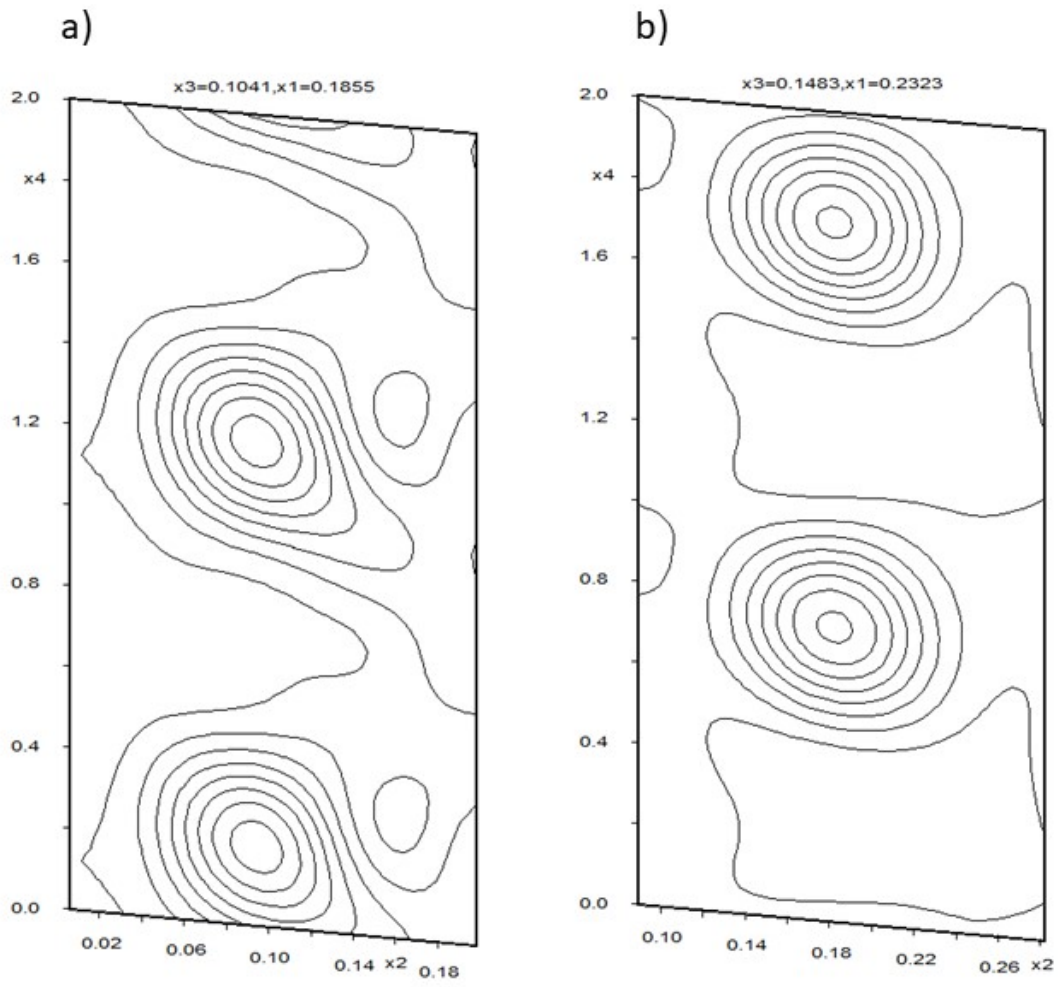

Figure S3. De Wolff section based on the electron density map from charge flipping, (a) at the position of C7a; (b) at the position of C7b. The atoms can be described by crenel modulation functions with complementary widths.

Table S2. Bond lengths of modulated structure Me_4N**15b.** The table summarizes the distances in the main molecule and in the first position of the solvent molecule. The solvent molecule has the same geometry in all positions. The positions differ only in their location in the crystal structure.

	Ave [Å]	Min [Å]	Max [Å]
Co1-C12	2.035(5)	2.021(5)	2.057(5)
Co1-C22	2.033(6)	2.018(6)	2.051(6)
Co1-B92	2.085(7)	2.075(7)	2.095(7)
Co1-B82	2.120(6)	2.116(6)	2.124(6)
Co1-B72	2.106(6)	2.092(6)	2.123(6)
Co1-C11	2.032(6)	2.022(6)	2.040(6)
Co1-C21	2.034(6)	2.016(6)	2.054(6)
Co1-B71	2.078(7)	2.058(7)	2.088(7)
Co1-B91	2.103(6)	2.092(6)	2.127(6)
Co1-B81	2.137(6)	2.127(6)	2.146(6)
C5-C6	1.537(9)	1.532(9)	1.546(9)
C5-C11	1.532(8)	1.524(8)	1.540(8)
C6-B82	1.598(8)	1.579(8)	1.617(8)
C12-C22	1.635(8)	1.633(8)	1.638(8)
C12-B72	1.697(8)	1.696(9)	1.701(9)
C12-B22	1.722(8)	1.721(8)	1.724(8)
C12-B32	1.704(7)	1.704(7)	1.704(7)
C22-B92	1.712(9)	1.710(9)	1.715(9)
C22-B22	1.714(7)	1.713(7)	1.716(7)
C22-B62	1.706(8)	1.705(8)	1.706(8)
B92-B52	1.779(7)	1.779(7)	1.780(7)
B12-B22	1.768(7)	1.767(7)	1.769(7)
B12-B62	1.777(7)	1.776(7)	1.779(7)
B12-B32	1.771(7)	1.770(7)	1.774(7)
B72-B32	1.782(8)	1.781(8)	1.785(8)
B72-B42	1.777(8)	1.777(8)	1.778(8)
B22-B62	1.765(8)	1.763(8)	1.768(8)
B22-B32	1.759(8)	1.757(8)	1.762(8)
B32-B42	1.782(8)	1.780(8)	1.785(8)
B52-B42	1.776(8)	1.774(8)	1.779(8)
C11-C21	1.645(8)	1.643(8)	1.650(8)
C11-B21	1.735(6)	1.733(6)	1.737(6)
C11-B71	1.746(9)	1.744(9)	1.750(9)
C11-B31	1.714(8)	1.714(8)	1.715(8)
C21-B21	1.719(8)	1.718(8)	1.722(8)
C21-B61	1.716(8)	1.715(8)	1.716(8)
C21-B91	1.728(9)	1.726(9)	1.733(9)
B11-B21	1.763(7)	1.762(7)	1.764(7)
B11-B61	1.777(7)	1.776(7)	1.780(7)
B11-B31	1.783(7)	1.781(7)	1.786(7)
B11-B41	1.780(7)	1.778(7)	1.785(7)

B21-B61	1.771(8)	1.769(8)	1.776(8)
B21-B31	1.760(8)	1.758(8)	1.765(8)
B71-B31	1.772(8)	1.770(8)	1.776(8)
B71-B41	1.766(7)	1.765(7)	1.766(7)
B61-B51	1.771(8)	1.769(8)	1.775(8)
B51-B81	1.783(7)	1.782(8)	1.786(8)
B51-B41	1.784(8)	1.782(8)	1.789(8)
B91-B81	1.774(9)	1.772(9)	1.779(9)
B31-B41	1.783(8)	1.781(8)	1.787(8)
C7a-N1a	1.522(17)	1.46(2)	1.77(2)
C8a-N1a	1.518(17)	1.46(2)	1.74(2)
C9a-N1a	1.499(16)	1.47(2)	1.80(2)
C10a-N1a	1.492(16)	1.453(18)	1.810(18)

Table S3. Bond angles of modulated structure Me_4N**15b.** The table summarizes the angles in the main molecule and in the first position of the solvent molecule. The solvent molecule has the same geometry in all positions. The positions differ only in their location in the crystal structure.

	Ang [˚]	Min [˚]	Max [˚]
C12-Co1-C22	47.4(2)	47.0(2)	47.7(2)
C12-Co1-B92	84.1(2)	83.6(2)	84.6(2)
C12-Co1-B82	84.3(2)	83.9(2)	84.6(2)
C12-Co1-B72	48.4(2)	48.0(2)	48.7(2)
C12-Co1-C11	141.3(2)	139.8(2)	142.7(2)
C12-Co1-C21	170.9(2)	169.6(2)	172.4(2)
C12-Co1-B71	102.5(2)	101.1(2)	103.6(2)
C12-Co1-B91	124.3(2)	123.1(2)	124.8(2)
C12-Co1-B81	95.4(2)	94.8(2)	96.2(2)
C22-Co1-B92	49.1(3)	48.8(3)	49.5(3)
C22-Co1-B82	85.0(2)	84.7(2)	85.3(2)
C22-Co1-B72	83.7(2)	83.2(2)	84.1(2)
C22-Co1-C11	167.9(3)	166.7(3)	169.0(3)
C22-Co1-C21	123.9(2)	122.6(2)	125.1(2)
C22-Co1-B71	141.8(3)	140.9(3)	143.0(3)
C22-Co1-B91	93.7(2)	92.9(2)	94.3(2)
C22-Co1-B81	102.6(2)	102.2(2)	103.1(2)
B92-Co1-B82	51.1(2)	51.0(2)	51.2(2)
B92-Co1-B72	86.9(2)	86.7(2)	87.1(2)
B92-Co1-C11	119.0(2)	118.2(2)	119.6(3)
B92-Co1-C21	90.5(2)	89.8(2)	91.3(2)
B92-Co1-B71	168.2(3)	167.3(3)	168.9(3)
B92-Co1-B91	98.0(2)	97.1(2)	98.7(2)
B92-Co1-B81	139.4(2)	138.2(2)	140.1(2)
B82-Co1-B72	50.4(2)	50.2(2)	50.5(2)
B82-Co1-C11	87.7(2)	87.5(2)	87.9(2)
B82-Co1-C21	97.9(2)	97.4(2)	98.3(2)
B82-Co1-B71	119.2(2)	118.5(2)	120.1(3)
B82-Co1-B91	138.3(2)	137.0(2)	139.0(2)
B82-Co1-B81	169.4(3)	168.7(3)	170.8(3)
B72-Co1-C11	99.0(2)	97.9(2)	100.1(2)
B72-Co1-C21	138.7(3)	137.8(3)	139.7(3)
B72-Co1-B71	90.2(2)	89.1(2)	91.1(2)
B72-Co1-B91	170.9(3)	169.9(3)	171.9(3)
B72-Co1-B81	122.5(2)	121.8(2)	123.9(2)
C11-Co1-C21	47.7(2)	47.4(2)	48.1(2)
C11-Co1-B71	50.3(2)	50.0(2)	50.7(2)
C11-Co1-B91	85.3(2)	84.8(2)	85.7(2)
C11-Co1-B81	85.9(2)	85.7(2)	86.2(2)
C21-Co1-B71	84.2(2)	84.0(2)	84.6(2)
C21-Co1-B91	49.3(2)	48.8(2)	49.7(2)

C21-Co1-B81	84.0(2)	83.6(2)	84.3(2)
B71-Co1-B91	86.4(2)	86.3(2)	86.6(2)
B71-Co1-B81	50.5(2)	50.2(2)	50.8(2)
B91-Co1-B81	49.5(2)	49.2(2)	49.7(2)
C6-C5-C11	112.5(5)	112.1(5)	112.8(5)
C5-C6-B82	109.6(5)	108.9(5)	110.4(5)
Co1-C12-C22	66.2(3)	65.8(3)	66.7(3)
Co1-C12-B72	68.0(3)	67.6(3)	68.4(3)
Co1-C12-B22	123.7(3)	123.3(3)	124.1(3)
Co1-C12-B32	125.1(4)	124.8(4)	125.3(4)
C22-C12-B72	111.9(4)	111.9(4)	111.9(4)
C22-C12-B22	61.3(3)	61.3(3)	61.4(3)
C22-C12-B32	110.8(4)	110.8(4)	110.8(4)
B72-C12-B22	114.5(4)	114.4(4)	114.6(4)
B72-C12-B32	63.2(3)	63.2(3)	63.3(3)
B22-C12-B32	61.8(3)	61.7(3)	61.8(3)
Co1-C22-C12	66.3(3)	65.9(3)	66.9(3)
Co1-C22-B92	67.0(3)	66.6(3)	67.3(3)
Co1-C22-B22	124.2(4)	123.8(4)	124.7(4)
Co1-C22-B62	124.4(4)	124.2(4)	124.6(4)
C12-C22-B92	111.0(5)	111.0(5)	111.0(5)
C12-C22-B22	61.8(3)	61.8(3)	61.9(3)
C12-C22-B62	111.2(3)	111.1(3)	111.2(3)
B92-C22-B22	114.4(4)	114.3(4)	114.5(4)
B92-C22-B62	63.0(3)	63.0(3)	63.1(3)
B22-C22-B62	62.1(3)	62.1(3)	62.2(3)
Co1-B92-C22	63.9(3)	63.5(3)	64.3(3)
Co1-B92-B52	118.3(4)	118.0(4)	118.7(4)
C22-B92-B52	104.6(4)	104.5(4)	104.6(4)
Co1-B82-C6	106.1(4)	105.8(4)	106.6(4)
B22-B12-B62	59.7(3)	59.7(3)	59.8(3)
B22-B12-B32	59.6(3)	59.6(3)	59.6(3)
B62-B12-B32	107.2(3)	107.2(3)	107.4(3)
Co1-B72-C12	63.6(2)	63.2(2)	64.1(2)
Co1-B72-B32	117.1(4)	116.6(4)	117.5(4)
Co1-B72-B42	117.6(3)	117.3(3)	117.9(3)
C12-B72-B32	58.6(3)	58.5(3)	58.6(3)
C12-B72-B42	104.7(4)	104.6(4)	104.8(4)
B32-B72-B42	60.1(3)	60.0(3)	60.1(3)
C12-B22-C22	56.8(3)	56.8(3)	56.9(3)
C12-B22-B12	104.9(4)	104.8(4)	105.0(4)
C12-B22-B62	104.5(4)	104.4(4)	104.5(4)
C12-B22-B32	58.6(3)	58.5(3)	58.7(3)
C22-B22-B12	105.2(4)	105.1(4)	105.2(4)
C22-B22-B62	58.7(3)	58.6(3)	58.7(3)
C22-B22-B32	104.7(4)	104.6(4)	104.7(4)

B12-B22-B62	60.4(3)	60.4(3)	60.4(3)
B12-B22-B32	60.3(3)	60.3(3)	60.3(3)
B62-B22-B32	108.4(4)	108.4(4)	108.4(4)
C22-B62-B12	105.2(4)	105.1(4)	105.2(4)
C22-B62-B22	59.2(3)	59.2(3)	59.2(3)
B12-B62-B22	59.9(3)	59.8(3)	59.9(3)
C12-B32-B12	105.5(3)	105.5(3)	105.6(3)
C12-B32-B72	58.2(3)	58.2(3)	58.3(3)
C12-B32-B22	59.6(3)	59.6(3)	59.7(3)
C12-B32-B42	104.2(4)	104.2(4)	104.3(4)
B12-B32-B72	108.6(4)	108.6(4)	108.7(4)
B12-B32-B22	60.1(3)	60.0(3)	60.2(3)
B12-B32-B42	60.4(3)	60.4(3)	60.4(3)
B72-B32-B22	108.6(4)	108.6(4)	108.7(4)
B72-B32-B42	59.8(3)	59.7(3)	59.9(3)
B22-B32-B42	108.2(4)	108.2(4)	108.3(4)
B92-B52-B42	107.9(4)	107.9(4)	108.0(4)
B72-B42-B32	60.1(3)	60.1(3)	60.1(3)
B72-B42-B52	108.3(4)	108.3(4)	108.4(4)
B32-B42-B52	107.8(4)	107.8(4)	107.8(4)
Co1-C11-C5	109.0(3)	108.4(3)	109.9(3)
Co1-C11-C21	66.2(3)	65.7(3)	67.1(3)
Co1-C11-B21	122.8(3)	122.4(3)	123.5(3)
Co1-C11-B71	66.2(3)	65.6(3)	66.7(3)
Co1-C11-B31	122.3(4)	122.0(4)	122.7(4)
C5-C11-C21	119.6(5)	118.9(5)	120.5(5)
C5-C11-B21	115.0(4)	113.5(4)	116.1(4)
C5-C11-B71	124.2(4)	123.1(4)	125.6(4)
C5-C11-B31	119.5(5)	119.0(5)	119.9(5)
C21-C11-B21	61.1(3)	61.0(3)	61.1(3)
C21-C11-B71	108.7(4)	108.7(4)	108.7(4)
C21-C11-B31	109.4(3)	109.4(3)	109.5(3)
B21-C11-B71	111.5(3)	111.5(3)	111.6(3)
B21-C11-B31	61.4(3)	61.3(3)	61.5(3)
B71-C11-B31	61.6(3)	61.6(3)	61.6(3)
Co1-C21-C11	66.1(3)	65.3(3)	66.4(3)
Co1-C21-B21	123.5(4)	122.8(3)	123.9(4)
Co1-C21-B61	124.3(4)	124.1(4)	124.6(4)
Co1-C21-B91	67.4(3)	67.1(3)	67.9(3)
C11-C21-B21	62.0(3)	62.0(3)	62.0(3)
C11-C21-B61	112.2(4)	112.2(4)	112.3(4)
C11-C21-B91	112.3(4)	112.3(4)	112.4(4)
B21-C21-B61	62.1(3)	62.0(3)	62.2(3)
B21-C21-B91	114.2(4)	114.1(4)	114.3(4)
B61-C21-B91	62.9(3)	62.8(3)	62.9(3)
B21-B11-B61	60.0(3)	60.0(3)	60.1(3)

B21-B11-B31	59.5(3)	59.5(3)	59.6(3)
B21-B11-B41	108.0(3)	107.9(3)	108.0(3)
B61-B11-B31	107.1(4)	107.0(4)	107.3(4)
B61-B11-B41	107.5(4)	107.5(4)	107.5(4)
B31-B11-B41	60.1(3)	60.1(3)	60.1(3)
C11-B21-C21	56.9(3)	56.9(3)	57.0(3)
C11-B21-B11	106.4(4)	106.2(4)	106.5(4)
C11-B21-B61	105.5(4)	105.4(4)	105.5(4)
C11-B21-B31	58.7(3)	58.6(3)	58.8(3)
C21-B21-B11	105.3(4)	105.2(4)	105.4(4)
C21-B21-B61	58.9(3)	58.7(3)	58.9(3)
C21-B21-B31	104.0(4)	104.0(4)	104.0(4)
B11-B21-B61	60.4(3)	60.4(3)	60.4(3)
B11-B21-B31	60.8(3)	60.8(3)	60.8(3)
B61-B21-B31	108.4(4)	108.4(4)	108.4(4)
Co1-B71-C11	63.5(3)	63.0(3)	63.9(3)
Co1-B71-B31	116.9(4)	116.5(4)	117.6(4)
Co1-B71-B41	119.4(4)	119.1(4)	120.0(4)
C11-B71-B31	58.3(3)	58.2(3)	58.4(3)
C11-B71-B41	105.8(3)	105.7(3)	105.8(3)
B31-B71-B41	60.5(3)	60.5(3)	60.6(3)
C21-B61-B11	104.9(4)	104.7(4)	104.9(4)
C21-B61-B21	59.1(3)	59.0(3)	59.1(3)
C21-B61-B51	105.1(4)	105.0(4)	105.1(4)
B11-B61-B21	59.6(3)	59.5(3)	59.6(3)
B11-B61-B51	60.5(3)	60.5(3)	60.5(3)
B21-B61-B51	108.3(4)	108.3(4)	108.3(4)
B61-B51-B81	108.8(4)	108.7(4)	108.9(4)
B61-B51-B41	107.6(4)	107.6(4)	107.6(4)
B81-B51-B41	60.5(3)	60.4(3)	60.5(3)
Co1-B91-C21	63.2(3)	62.8(3)	63.6(3)
Co1-B91-B81	66.3(3)	65.7(3)	66.8(3)
C21-B91-B81	105.8(4)	105.7(4)	105.8(4)
Co1-B81-B51	116.5(4)	116.0(4)	117.2(4)
Co1-B81-B91	64.3(3)	63.8(3)	65.1(3)
B51-B81-B91	60.2(3)	60.1(3)	60.2(3)
C11-B31-B11	106.4(4)	106.3(4)	106.5(4)
C11-B31-B21	59.9(3)	59.9(3)	59.9(3)
C11-B31-B71	60.1(3)	60.0(3)	60.2(3)
C11-B31-B41	106.4(4)	106.3(4)	106.5(4)
B11-B31-B21	59.7(3)	59.6(3)	59.7(3)
B11-B31-B71	107.9(4)	107.8(4)	107.9(4)
B11-B31-B41	59.9(3)	59.9(3)	59.9(3)
B21-B31-B71	109.1(4)	109.1(4)	109.2(4)
B21-B31-B41	107.9(4)	107.9(4)	107.9(4)
B71-B31-B41	59.6(3)	59.4(3)	59.6(3)

B11-B41-B71	108.3(4)	108.3(4)	108.3(4)
B11-B41-B51	60.2(3)	60.2(3)	60.2(3)
B11-B41-B31	60.0(3)	60.0(3)	60.1(3)
B71-B41-B51	107.9(4)	107.8(4)	107.9(4)
B71-B41-B31	59.9(3)	59.9(3)	60.0(3)
B51-B41-B31	107.8(4)	107.8(4)	107.8(4)
C7a-N1a-C8a	109.1(10)	108.0(9)	114.1(9)
C7a-N1a-C9a	108.9(10)	103.9(10)	110.9(10)
C7a-N1a-C10a	110.1(10)	103.5(10)	112.0(9)
C8a-N1a-C9a	109.0(11)	102.1(11)	110.9(10)
C8a-N1a-C10a	109.7(10)	104.7(10)	111.8(10)
C9a-N1a-C10a	110.0(10)	107.9(10)	112.7(10)

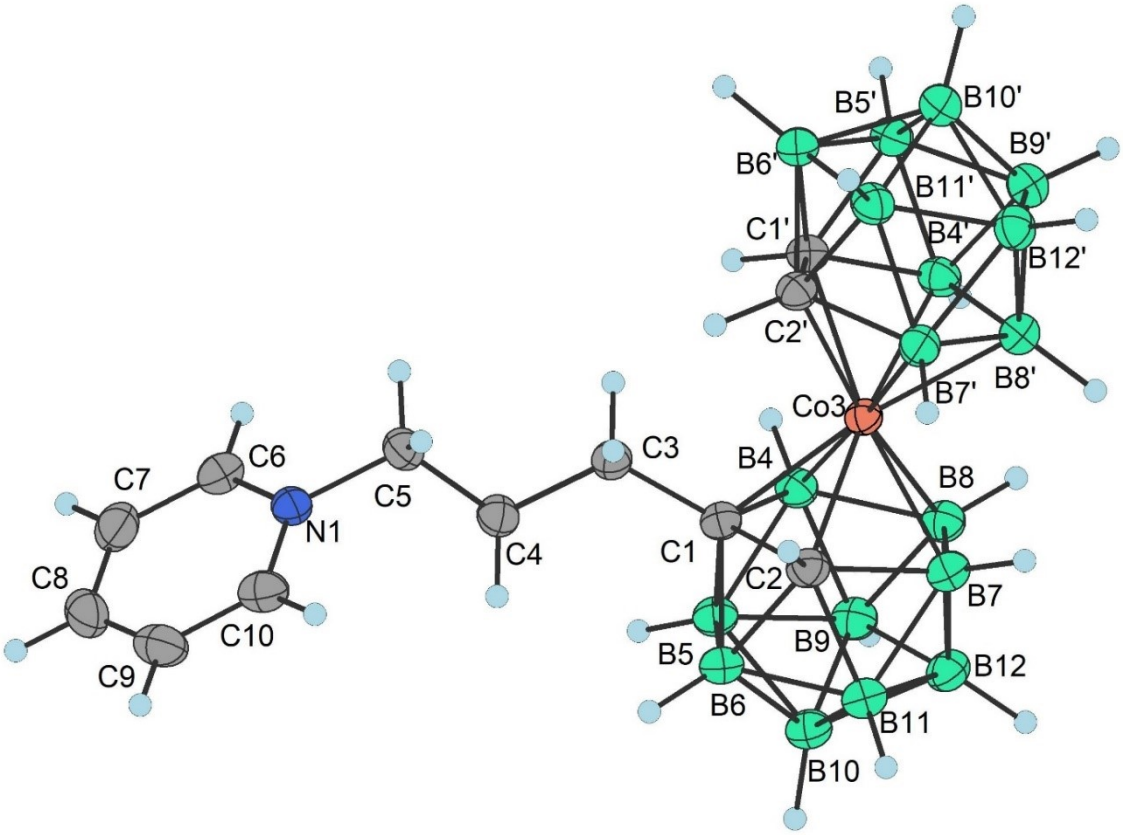

*Figure S4. X-ray structure of **16**.*

Crystallographic Data $[(1\text{-}C_6H_5N\text{-}(CH_2)_3\text{-}1,2\text{-}C_2B_9H_{10})(1',2'\text{-}C_2B_9H_{11})\text{-}3,3'\text{-}Co]^0$ (**16**) $C_{10}H_{36}B_{18}CoN$ (M =423.91 g/mol), **CCDC 2246097**: monoclinic, space group $P2_1/c$ (no. 14), a = 13.7657(3) Å, b = 11.6644(2) Å, c = 14.2364(3) Å, β = 94.582(2)°, V = 2278.61(8) Å^3, Z = 4, T = 100.00(10) K, μ(Cu Kα) = 5.836 mm^{-1}, D_{calc} = 1.236 g/cm^3, 20741 reflections measured (6.442° ≤ 2Θ ≤ 133.198°), 4007 unique (R_{int} = 0.0476, R_{sigma} = 0.0350) which were used in all calculations. The final R_1 was 0.0466 (I > 2σ(I)) and wR_2 was 0.1257 (all data).

Data were collected on the Rigaku XtaLAB Synergy S diffractometer equipped with micro-focus CuKα/MoKα radiation and a Hybrid Pixel Array Detector (HyPix-6000HE). An Oxford Cryosystems (Cryostream 800) cooling device was used for data collection and the crystals were kept at 100.00(10) K during data collection. CrysAlisPro software[3] was used for data collection, cell refinement and data reduction. Data was corrected for absorption effects using empirical absorption correction (spherical harmonics), implemented in SCALE3 ABSPACK scaling algorithm and numerical absorption correction based on gaussian integration over a three-dimensional grid.[14] Using Olex2[5], the structure was solved with the SHELXT[6] structure solution program using Intrinsic Phasing and refined with the SHELXL [7] refinement package using Least Squares minimization. Hydrogen atoms of **16** were placed in calculated positions. A molecular graphic for **16** was generated using DIAMOND software (Diamond, v4.6.3).[8]

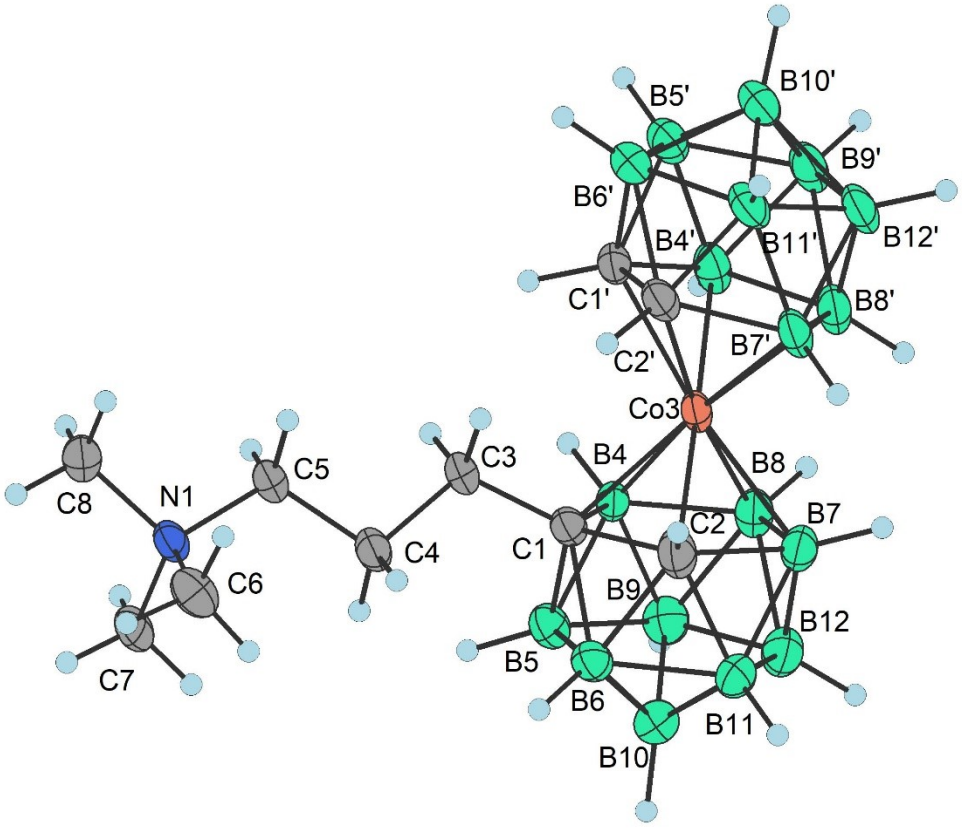

*Figure S5. X-ray structure of **18**.*

Crystallographic Data $[(1\text{-}(CH_3)_3N\text{-}(CH_2)_3\text{-}1,2\text{-}C_2B_9H_{10})(1',2'\text{-}C_2B_9H_{11})\text{-}3,3'\text{-}Co]^0$ (**18**) $C_{12}H_{32}B_{18}CoN$ (M =443.89 g/mol), **CCDC 2246098**: monoclinic, space group $P2_1/c$ (no. 14), a = 14.2945(2) Å, b = 12.39900(10) Å, c = 13.30760(10) Å, β = 106.1000(10)°, V = 2266.10(4) Å^3, Z = 4, T = 100.00(10) K, μ(Cu Kα) = 5.899 mm^{-1}, D_{calc} = 1.301 g/cm^3, 34472 reflections measured (6.436° ≤ 2Θ ≤ 133.17°), 4003 unique (R_{int} = 0.0404, R_{sigma} = 0.0219) which were used in all calculations. The final R_1 was 0.0306 (I > 2σ(I)) and wR_2 was 0.0852 (all data).

Data were collected on the Rigaku XtaLAB Synergy S diffractometer equipped with micro-focus CuKα/MoKα radiation and a Hybrid Pixel Array Detector (HyPix-6000HE). An Oxford Cryosystems (Cryostream 800) cooling device was used for data collection and the crystals were kept at 100.00(10) K during data collection. CrysAlisPro software[3] was used for data collection, cell refinement and data reduction. Data was corrected for absorption effects using empirical absorption correction (spherical harmonics), implemented in SCALE3 ABSPACK scaling algorithm and numerical absorption correction based on gaussian integration over a three-dimensional grid.[14] Using Olex2[5], the structure was solved with the SHELXT[6] structure solution program using Intrinsic Phasing and refined with the SHELXL [7] refinement package using Least Squares minimisation. Hydrogen atoms of **18** were placed in calculated positions. Molecular graphic for **18** was generated using DIAMOND software (Diamond, v4.6.3).[8]

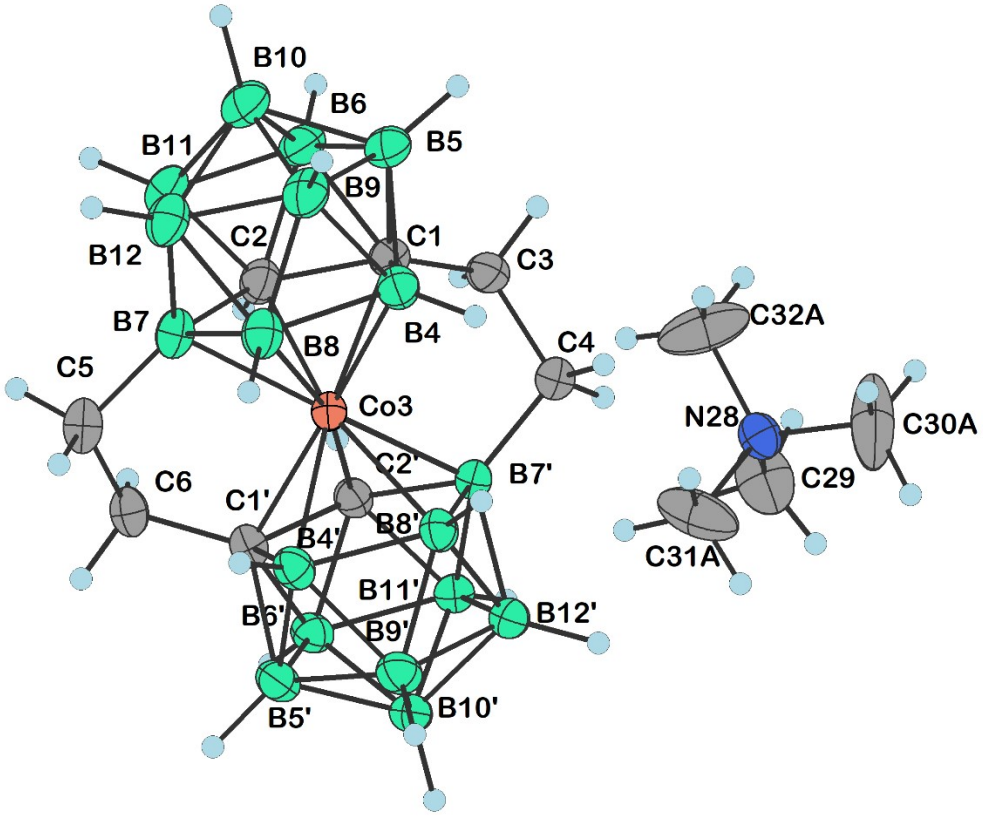

*Figure S6. X-ray structure of **20a**.*

Crystallographic Data [(1,7-μ-C_2H_4-1,2-$C_2B_9H_9)_2$-3,3'-Co]Me_4N (Me_4N**20a**) $C_{13}H_{40}B_{18}Cl_2CoN$ (M =534.87 g/mol), **CCDC 2313358** : monoclinic, space group $P2_1/c$ (no. 14), a = 15.3274(4) Å, b = 12.8952(3) Å, c =14.3700(3) Å, β = 109.088(3)°, V = 2684.07(11) Å^3, Z = 4, T = 99.99(10) K, μ(Cu Kα) = 6.855 mm^{-1}, D_{calc} = 1.324 g/cm^3, 39000 reflections measured (6.102° ≤ 2Θ ≤ 133.172°), 4743 unique (R_{int} = 0.0542, R_{sigma} = 0.0268) which were used in all calculations. The final R_1 was 0.0352 (I > 2σ(I)) and wR_2 was 0.0950 (all data).

Data were collected on the Rigaku XtaLAB Synergy S diffractometer equipped with micro-focus CuKα/MoKα radiation and a Hybrid Pixel Array Detector (HyPix-6000HE). An Oxford Cryosystems (Cryostream 800) cooling device was used for data collection and the crystals were kept at 99.99(10) K during data collection. CrysAlisPro software[3] was used for data collection, cell refinement and data reduction. Data was corrected for absorption effects using empirical absorption correction (spherical harmonics), implemented in SCALE3 ABSPACK scaling algorithm and numerical absorption correction based on gaussian integration over a three-dimensional grid.[14] Using Olex2[5], the structure was solved with the SHELXT[6] structure solution program using Intrinsic Phasing and refined with the SHELXL [7] refinement package using Least Squares minimisation. Hydrogen atoms of **20a** were placed in calculated positions. Molecular graphic for **20a** was generated using DIAMOND software (Diamond, v4.6.3).[8]

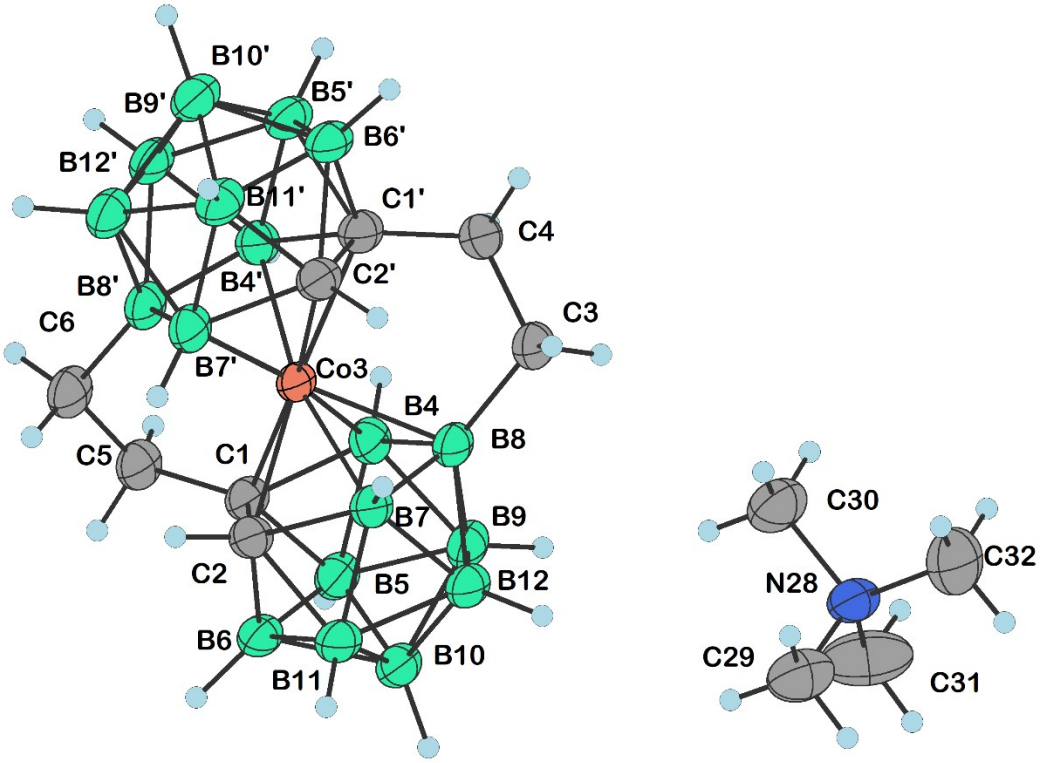

Figure S7. *Figure S7. X-ray structure of **20b**.*

Crystallographic Data [(1,8-μ-C_2H_4-1,2-$C_2B_9H_9$)$_2$-3,3'-Co]Me_4N (Me_4N**20b**) $C_{12}H_{38}B_{18}CoN$ (M =449.94 g/mol), **CCDC 2313381**: triclinic, space group P-1 (no. 2), a = 9.8900(2) Å, b = 10.5598(3) Å, c = 11.48866(18) Å, α = 84.7500(17)°, β = 87.7997(15)°, γ = 88.905(2)°, V = 1193.77(5) Å^3, Z = 2, T = 100.00(10) K, μ(Cu Kα) = 5.600 mm^{-1}, D_{calc} = 1.252 g/cm^3, 32591 reflections measured (7.732° ≤ 2Θ ≤ 133.162°), 4211 unique (R_{int} = 0.0689, R_{sigma} = 0.0349) which were used in all calculations. The final R_1 was 0.0513 (I > 2σ(I)) and wR_2 was 0.1471 (all data).

Data were collected on the Rigaku XtaLAB Synergy S diffractometer equipped with micro-focus CuKα/MoKα radiation and a Hybrid Pixel Array Detector (HyPix-6000HE). An Oxford Cryosystems (Cryostream 800) cooling device was used for data collection and the crystals were kept at 100.00(10)) K during data collection. CrysAlisPro software[3] was used for data collection, cell refinement and data reduction. Data was corrected for absorption effects using empirical absorption correction (spherical harmonics), implemented in SCALE3 ABSPACK scaling algorithm and numerical absorption correction based on gaussian integration over a three-dimensional grid.[14] Using Olex2[5], the structure was solved with the SHELXT[6] structure solution program using Intrinsic Phasing and refined with the SHELXL [7] refinement package using Least Squares minimisation. Hydrogen atoms of **20b** were placed in calculated positions. Molecular graphic for **20b** was generated using DIAMOND software (Diamond, v4.6.3).[8]

Spectral data and details on synthesis

[(1-(F_3C-SO_2)-O-(CH_2)$_3$-1,2-$C_2B_9H_{10}$)(1',2'-$C_2B_9H_{11}$)-3,3'-Co]$^-$ (**2c**)

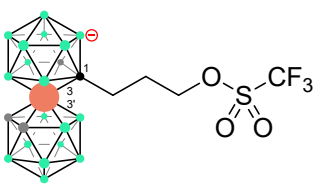

Dried hydroxy derivative **1c** (1 equiv.) was dissolved in dry CH_2Cl_2 (1 mL per 100 mg) and cooled down to 0 °C using an ice bath. Then the Tf_2O (1.1 equiv.) in dry CH_2Cl_2 and pyridine (1.1 equiv) were added dropwise *via* septum from a syringe at room temperature. The reaction was monitored by periodic ESI-MS check until no starting material was present (5 h).[15] The compound decomposed during all purification processes. **MS**: *m/z* (ESI^-) 517.20 (M^-, 16%), 514.28 (100%), calc. 517.26 and 514.28.

$[(1\text{-Br-}CH_2\text{-}1,2\text{-}C_2B_9H_{10})(1',2'\text{-}C_2B_9H_{11})\text{-}3,3'\text{-Co}]^-\ Me_4N^+$ (**3a**$^-$)

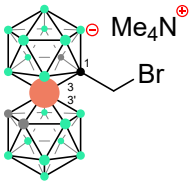

Prepared accordingly to General procedure **A**. Reaction time 12 h. Yield 91%. **^{1}H NMR** (600 MHz, Acetonitrile-d_3) δ 4.48 (dd, *J* = 95.9, 11.8 Hz, 2H), 4.11 (s, 1H), 3.95 (s, 1H), 3.93 (s, 1H), 3.06 (s, 12H); **^{11}B NMR** (193 MHz, Acetonitrile-d_3) δ 5.82 (2d, *J* = 137.5 Hz, 2B), 0.41 (d, *J* = 142.9 Hz, 2B), -6.82 (4d, *overlap*, 8B), -13.90 (d, *J* = 159.9 Hz, 1B), -17.91 (m, *overlap*, 3B), -20.62 (d, *J* = 171.8 Hz, 1B), -23.59 (d, *J* = 169.8 Hz, 1B); **^{13}C NMR** (151 MHz, Acetonitrile-d_3) δ 56.28, 55.25, 50.11, 39.61, 29.42; **HRMS**: *m/z* (ESI^-) 420.2008 (M^-, 21%), 417.2099 (100%), calc. 420.2017 and 417.2100.

$[(1\text{-Br-}(CH_2)_2\text{-}1,2\text{-}C_2B_9H_{10})(1',2'\text{-}C_2B_9H_{11})\text{-}3,3'\text{-Co}]^-\ Me_4N^+$ (**3b**$^-$)

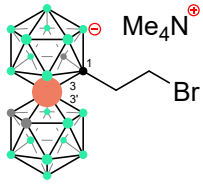

Prepared accordingly to General procedure **A**. Reaction time 12 h. Yield 89%. **^{1}H NMR** (600 MHz, Acetonitrile-d_3) δ 4.10 – 4.05 (m, 2H), 3.93 (s, 1H), 3.70 (s, 1H), 3.61 (s, 1H), 3.48 (dddd, *J* = 43.6, 11.6, 9.5, 5.3 Hz, 1H), 3.04 (s, 12H), 3.00 – 2.95 (m, 1H), 2.56 (dtd, *J* = 15.6, 9.4, 6.0 Hz, 2H); **^{11}B NMR** (193 MHz, Acetonitrile-d_3) δ 5.25 (d, *J* = 145.6 Hz, 2B), -0.10 (d, *J* = 97.1 Hz, 2B), -5.06 – -9.00 (4d, *overlap*, 8B), -15.53 – -19.76 (2d, *overlap*, 4B), -20.68 (d, *J* = 162.3 Hz, 1B), -23.84 (d, *J* = 168.6 Hz, 1B); **^{13}C NMR** (151 MHz, Acetonitrile-d_3) δ 64.84, 56.70, 55.29, 53.54, 51.42, 45.06, 39.55; **HRMS**: *m/z* (ESI^-) 435.2127 (M^-, 5%), 431.2249 (100%), calc. 435.2145 and 431.2252.

$[(1\text{-Br-}(CH_2)_3\text{-}1,2\text{-}C_2B_9H_{10})(1',2'\text{-}C_2B_9H_{11})\text{-}3,3'\text{-Co}]^-\ Me_4N^+$ (**3c**$^-$)

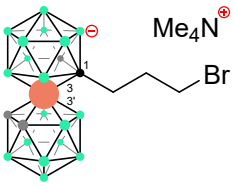

Prepared accordingly to General procedure **A**. Reaction time 4 h. Yield 90%. **^{1}H NMR** (600 MHz, Acetonitrile-d_3) δ 3.97 (s, 1H), 3.67 (s, 1H), 3.61 (s, 1H), 3.41 (td, *J* = 6.4, 2.3 Hz, 2H), 3.07 (s, 12H), 2.77 – 2.72 (m, 1H), 2.35 (ddd, *J* = 14.6, 9.4, 6.9 Hz, 1H), 2.06 – 2.00 (m, 2H); **^{11}B NMR** (193 MHz, Acetonitrile-d_3) δ 5.06 (2d, *J* = 102.0 Hz, 2B), -0.31 (d, *J* = 142.3 Hz, 2B), -7.26 (4d, *overlap*, 8B), -16.02 (d, *J* = 161.9 Hz, 1B), -17.32 (d, *J* = 159.0 Hz, 1B), -18.84 (2d, *overlap*, 4B), -23.89 (d, *J* = 169.4 Hz, 1B).; **^{13}C NMR** (151 MHz, Acetonitrile-d_3) δ 56.84, 55.91 – 54.82 (m), 53.28, 51.15, 38.36, 33.83, 33.37; **HRMS**: *m/z* (ESI^-) 449.2289 (M^-, 10%), 445.2398 (100%), calc. 449.2309 and 445.2414.

[(1-I-CH_2-1,2-$C_2B_9H_{10}$)(1′,2′-$C_2B_9H_{11}$)-3,3′-Co]$^-$ Me_4N^+ (**4a**$^-$)

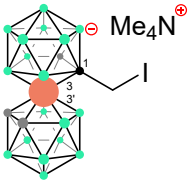

Prepared accordingly to General procedure **B**. Reaction time 72 h. Yield 93%. **^{1}H NMR** (600 MHz, Acetonitrile-d_3) δ 4.50 (dd, *J* = 38.0, 12.9 Hz, 2H), 4.09 (s, 1H), 3.92 (s, 2H), 3.06 (s, 12H); **^{11}B NMR** (193 MHz, Acetonitrile-d_3) δ 5.78 (2d, *J* = 148.9 Hz, 2B), 0.36 (d, *J* = 144.4 Hz, 2B), -7.21 (m, *overlap*, 8B), -12.82 (d, *J* = 159.9 Hz, 1B), -15.66 – -20.37 (2d, *overlap*, 4B), -23.79 (d, *J* = 178.4 Hz, 1B); **^{13}C NMR** (151 MHz, Acetonitrile-d_3) δ 58.16, 55.29 – 54.23 (m), 52.08, 50.33, 14.09; **HRMS**: *m/z* (ESI$^-$) 467.1859 (*M*$^-$, 11%), 464.1963 (100%), calc. 467.1870 and 464.1969.

[(1-I-$(CH_2)_2$-1,2-$C_2B_9H_{10}$)(1′,2′-$C_2B_9H_{11}$)-3,3′-Co]$^-$ Me_4N^+ (**4b**$^-$)

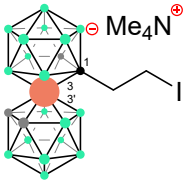

Prepared accordingly to General procedure **B**. Reaction time 24 h. Yield 94%. **^{1}H NMR** (600 MHz, Acetone-d_6) δ 4.15 (s, 1H), 3.81 (s, 1H), 3.70 (s, 1H), 3.46 (s, 12H), 3.39 – 3.33 (m, 1H), 3.33 – 3.27 (m, 1H), 3.19 – 3.17 (m, 1H), 2.92 (td, *J* = 12.9, 11.8, 2.8 Hz, 1H); **^{11}B NMR** (193 MHz, Acetone-d_6) δ 5.83 (d, *J* = 147.4 Hz, 2B), -0.12 (t, *J* = 125.1 Hz, 2B), -6.93 (m, *overlap*, 9B), -17.88 (m, *overlap*, 3B), -20.88 (d, *J* = 165.2 Hz, 1B), -24.16 (d, *J* = 170.9 Hz, 1B); **^{13}C NMR** (151 MHz, Acetone-d_6) δ 56.12, 55.62 – 54.35 (m), 52.77, 51.15, 44.57, 3.27; **HRMS**: *m/z* (ESI$^-$) 481.1992 (*M*$^-$, 11%), 478.2116 (100%), calc. 481.2017 and 478.2115.

[(1-I-$(CH_2)_3$-1,2-$C_2B_9H_{10}$)(1′,2′-$C_2B_9H_{11}$)-3,3′-Co]$^-$ Me_4N^+ (**4c**$^-$)

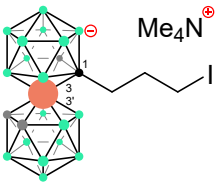

Prepared accordingly to General procedure **B**. Reaction time 4 h. Yield 91%. **^{1}H NMR** (600 MHz, Acetone-d_6) δ 4.09 (s, 1H), 3.73 (s, 1H), 3.68 (s, 1H), 3.46 (s, 12H), 3.26 (tt, *J* = 6.8, 2.2 Hz, 2H), 3.22 – 3.21 (m, 2H) 2.90 – 2.86 (m, 1H), 2.45 (dddd, *J* = 14.4, 10.8, 5.5, 1.8 Hz, 1H); **^{11}B NMR** (193 MHz, Acetone-d_6) δ 5.54 (t, *J* = 118.4 Hz, 2B), -0.23 (d, *J* = 142.7 Hz, 2B), -4.86 – -9.07 (m, *overlap*, 8B), -15.16 – -21.21 (m, *overlap*, 4B), -24.02 (d, *J* = 170.2 Hz, 1B); **^{13}C NMR** (151 MHz, Acetone-d_6) δ 56.94, 55.22, 53.11, 50.92, 45.25, 40.88, 34.30, 6.27; **HRMS**: *m/z* (ESI$^-$) 494.2212 (*M*$^-$, 7%), 492.2283 (100%), calc. 494.2215 and 492.2283.

[(1-(4-CH_3O-C_6H_4)-NH_2-$(CH_2)_3$-1,2-$C_2B_9H_{10}$)(1′,2′-$C_2B_9H_{11}$)-3,3′-Co]^0 (**7**)

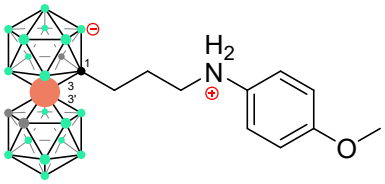

Prepared accordingly to General procedure C. Orange solid. Yield 71%. **^{1}H NMR** (600 MHz, Acetonitrile-d_3) δ 7.35 (d, *J* = 8.7 Hz, 2H), 7.08 (t, *J* = 8.9 Hz, 2H), 6.93 (d, *J* = 8.9 Hz, 2H), 3.91 (s, 1H), 3.66 (s, 1H), 3.54 (s, 1H), 3.30 (t, *J* = 7.1 Hz, 1H), 3.16 – 3.06 (m, 2H), 2.71 (s, 3H), 2.69 – 2.61 (m, 1H), 1.87 – 1.82 (m, 1H).**^{11}B NMR** (193 MHz, Acetone-d_6) δ 4.96 (d, *J* = 98.3 Hz, 2B), -0.29 (d, *J* = 133.1 Hz, 2B), -7.19 (overlap, 8B), -15.88 (d, *J* = 142.3 Hz, 1B), -17.45 (d, *J* = 163.5 Hz, 1B), -18.04 – -21.59 (overlap, 3B), -24.16 (d, *J* = 148.7 Hz, 1B); **^{13}C NMR** (151 MHz, Acetone-d_6) δ 114.69, 113.61, 57.01, 55.00, 53.15, 50.81, 44.10, 37.74, 30.71. **HRMS**: *m/z* (ESI$^-$) 490.3781 (*M*$^-$, 18%), 487.3855 (100%), calc. 490.3765 and 487.3848.

[(1-(3,4,5-$(CH_3O)_3$-C_6H_2)-NH_2-$(CH_2)_3$-1,2-$C_2B_9H_{10}$)(1′,2′-$C_2B_9H_{11}$)-3,3′-Co]^0 (**8**)

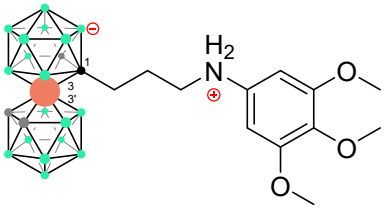

Prepared accordingly to General procedure C. Orange solid. Yield 70%. **^{1}H NMR** (600 MHz, Acetonitrile-d_3) δ 6.20 (s, 2H), 3.92 (s, 1H), 3.65 (s, 1H), 3.54 (s, 1H), 3.11 (qt, *J* = 12.7, 7.1 Hz, 2H), 2.70 – 2.63 (m, 1H), 2.48 (s, 9H), 2.27 – 2.20 (m, 1H), 1.86 – 1.79 (m, 2H); **^{11}B NMR** (193 MHz, Acetonitrile-d_3) δ 4.99 (d, *J* = 143.0 Hz, 2B), -0.29 (d, *J* = 149.4 Hz, 2B), -7.77 (4d, *overlap*, 8B), -15.13 – -21.67 (3d, *overlap*, 5B), -24.00 (d, *J* = 171.6 Hz, 1B); **^{13}C NMR** (151 MHz, Acetonitrile-d_3) δ 155.08, 95.89, 60.96, 57.91, 56.76, 54.29, 52.09, 48.33, 41.35, 37.85, 31.61, 30.33, 29.58, 14.36; **HRMS**: *m/z* (ESI^-) 550.3979 (M^-, 15%), 547.4065 (100%), calc. 550.3983 and 547.4061.

[(1-(4-CH_3-C_6H_4)-NH_2-$(CH_2)_3$-1,2-$C_2B_9H_{10}$)(1′,2′-$C_2B_9H_{11}$)-3,3′-Co]^0 (**9**)

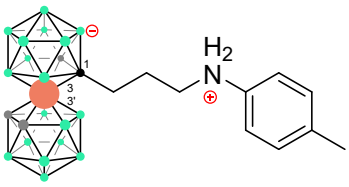

Prepared accordingly to General procedure C. Orange solid. Yield 62%. **^{1}H NMR** (600 MHz, Acetone-d_6) δ 6.89 (d, *J* = 8.0 Hz, 2H), 6.50 (d, *J* = 8.5 Hz, 2H), 4.69 (s, 2H), 4.02 (s, 1H), 3.68 (s, 1H), 3.63 (s, 1H), 3.53 – 3.45 (m, 3H), 3.11 – 3.00 (m, 2H), 2.50 – 2.42 (m, 2H), 1.90 – 1.81 (m, 2H).**^{11}B NMR** (193 MHz, Acetone-d_6) δ 5.03 (2d, *J* = 130.9 Hz, 2B), -0.31 (d, *J* = 142.7 Hz, 2B), -7.30 (m, *overlap*, 8B), -15.87 (d, *J* = 141.5 Hz, 2B), -17.43 (d, *J* = 161.4 Hz, 2B), -19.62 (m, *overlap*, 3B), -24.15 (d, *J* = 166.0 Hz, 1B); **^{13}C NMR** (151 MHz, Acetone-d_6) δ 129.46, 112.55, 57.05, 53.24, 50.85, 47.24, 43.42, 37.73, 30.70, 19.64, 8.55; **HRMS**: *m/z* (ESI^-) 474.3774 (M^-, 13%), 471.3895 (100%), calc. 474.3783 and 471.3891.

[(1-(4-NO_2-C_6H_4)-NH_2-$(CH_2)_3$-1,2-$C_2B_9H_{10}$)(1′,2′-$C_2B_9H_{11}$)-3,3′-Co]^0 (**10**)

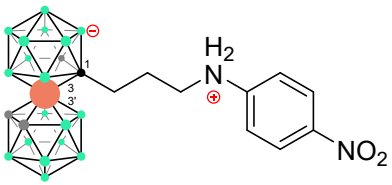

Prepared accordingly to General procedure C. Orange solid. Yield 55%. **^{1}H NMR** (600 MHz, Acetone-d_6) δ 8.02 (d, *J* = 9.3 Hz, 2H), 6.68 (d, *J* = 9.3 Hz, 2H), 4.03 (s, 1H), 3.66 (s, 1H), 3.61 (s, 1H), 3.26 – 3.21 (m, 2H), 2.48 (ddd, *J* = 14.4, 11.5, 4.9 Hz, 2H), 1.96 – 1.86 (m, 2H).**^{11}B NMR** (193 MHz, Acetone-d_6) δ 5.11 (d, *J* = 125.8 Hz, 2B), -0.28 (d, *J* = 144.3 Hz, 2B), -7.11 (m, *overlap*, 8B), -15.01 – -21.16 (m, *overlap*, 5B), -24.08 (d, *J* = 169.8 Hz, 1B); **^{13}C NMR** (151 MHz, Acetone-d_6) δ 126.11, 110.83, 57.14, 53.19, 50.83, 42.51 (d, *J* = 18.2 Hz), 37.41, 30.22, 29.54; **HRMS**: *m/z* (ESI^-) 505.3478 (M^-, 14%), 502.3586 (100%), calc. 505.3475 and 502.3592.

[(1-(2-Cl-6-CH_3-C_6H_3)-NH_2-$(CH_2)_3$-1,2-$C_2B_9H_{10}$)(1′,2′-$C_2B_9H_{11}$)-3,3′-Co]^0 (**11**)

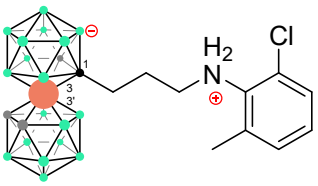

Prepared accordingly to General procedure C. Orange solid. Yield 59%. **^{1}H NMR** (600 MHz, Acetonitrile-d_3) δ 7.14 (dd, *J* = 8.0, 1.5 Hz, 1H), 7.02 (d, *J* = 6.8 Hz, 1H), 6.77 (t, *J* = 7.7 Hz, 1H), 6.24 – 5.91 (m, 2H), 3.88 (s, 1H), 3.57 (s, 1H), 3.52 (s, 1H), 3.03 – 2.95 (m, *J* = 6.6 Hz, 2H), 2.62 (ddd, *J* = 14.5, 10.7, 6.0 Hz, 1H), 2.26 (ddd, *J* = 14.6, 11.1, 5.8 Hz, 1H), 2.23 (s, 2H), 1.72 – 1.65 (m, 2H); **^{11}B NMR** (193 MHz, Acetonitrile-d_3) δ 4.88 (2d, *J* = 130.0 Hz, 2B), -0.28 (d, *J* = 120.6 Hz, 2B), -7.26 (m, *overlap*, 8B), -16.05 (d, *J* = 155.3 Hz, 1B), -17.51 (d, *J* = 160.1 Hz, 1B), -18.98 (d, *J* = 169.4 Hz, 2B), -20.62 (d, *J* = 163.5 Hz, 1B), -23.98 (d, *J* = 167.9 Hz, 1B); **^{13}C NMR** (151 MHz,

Acetonitrile-d_3) δ 130.05, 127.27, 121.95, 57.39, 53.62, 51.06, 46.97, 37.27, 31.81, 18.54. **HRMS**: *m/z* (ESI^-) 509.3381 (M^-, 10%), 505.3508 (100%), calc. 509.3402 and 505.3504.

[(1,7'-μ-CH_2CH_2)-(1,2-$C_2B_9H_{10}$)(1',2'-$C_2B_9H_{10}$)-3,3'-Co]$^-Me_4N^+$ (Me_4N**15a**)

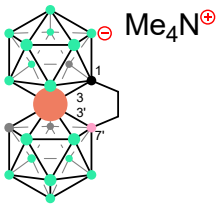

^{1}H NMR (600 MHz, Acetone-d_6) δ 4.40 (s, 1H), 4.07 (s, 1H), 4.04 (s, 1H), 3.47 (s, 12H), 2.81 (dt, *J* = 14.5, 6.1 Hz, 1H), 2.42 – 2.47 (m, 1H), 1.66 – 1.52 (m, 1H), 1.08 (dt, *J* = 14.2, 5.7 Hz, 1H); **^{11}B NMR** (193 MHz, Acetone-d_6) δ 7.95 (s, 1B), 6.12 (d, *J* = 147.3 Hz, 1B), 4.95 (d, *J* = 142.4 Hz, 1B), -1.07 (d, *J* = 148.1 Hz, 1B), -2.52 (d, *J* = 148.1 Hz, 1B), -3.31 (d, *J* = 148.1 Hz, 1B), -4.87 (d, *J* = 148.1 Hz, 1B), -5.59 (d, *J* = 148.1 Hz, 1B), -7.79, -8.22 (2d, *overlap*, 3B), -11.01 (d, *J* = 151.7 Hz, 1B), -12.85 (d, *J* = 151.7 Hz, 1B),-16.91 (t, *J* = 153.0 Hz, 2B), -20.90 (d, *J* = 153.0 Hz, 2B), -23.34 (d, *J* = 168.5 Hz, 1B); **^{13}C NMR** (151 MHz, Acetone-d_6) δ 61.69 (1C), 55.22 (4C), 49.63 (1C), 45.41 (1C); **HRMS**: *m/z* (ESI^-) 353.2868 (M^-, 10%), 350.2982 (100%), calc. 353.3002 and 350.2932.

[(1,8'-μ-CH_2CH_2)-(1,2-$C_2B_9H_{10}$)(1',2'-$C_2B_9H_{10}$)-3,3'-Co]$^-Me_4N^+$(Me_4N**15b**)

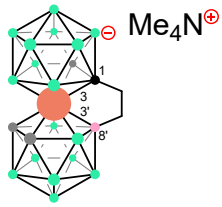

^{1}H NMR (600 MHz, Acetone-d_6) δ 4.89 (s, 1H), 4.17 (s, 1H), 4.12 (s, 1H), 3.43 (s, 12H), 2.65 (dt, *J* = 14.5, 6.1 Hz, 1H), 2.59 – 2.52 (m, 1H), 1.51 – 1.43 (m, 1H), 0.98 (dt, *J* = 14.2, 5.7 Hz, 1H); **^{11}B NMR** (193 MHz, Acetone-d_6) δ 20.80 (s, 1B), 1.47 (d, *J* = 147.3 Hz, 1B), -1.03 (d, *J* = 142.4 Hz, 1B), -2.77 (d, *J* = 148.1 Hz, 2B), -6.16 – -8.75 (m, *overlap*, 6B), -12.56 (d, *J* = 151.7 Hz, 2B), -16.48 (2d, *J* = 153.0 Hz, 2B), -18.71 (2d, *J* = 162.1 Hz, 2B), -26.13 (d, *J* = 168.5 Hz); **^{13}C NMR** (151 MHz, Acetone-d_6) δ 60.61, 55.40 – 55.08 (m), 49.74; **HRMS**: *m/z* (ESI^-) 353.2885 (M^-, 10%), 350.2998 (100%), calc. 353.2890 and 350.2999.

[(1-C_6H_5N-$(CH_2)_3$-1,2-$C_2B_9H_{10}$)(1',2'-$C_2B_9H_{11}$)-3,3'-Co]^0 (**16**)

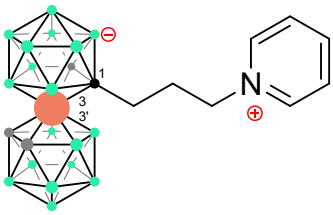

^{1}H NMR (600 MHz, Acetonitrile-d_3) δ 8.61 (t, *J* = 5.5 Hz, 2H), 8.46 (d, *J* = 7.9 Hz, 1H), 7.97 (t, *J* = 7.0 Hz, 2H), 4.40 (t, *J* = 7.3 Hz, 2H), 3.90 (s, 1H), 3.72 (s, 1H), 3.53 (s, 1H), 2.77 – 2.70 (m, 2H), 2.25 – 2.17 (m, 2H), 1.95 – 1.93 (m, 1H), 1.90 – 1.88 (m, 1H); **^{11}B NMR** (193 MHz, Acetonitrile-d_3) δ 5.29 (d, *J* = 144.7 Hz, 2B), -0.25 (d, *J* = 153.6 Hz, 2B), -4.49 – -10.89 (m, *overlap*, 8B), -14.95 – -21.52 (m, overlap, 5B), -24.03 (d, *J* = 173.9 Hz, 1B); **^{13}C NMR** (151 MHz, Acetonitrile-d_3) δ 145.92, 144.54, 128.53, 61.13, 57.00, 53.12, 51.24, 36.14, 32.09, 29.50; **HRMS**: *m/z* (ESI^-) 446.3646 (M^-, 21%), 443.3580 (100%), calc. 446.3496 and 443.3584.

[(1-CH_2=$CHCH_2$-1,2-$C_2B_9H_{10}$)(1',2'-$C_2B_9H_{11}$)-3,3'-Co]$^-$ (**17**$^-$)

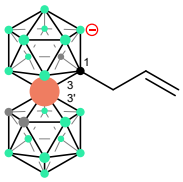

HRMS: *m/z* (ESI^-) 367.3051 (M^-, 14%), 364.3148 (100%), calc. 367.3062 and 364.3159.

[(1-$(CH_3)_3N$-$(CH_2)_3$-1,2-$C_2B_9H_{10}$)(1',2'-$C_2B_9H_{11}$)-3,3'-Co]^0 (**18**)

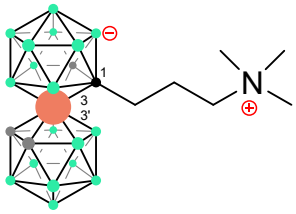

^{1}H NMR (600 MHz, Acetonitrile-d_3) δ 3.94 (s, 1H), 3.72 (s, 1H), 3.59 (s, 1H), 3.11 (td, *J* = 12.1, 11.6, 5.3 Hz, 1H), 3.04 (dt, *J* = 12.6, 6.8 Hz, 1H), 2.95 (s, 9H), 2.67 (ddd, *J* = 15.3, 10.2, 6.1 Hz, 2H), 2.21 – 2.16 (m, 2H); **^{11}B NMR** (193 MHz, Acetonitrile-d_3) δ 5.34 (d, *J* = 148.6 Hz, 2B), -0.17 (dd, *J* = 145.2Hz, 2B), -5.00 – -9.11 (m, *overlap*, 8B), -14.59 – -21.94 (m, *overlap*, 5B), -23.94 (d, *J* = 167.6 Hz, 1B); **^{13}C NMR** (151 MHz, Acetonitrile-d_3) δ 65.65, 57.33, 53.31, 53.03, 51.23, 36.06, 24.14; **HRMS**: *m/z* (ESI$^-$) 427.3263 (*M*$^-$, 16%), 424.3361 (100%), calc. 427.3884 and 424.3974.

[(1,7-*μ*-CH_2CH_2-1,2-$C_2B_9H_{10}$)$_2$-3,3'-Co]$^-$$Me_4N^+$ (**20a**)

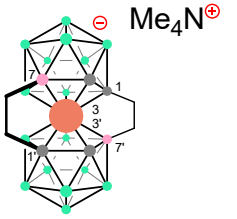

^{1}H NMR (600 MHz, Acetone-d_6) δ 4.56 (s, 2H), 3.43 (s, 12H), 2.45 – 2.42 (m, 4H), 1.66 – 1.52 (m, 2H), 0.99-095 (m, 2H); **^{11}B NMR** (193 MHz, Acetone-d_6) δ 7.19 (s, 2B), 5.43 (d, *J* = 147.3 Hz, 2B), -3.48 (d, *J* = 142.4 Hz, 2B), -4.70 (d, *J* = 148.1 Hz, 4B), -11.19 (d, *J* = 148.1 Hz, 2B), -15.48 (d, *J* = 148.1 Hz, 2B), -16.27 (d, *J* = 148.1 Hz, 1B), -20.28 (d, *J* = 153.0 Hz, 2B); **^{13}C NMR** (151 MHz, Acetone-d_6) δ 61.28 (2C), 55.21 (4C), 45.52 (2C); **HRMS**: *m/z* (ESI$^-$) 379.3040 (*M*$^-$, 10%), 376.3145 (100%), calc. 379.3059 and 376.3154.

[(1,8-*μ*-CH_2CH_2-1,2-$C_2B_9H_{10}$)$_2$-3,3'-Co]$^-$$Me_4N^+$ (**20b**)

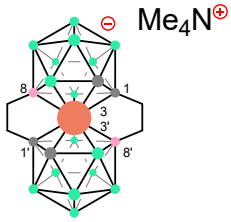

^{1}H NMR (600 MHz, Acetone-d_6) δ 4.73 (s, 2H), 3.42 (s, 12H), 2.40 – 2.78 (m, 4H), 1.83 – 1.69 (m, 2H), 0.90-086 (m, 2H); **^{11}B NMR** (193 MHz, Acetone-d_6) δ 19.88 (s, 2B), -4.10, -4.53 (2d, overlap, 4B), -7.09 (d, *J* = 142.4 Hz, 2B), -9.59 (d, *J* = 148.1 Hz, 2B), -11.60 (2d, *J* = 148.1 Hz, 4B), -15.62 (d, *J* = 148.1 Hz, 2B), -23.60 (d, *J* = 148.1 Hz, 1B); **^{13}C NMR** (151 MHz, Acetone-d_6) δ 63.28 (2C), 55.21 (4C), 49.21 (2C); **HRMS**: *m/z* (ESI$^-$) 379.3041 (*M*$^-$, 10%), 376.3152 (100%), calc. 379.3059 and 376.3154.

NMR spectra

*Figure S8. ^{1}H NMR spectrum of **3a**$^{-}$.*

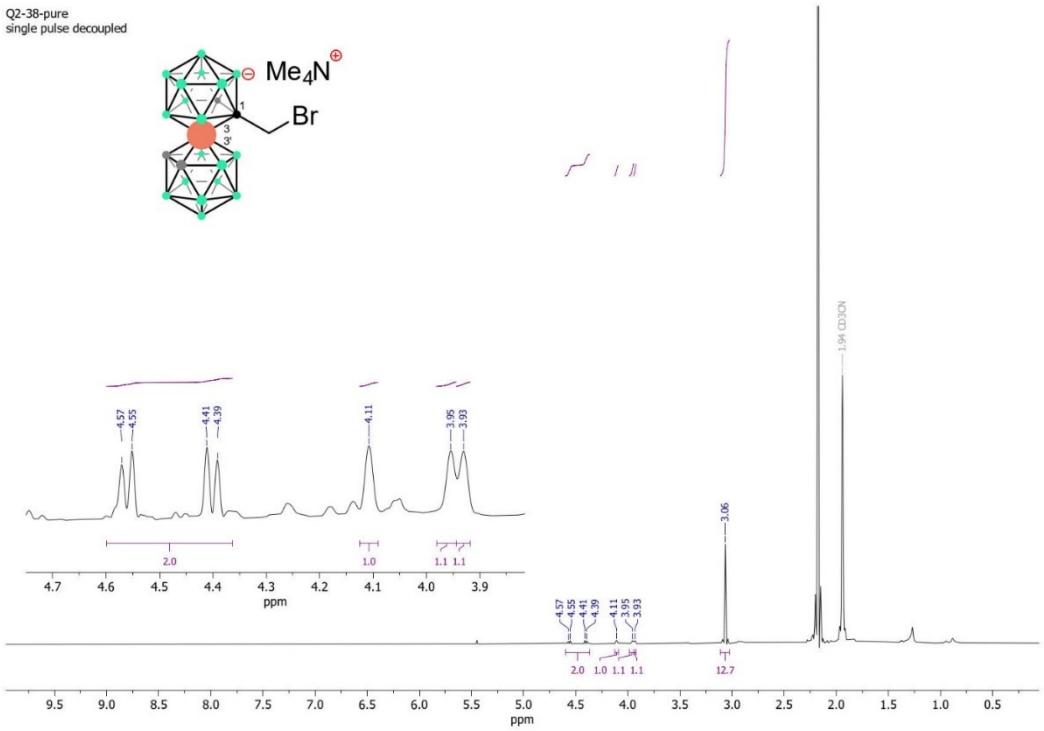

*Figure S9. $^{1}H\{^{11}B\}$ NMR spectrum of **3a**$^{-}$.*

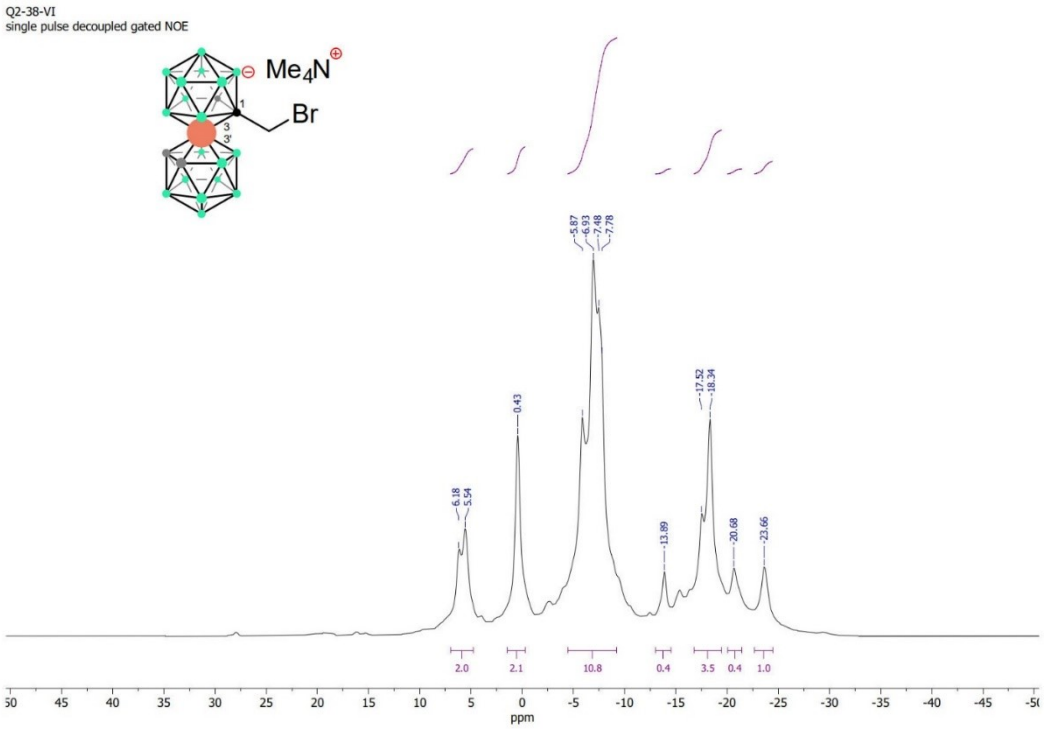

*Figure S10. ^{11}B NMR spectrum of **3a**$^-$.*

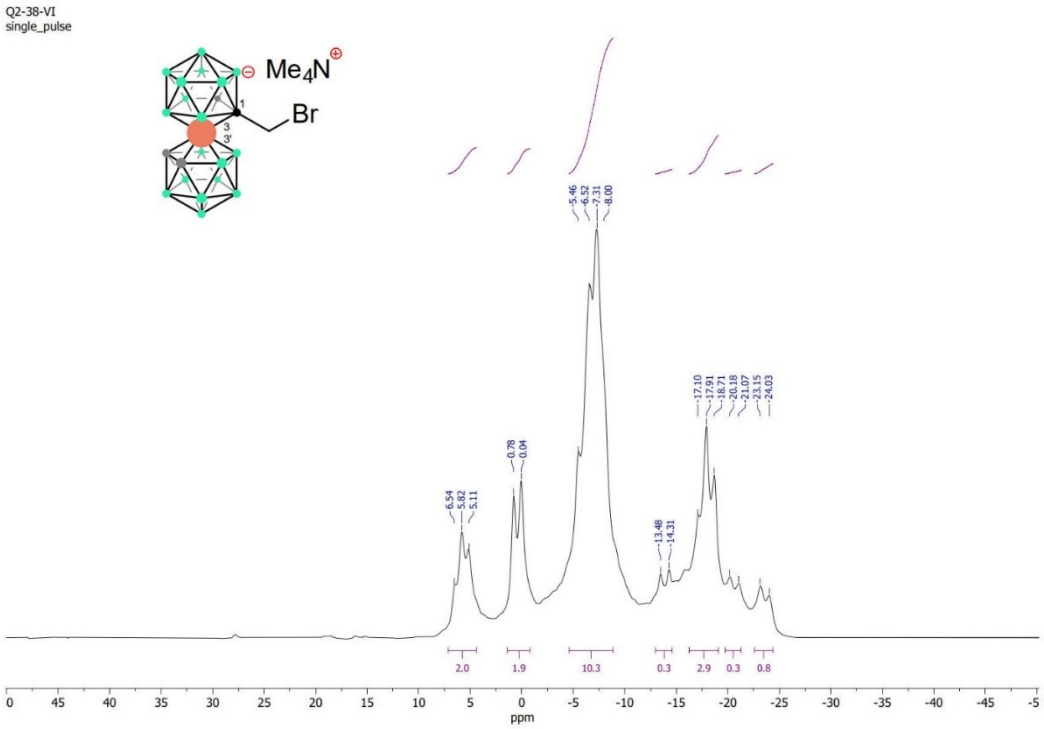

*Figure S11. ^{13}C NMR spectrum of **3a**$^-$.*

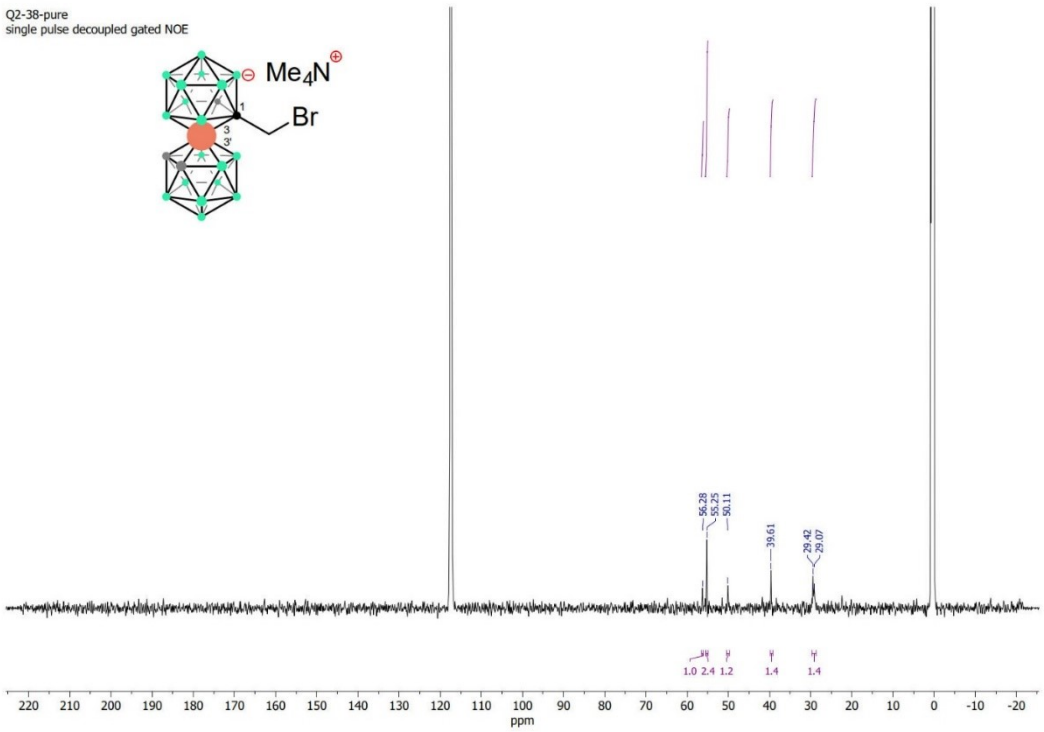

*Figure S12. ^{1}H NMR spectrum of **3b**$^{-}$.*

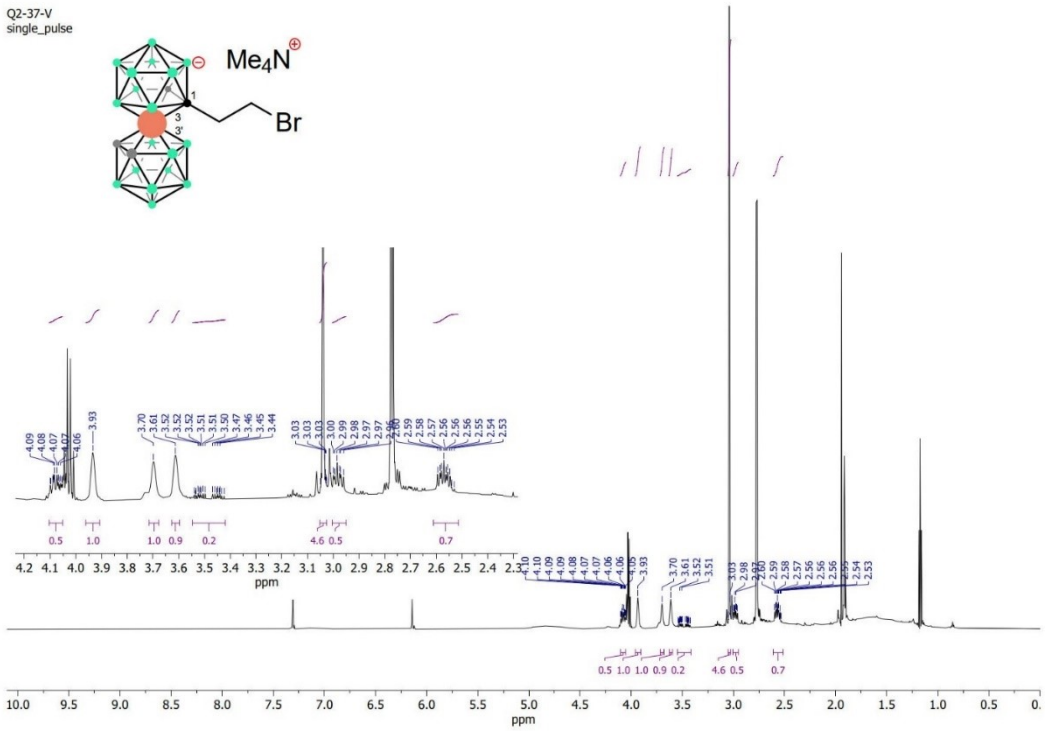

*Figure S13. $^{1}H\{^{11}B\}$ NMR spectrum of **3b**$^{-}$.*

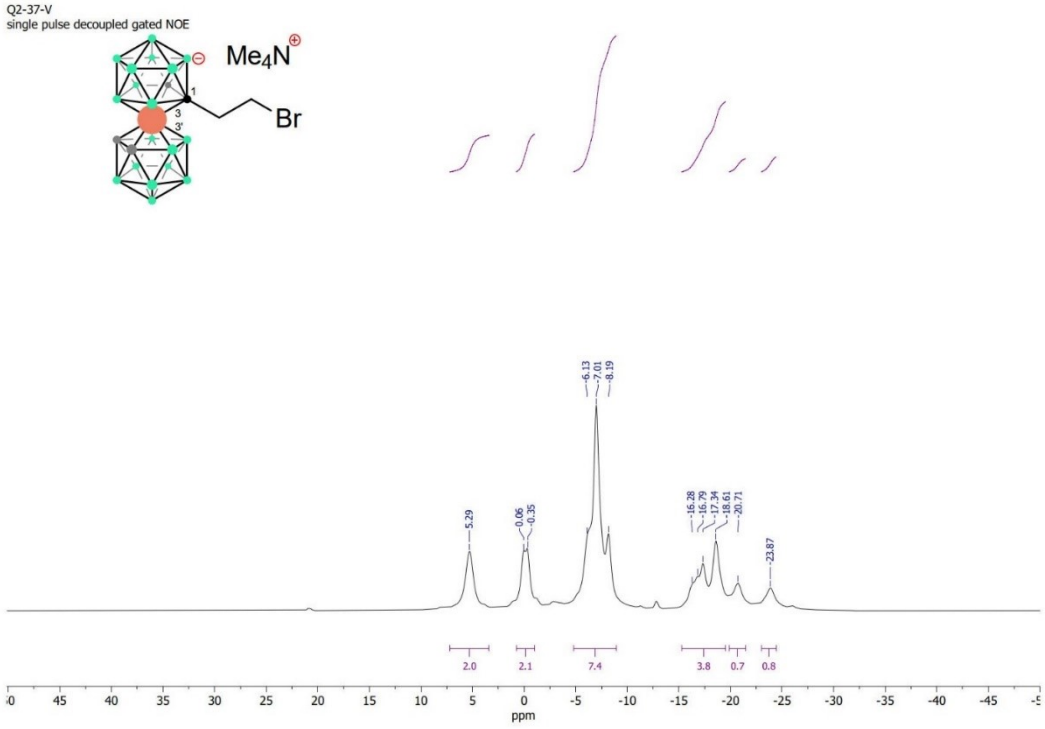

*Figure S14. ^{11}B NMR spectrum of **3b**$^{-}$.*

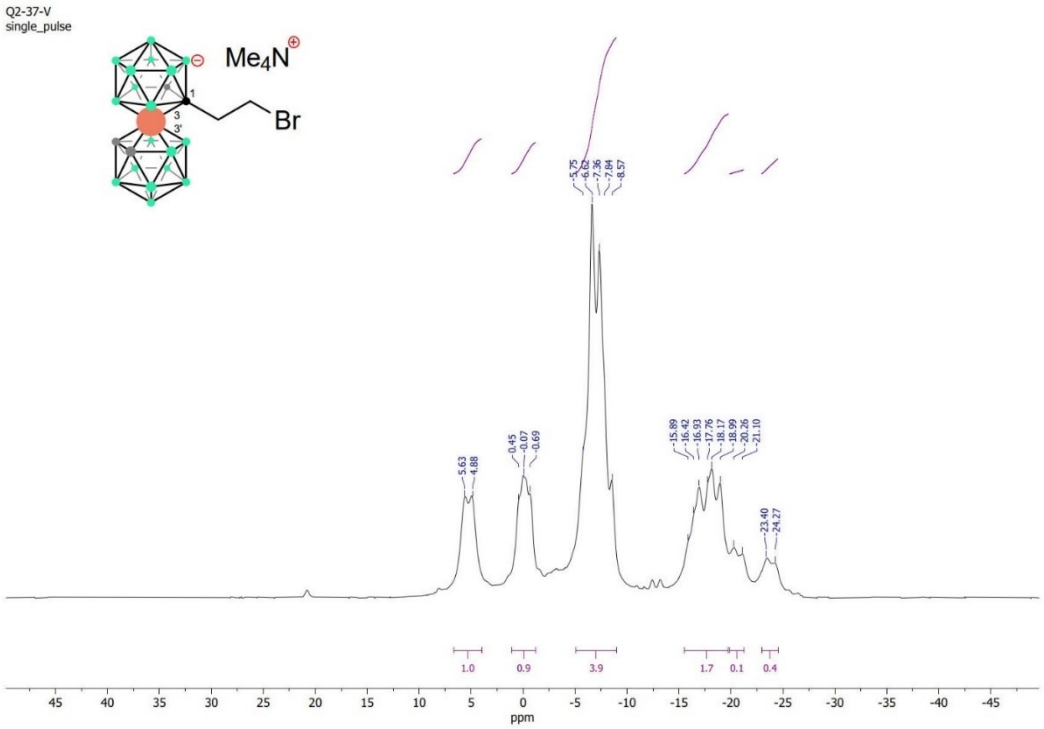

*Figure S15. ^{13}C NMR spectrum of **3b**$^{-}$.*

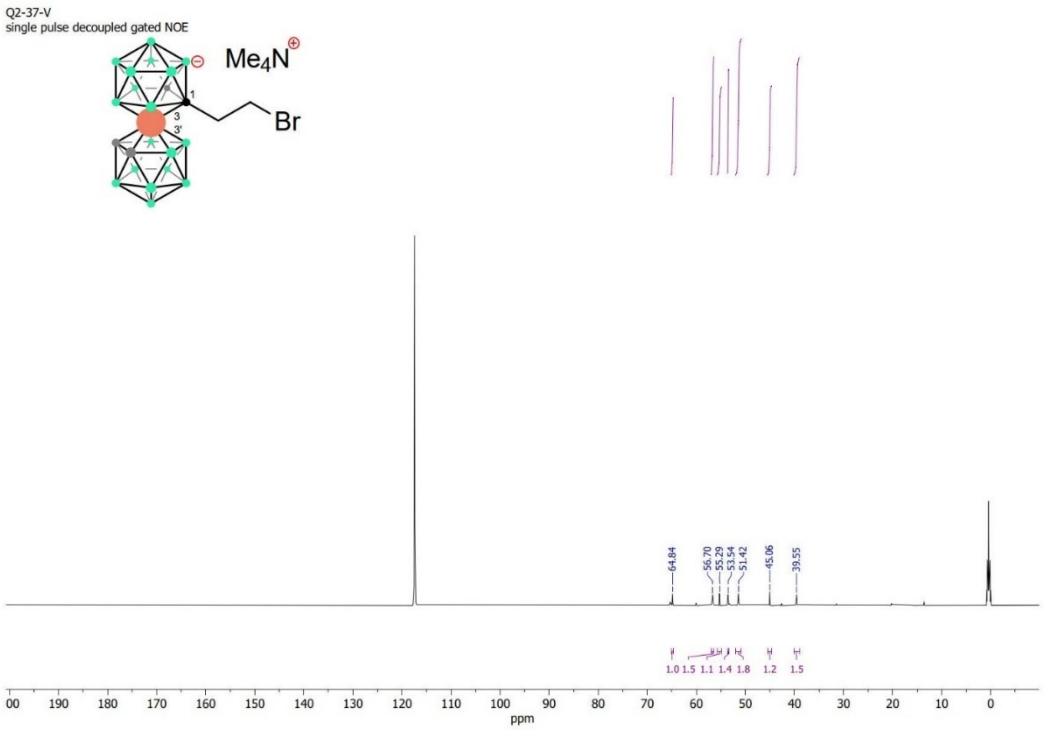

*Figure S16. ^{1}H NMR spectrum of **3c**$^{-}$.*

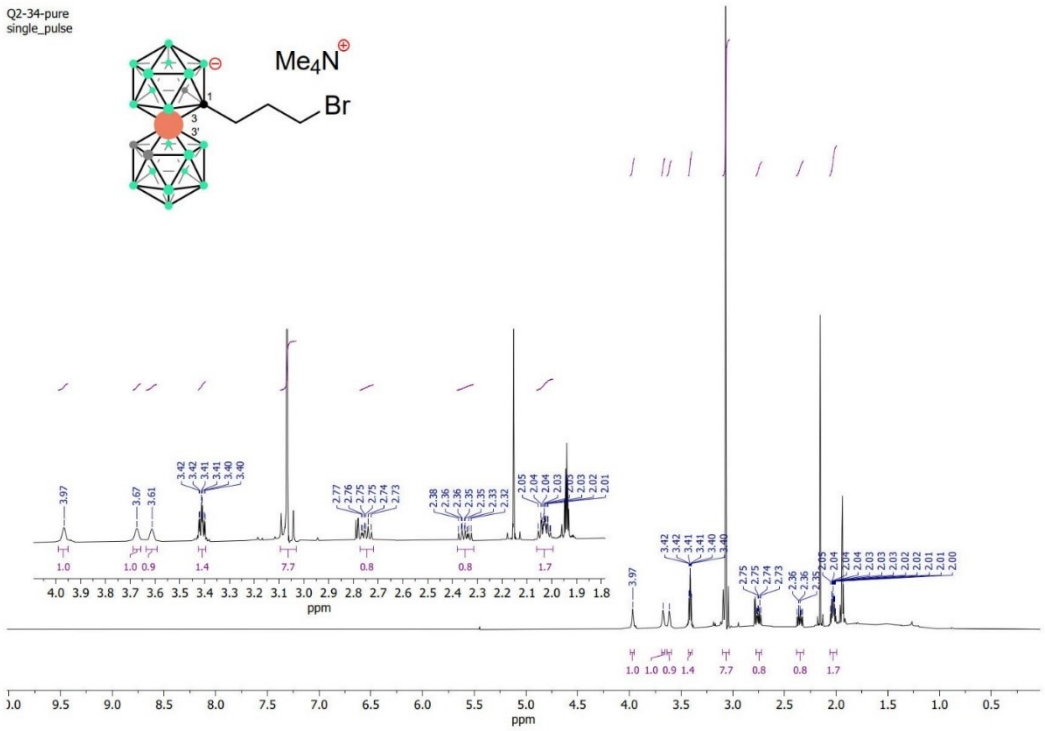

*Figure S17. $^{1}H\{^{11}B\}$ NMR spectrum of **3c**$^{-}$.*

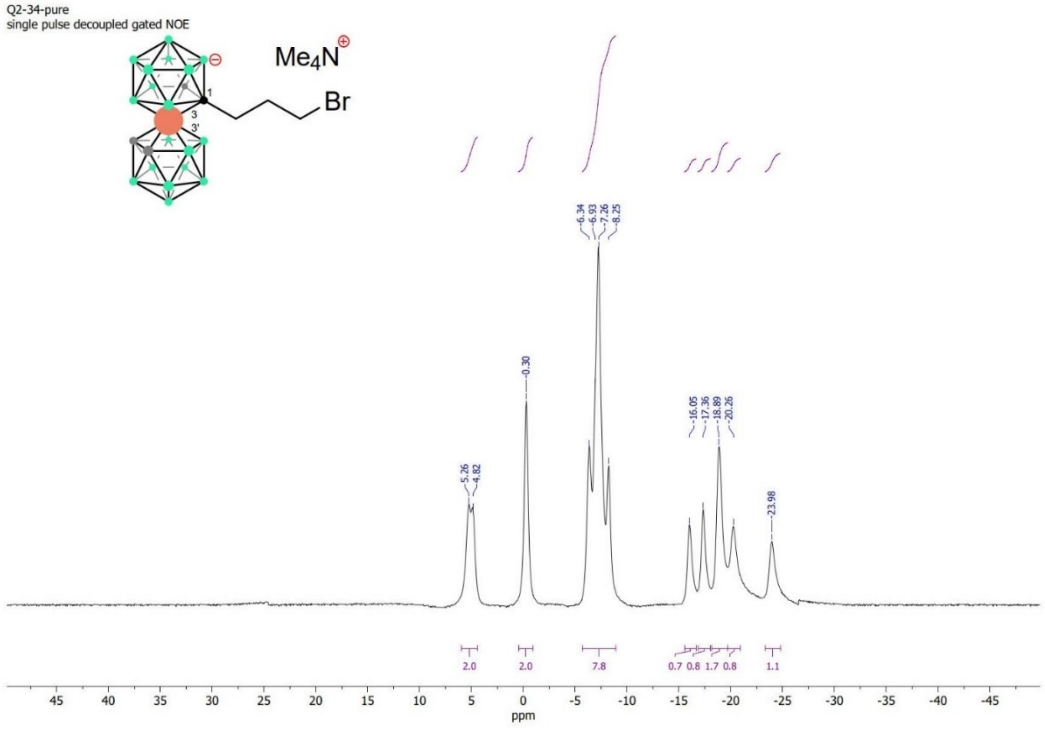

*Figure S18. ^{11}B NMR spectrum of **3c**$^{-}$.*

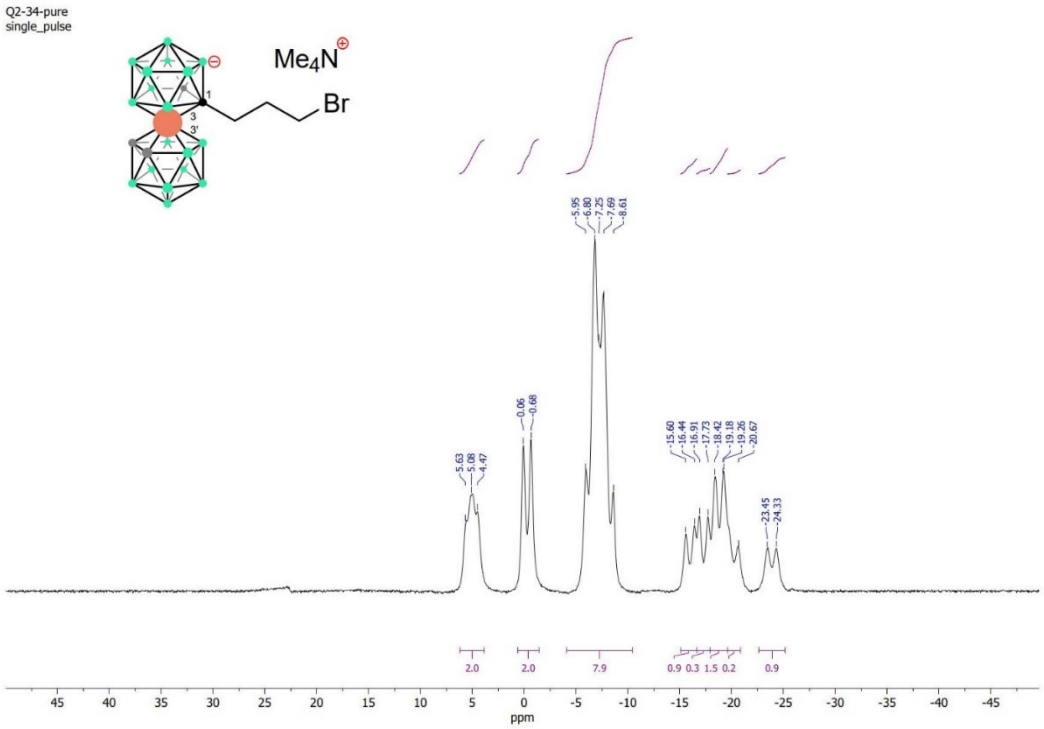

*Figure S19. ^{13}C NMR spectrum of **3c**$^{-}$.*

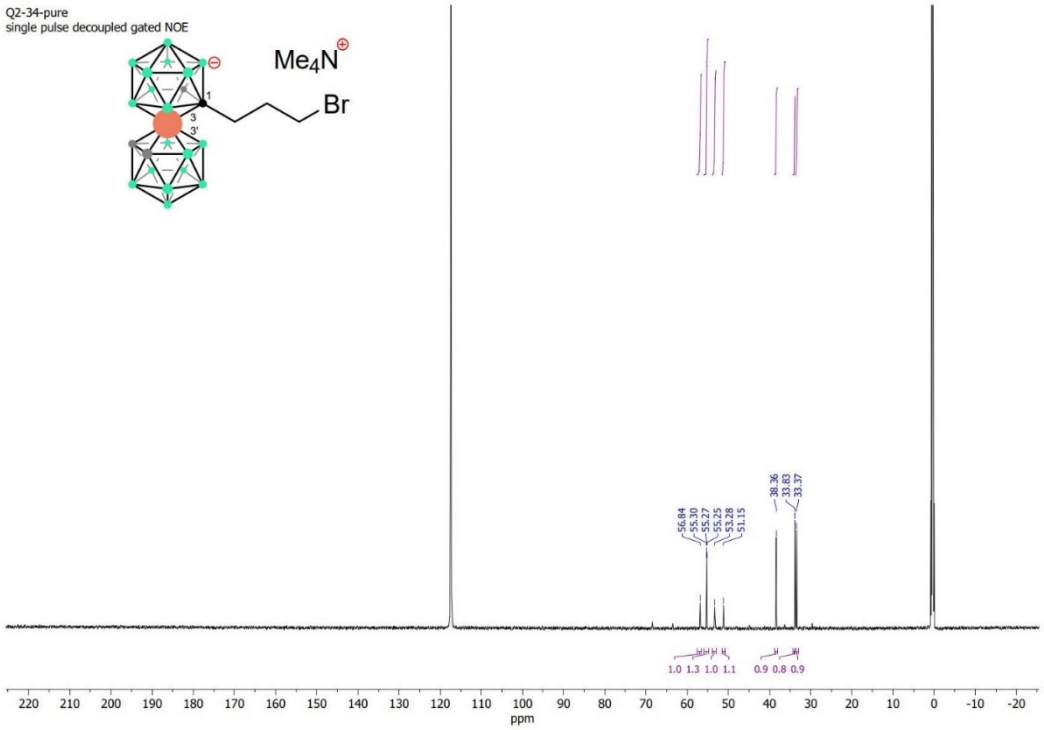

*Figure S20. ^{1}H NMR spectrum of **4a**$^{-}$.*

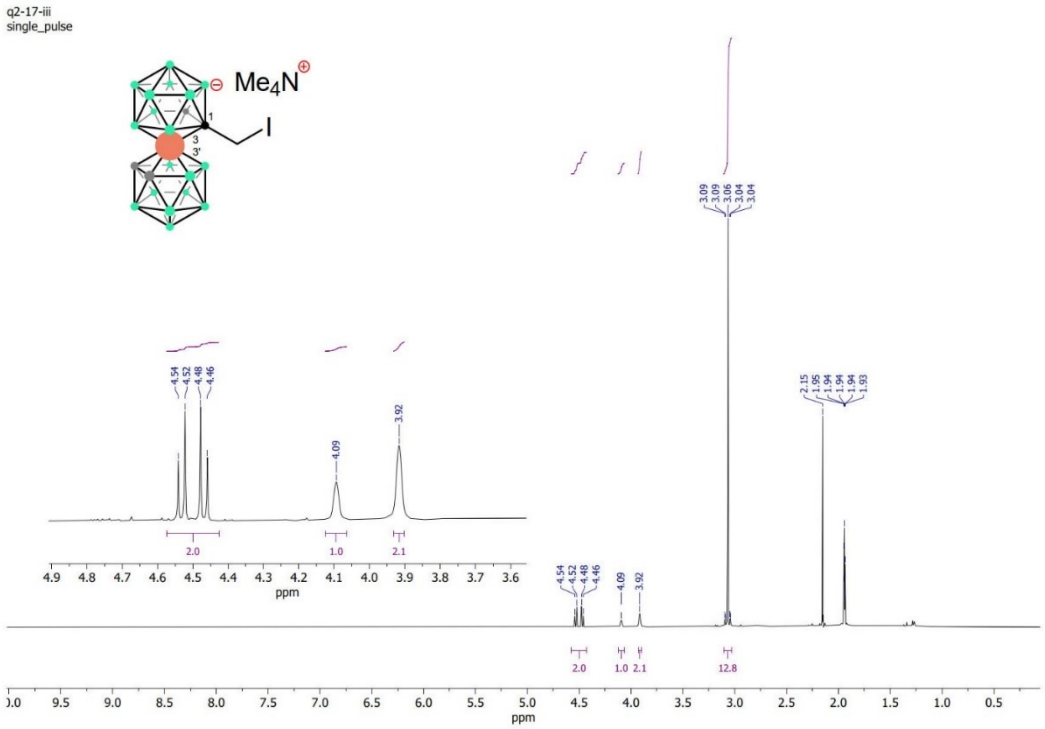

*Figure S21. $^{1}H\{^{11}B\}$ NMR spectrum of **4a**$^{-}$.*

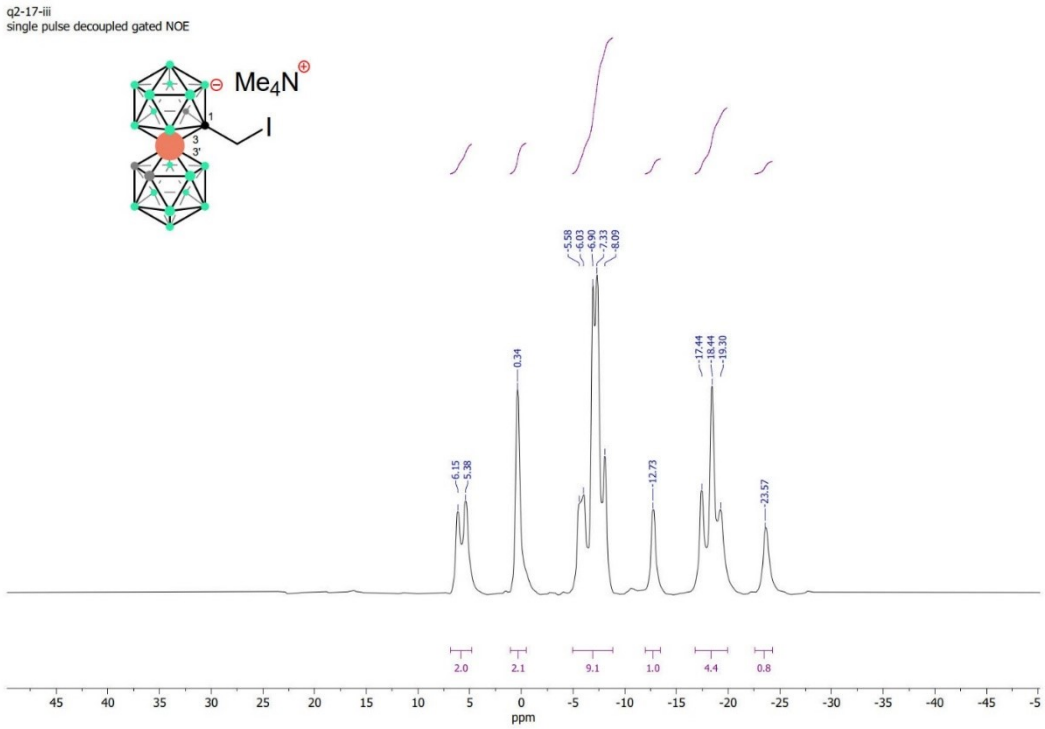

*Figure S22. ^{11}B NMR spectrum of **4a**$^-$.*

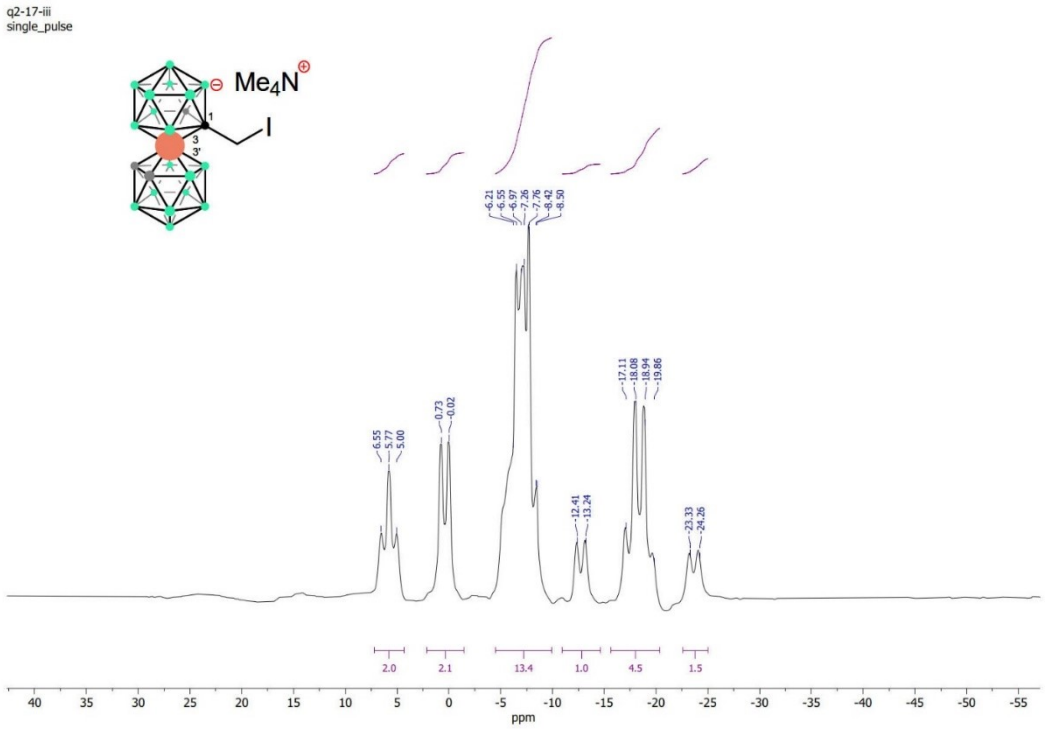

*Figure S23. ^{13}C NMR spectrum of **4a**$^-$.*

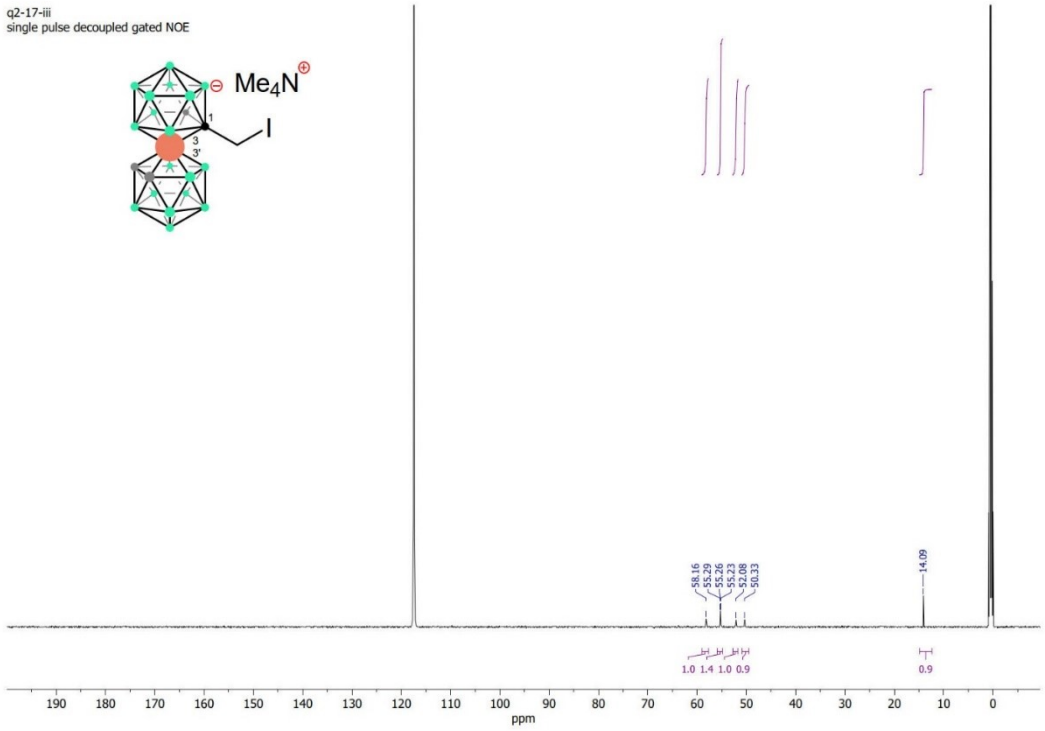

*Figure S24. ^{1}H NMR spectrum of **4b**$^{-}$.*

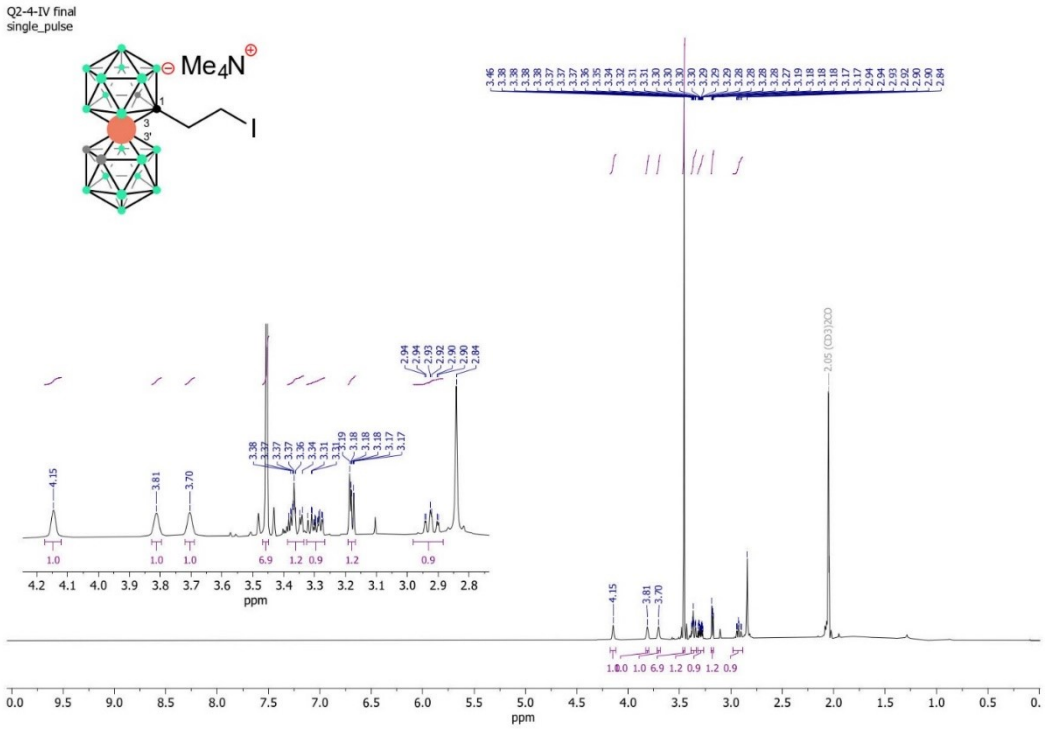

*Figure S25. $^{1}H\{^{11}B\}$ NMR spectrum of **4b**$^{-}$.*

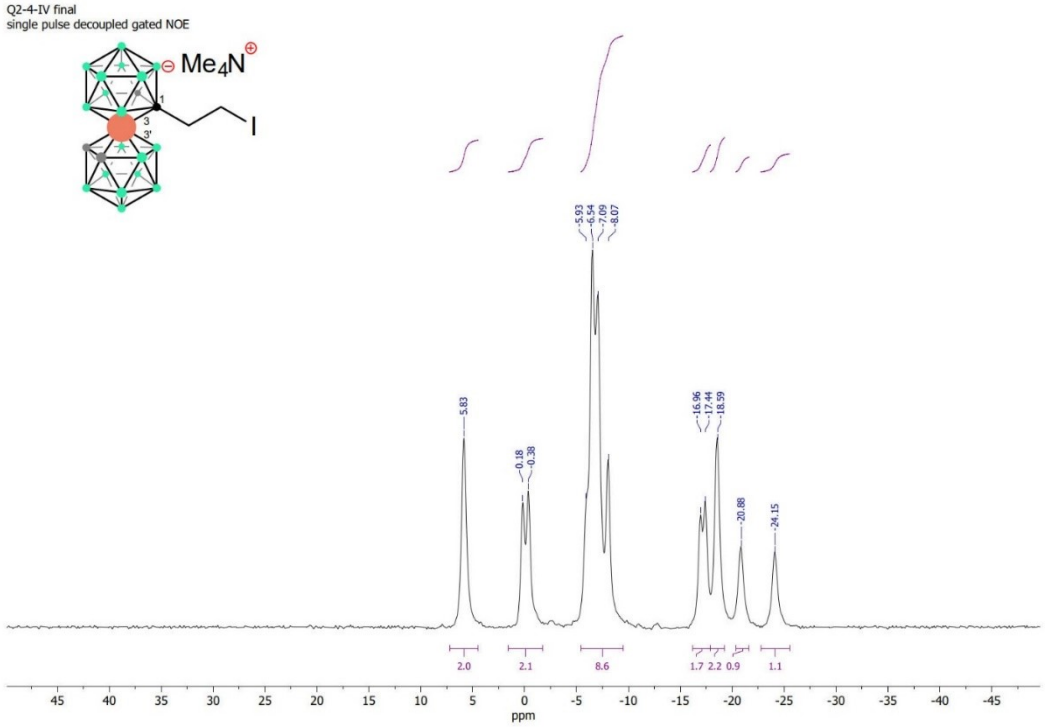

*Figure S26. ^{11}B NMR spectrum of **4b**$^-$.*

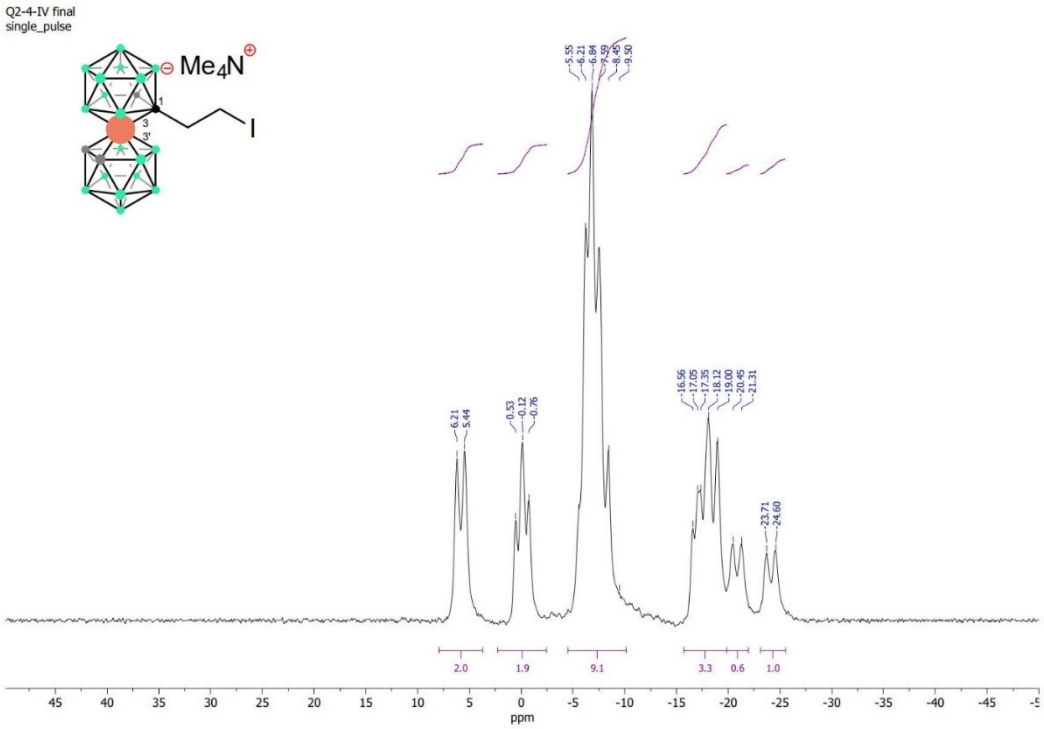

*Figure S27. ^{13}C NMR spectrum of **4b**$^-$.*

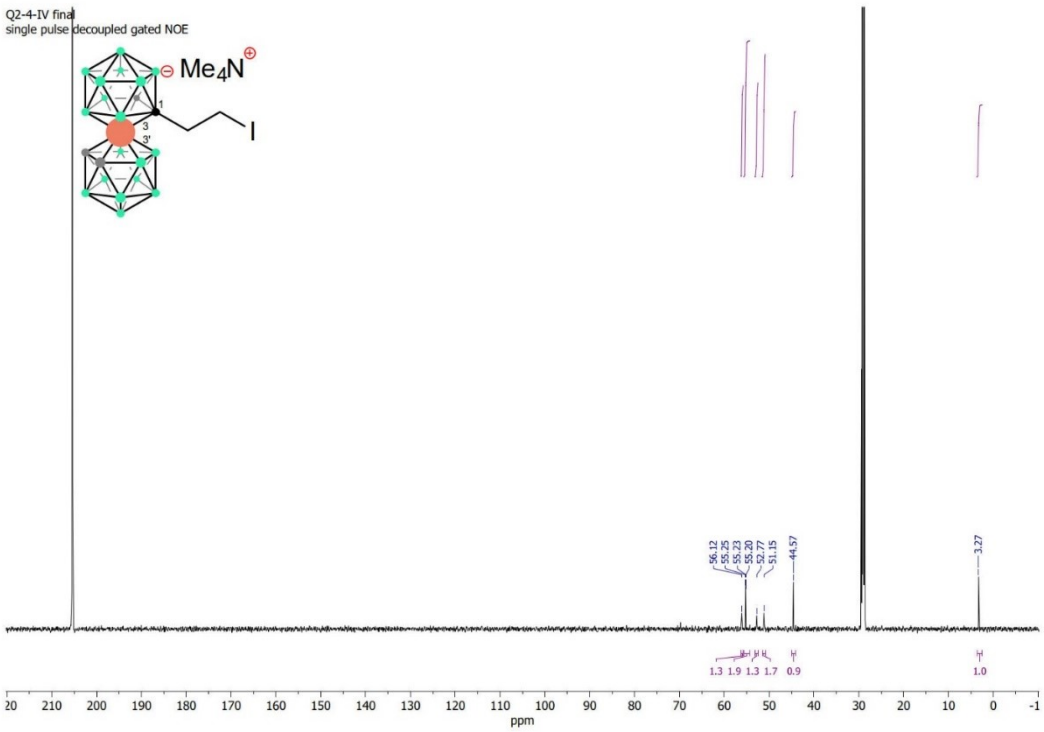

*Figure S28. ^{1}H NMR spectrum of **4c**$^{-}$.*

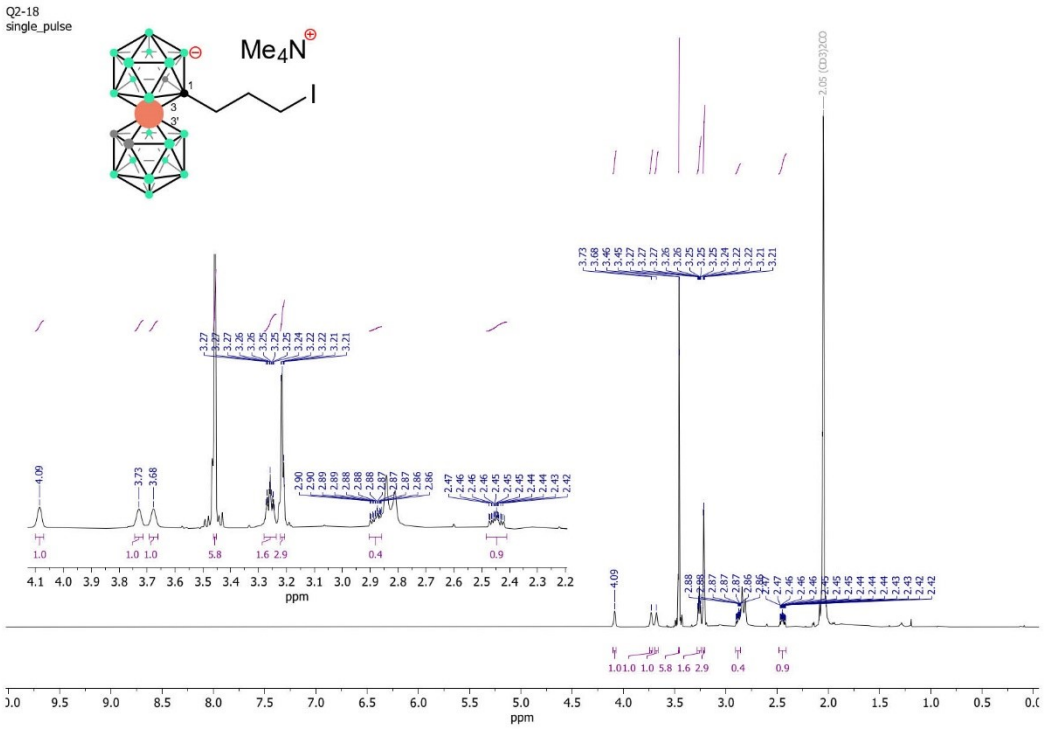

*Figure S29. $^{1}H\{^{11}B\}$ NMR spectrum of **4c**$^{-}$.*

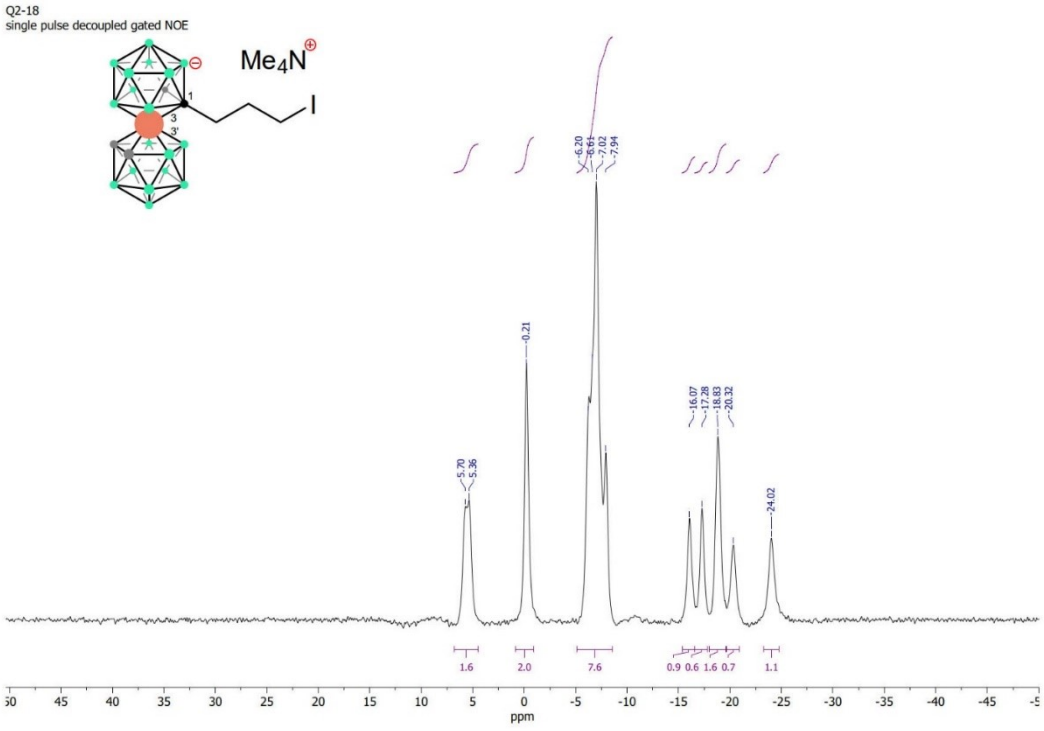

*Figure S30. ^{11}B NMR spectrum of **4c**$^-$.*

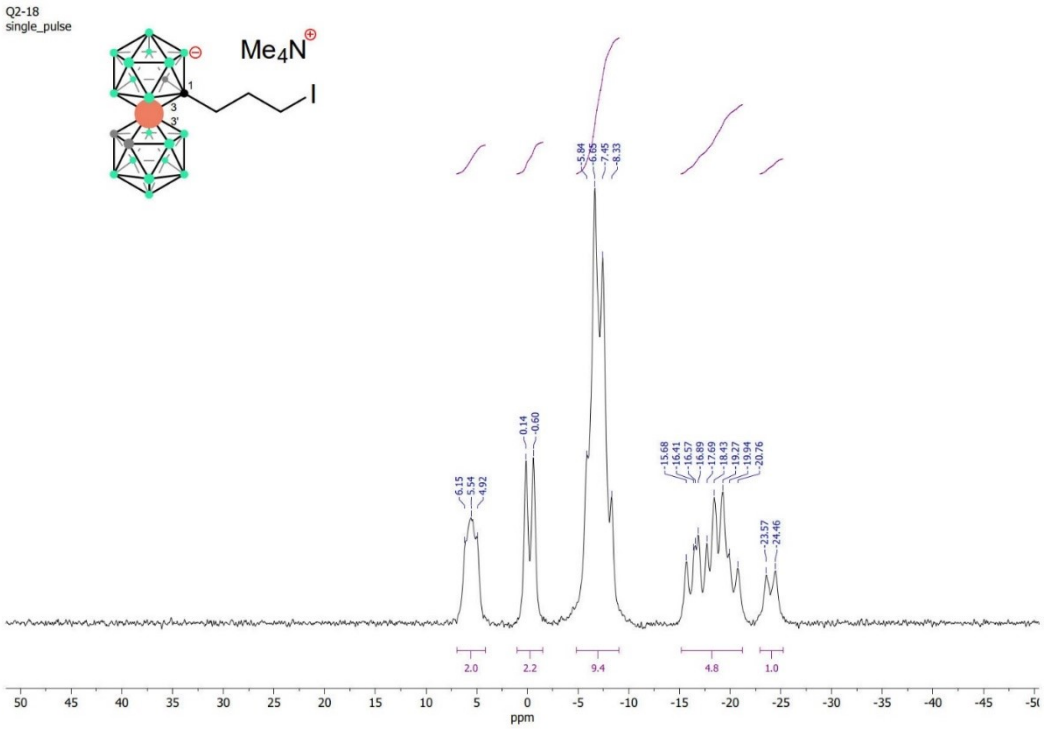

*Figure S31. ^{13}C NMR spectrum of **4c**$^-$.*

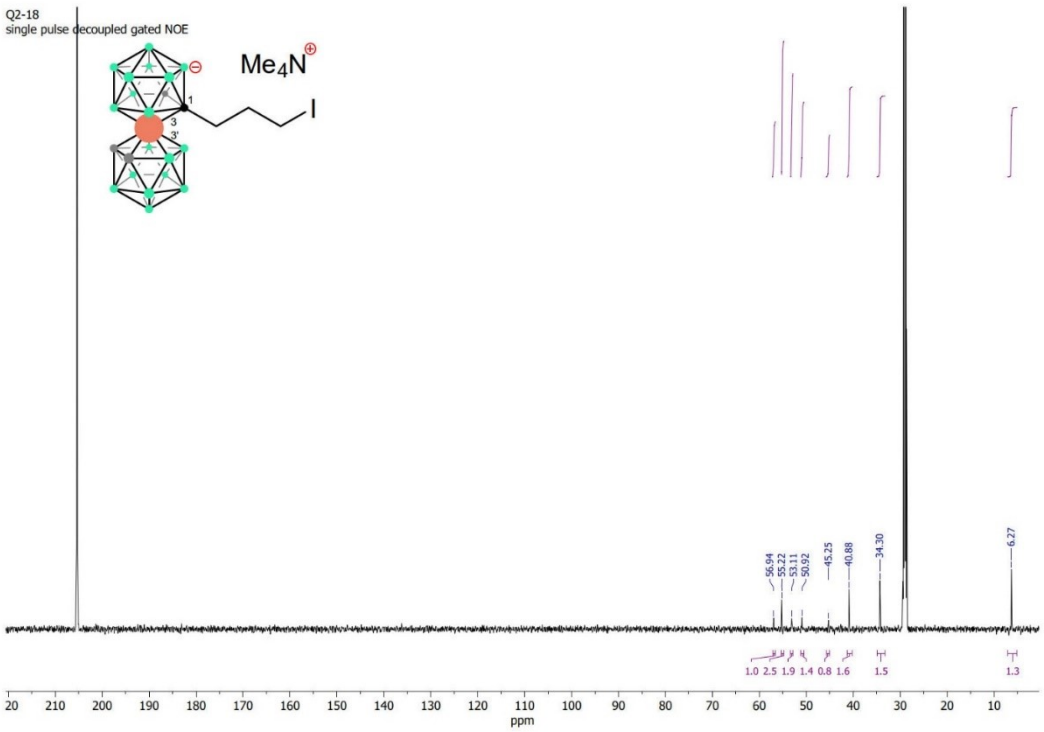

*Figure S32. ^{1}H NMR spectrum of **7**.*

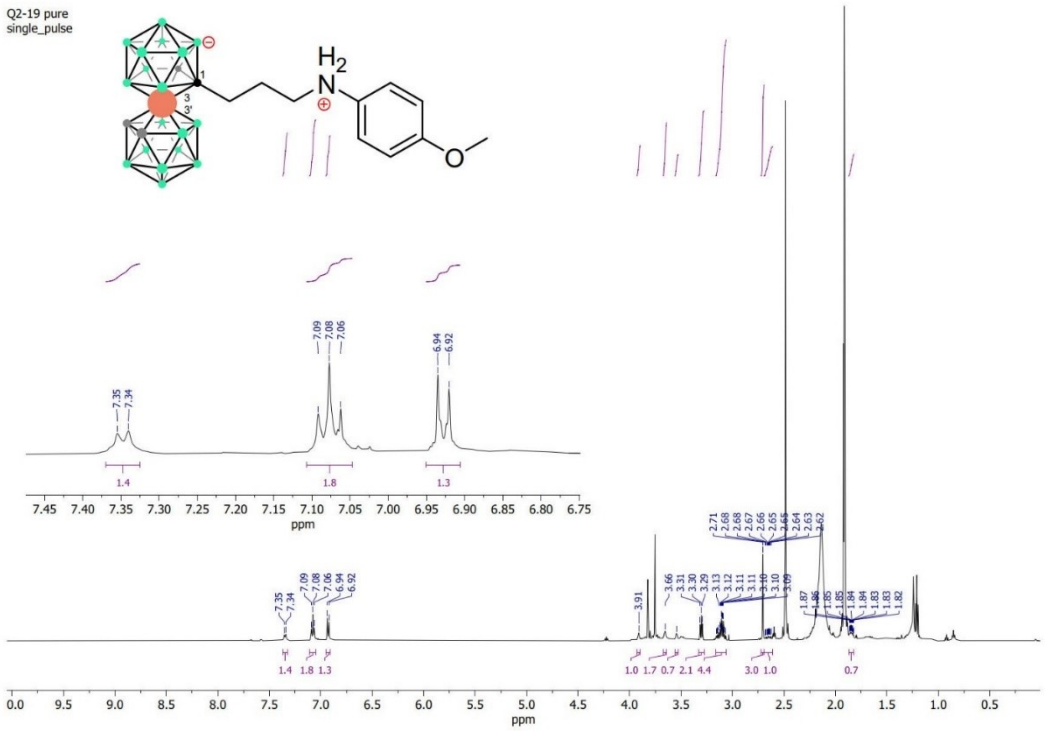

*Figure S33. $^{1}H\{^{11}B\}$ NMR spectrum of **7**.*

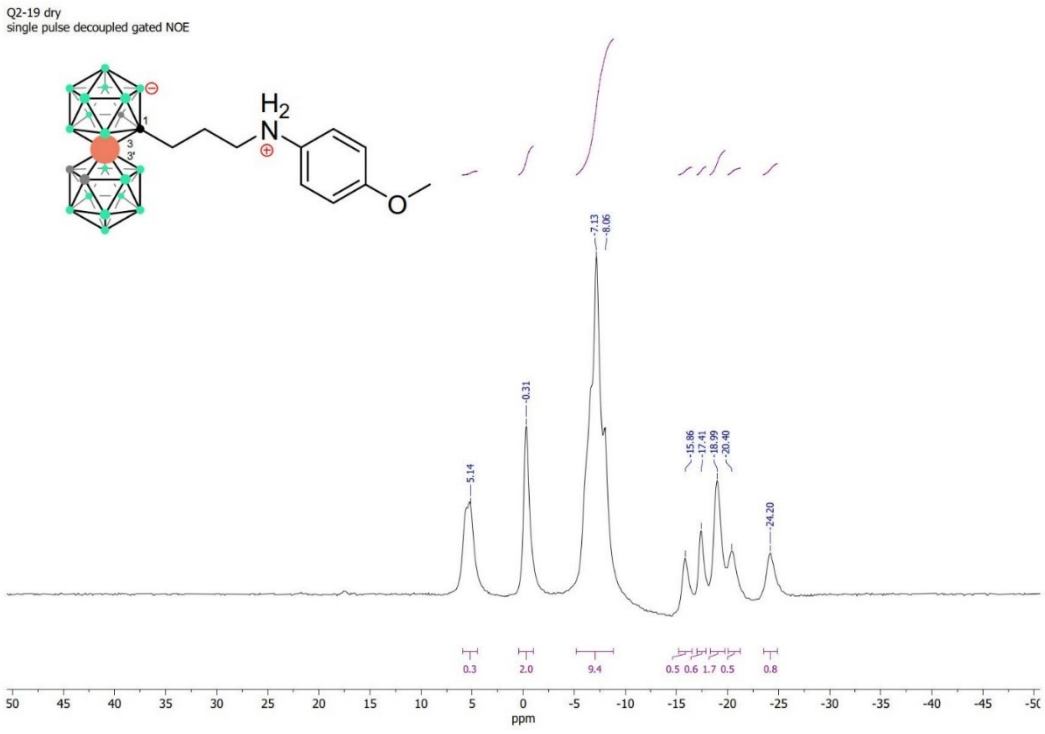

*Figure S34. ^{11}B NMR spectrum of **7**.*

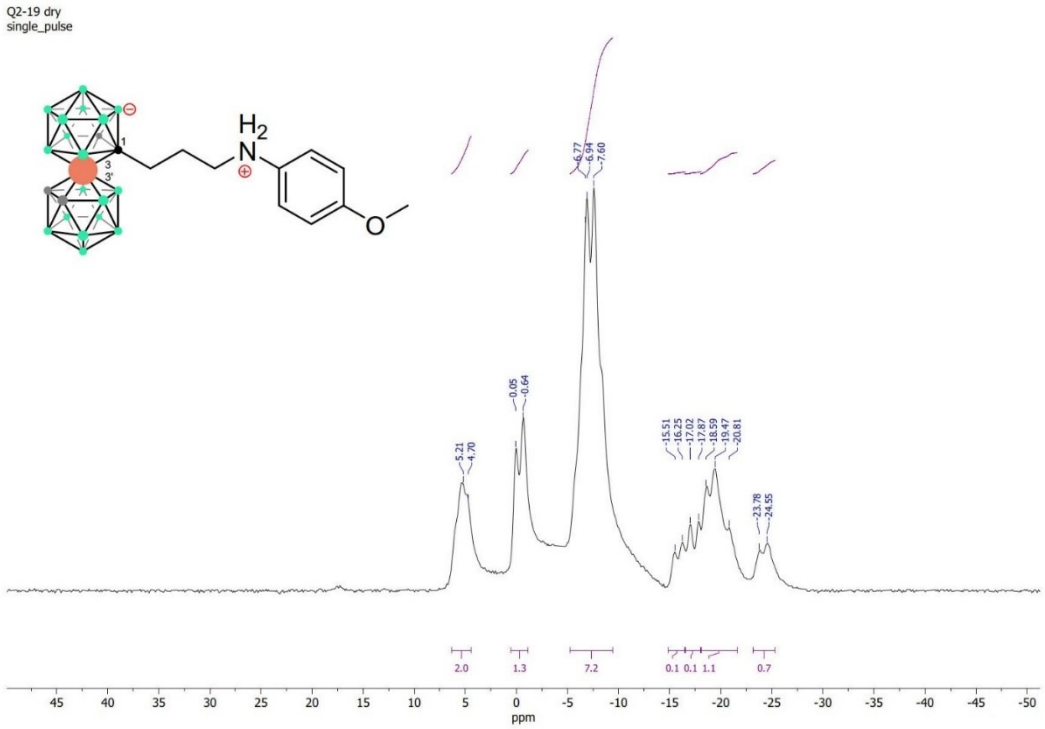

*Figure S35. ^{13}C NMR spectrum of **7**.*

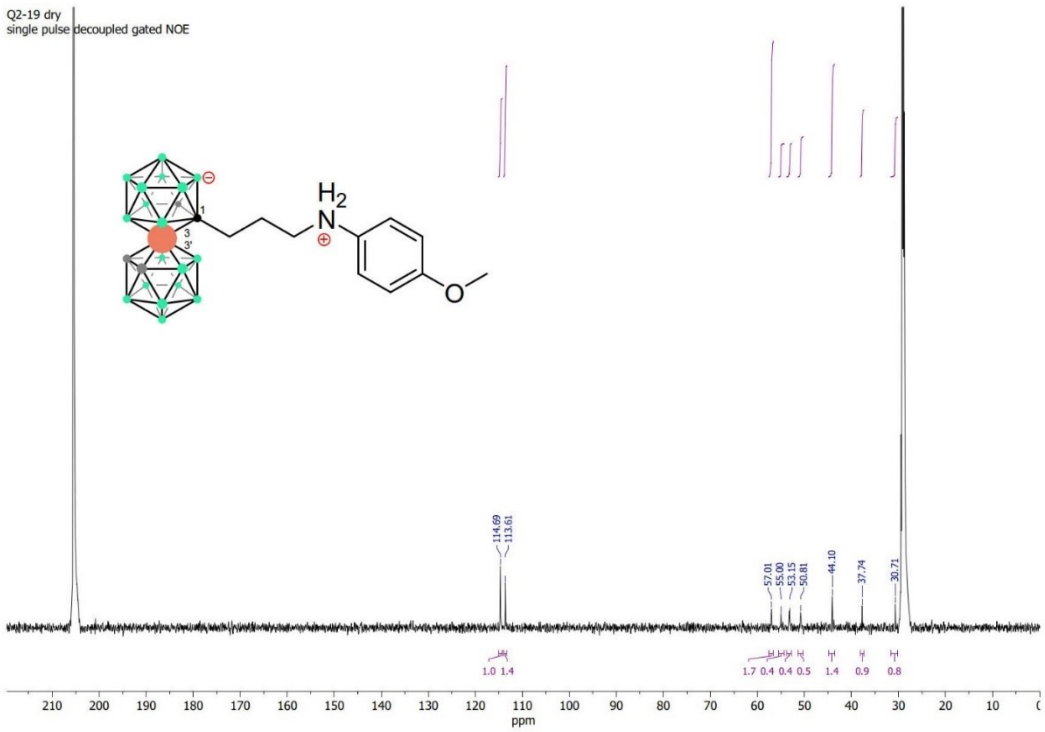

*Figure S36. ^{1}H NMR spectrum of **8**.*

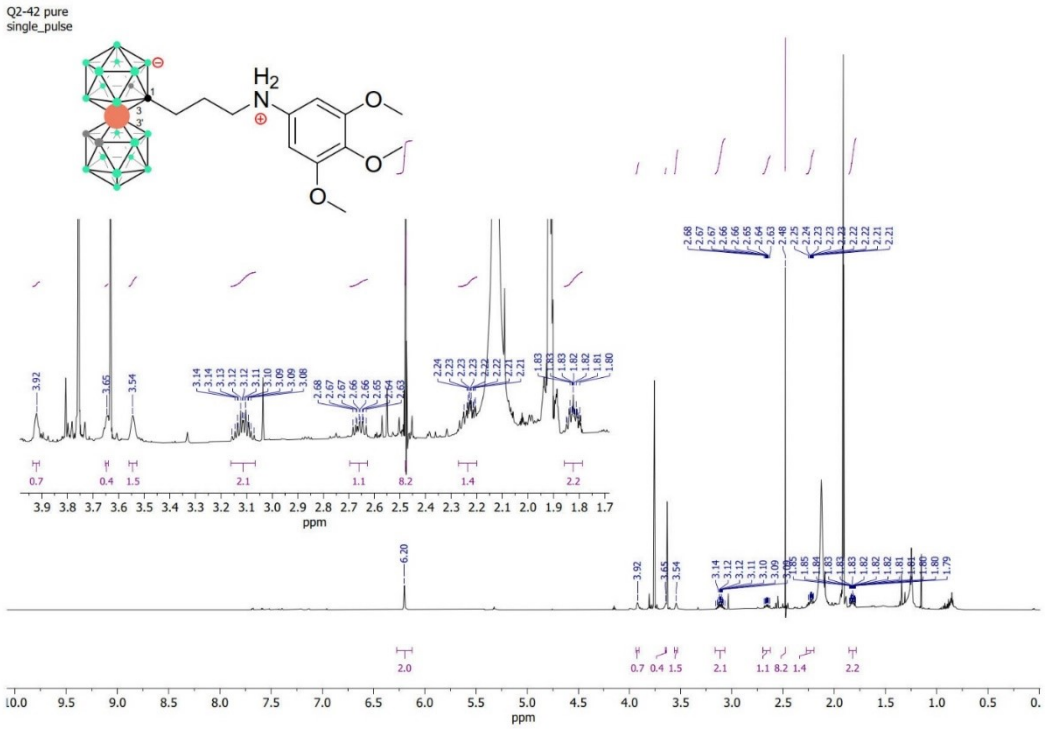

*Figure S37. $^{1}H\{^{11}B\}$ NMR spectrum of **8**.*

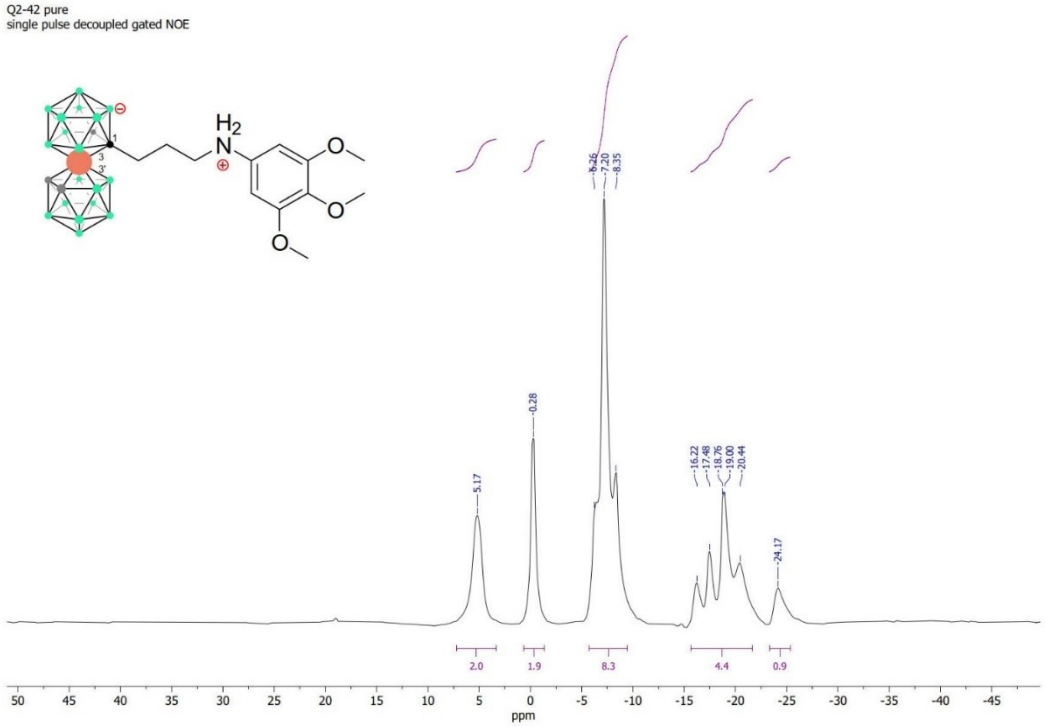

*Figure S38. ^{11}B NMR spectrum of **8**.*

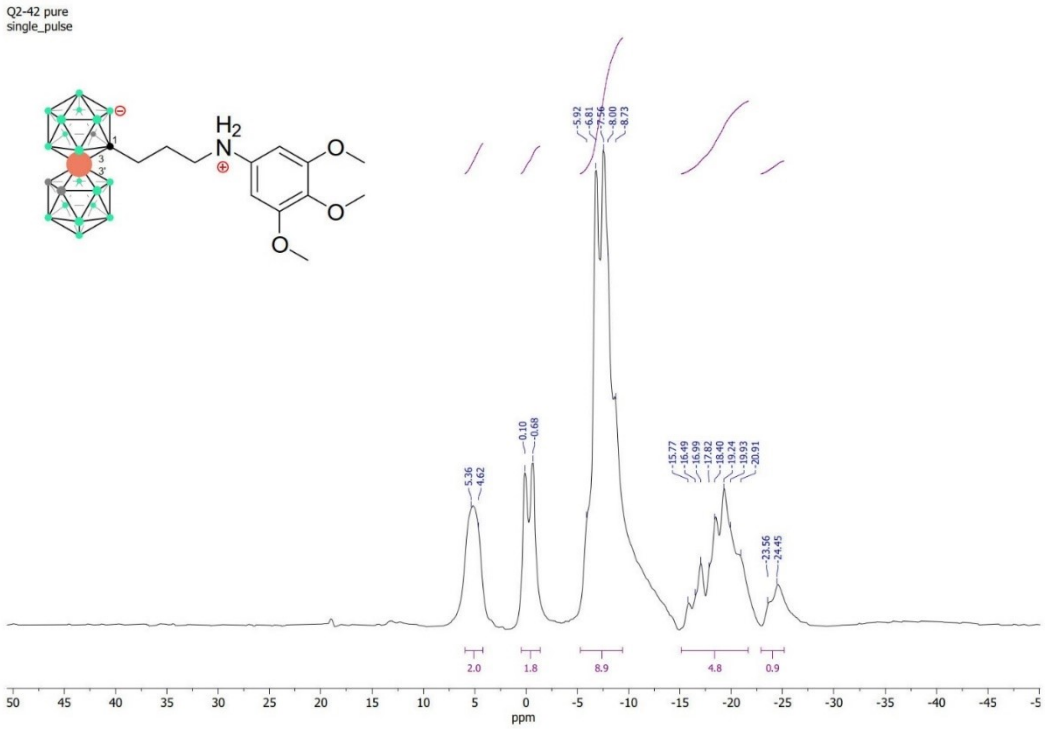

*Figure S39. ^{13}C NMR spectrum of **8**.*

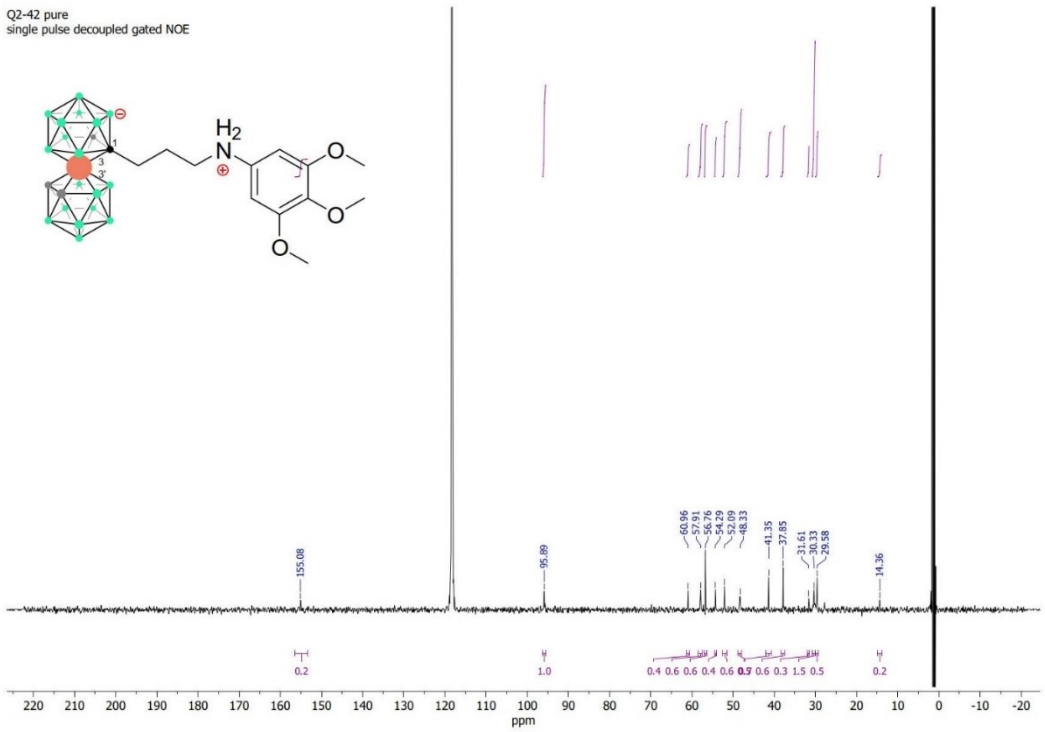

*Figure S40. ^{1}H NMR spectrum of **9**.*

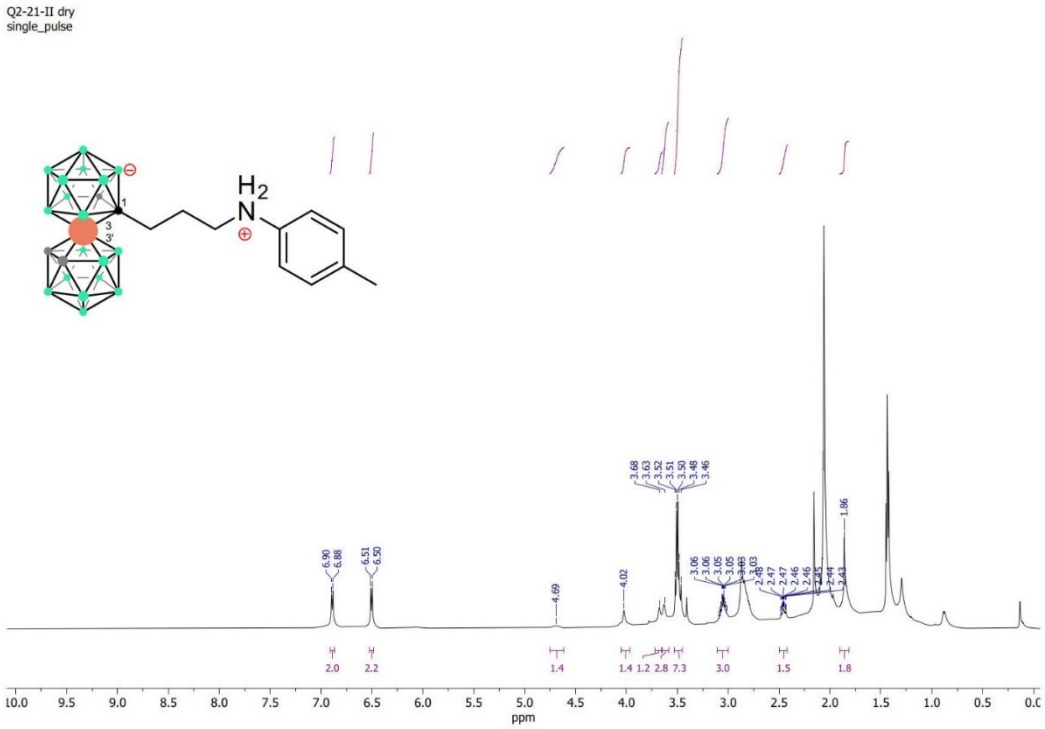

*Figure S41. $^{1}H\{^{11}B\}$ NMR spectrum of **9**.*

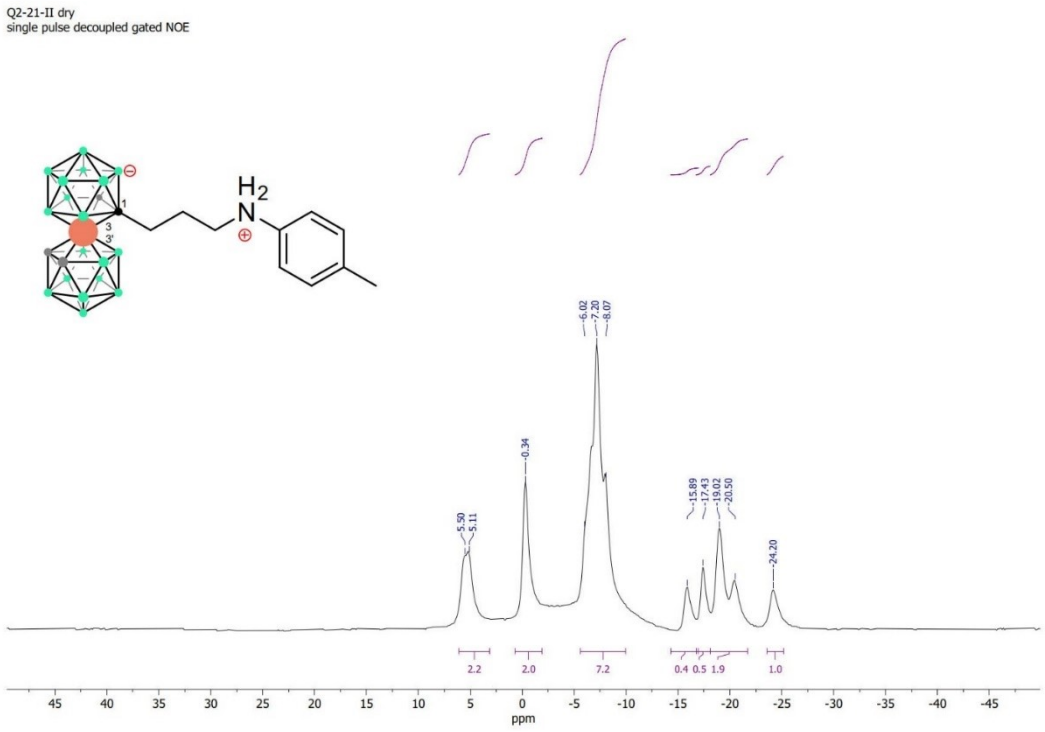

*Figure S42. ^{11}B NMR spectrum of **9**.*

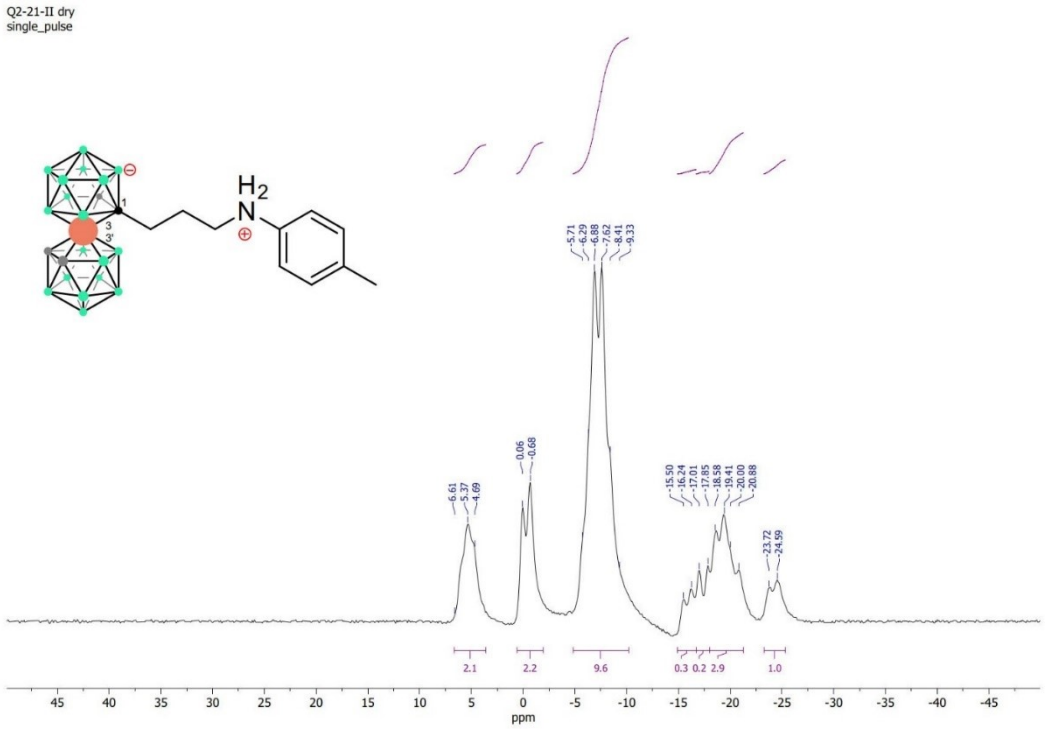

*Figure S43. ^{13}C NMR spectrum of **9**.*

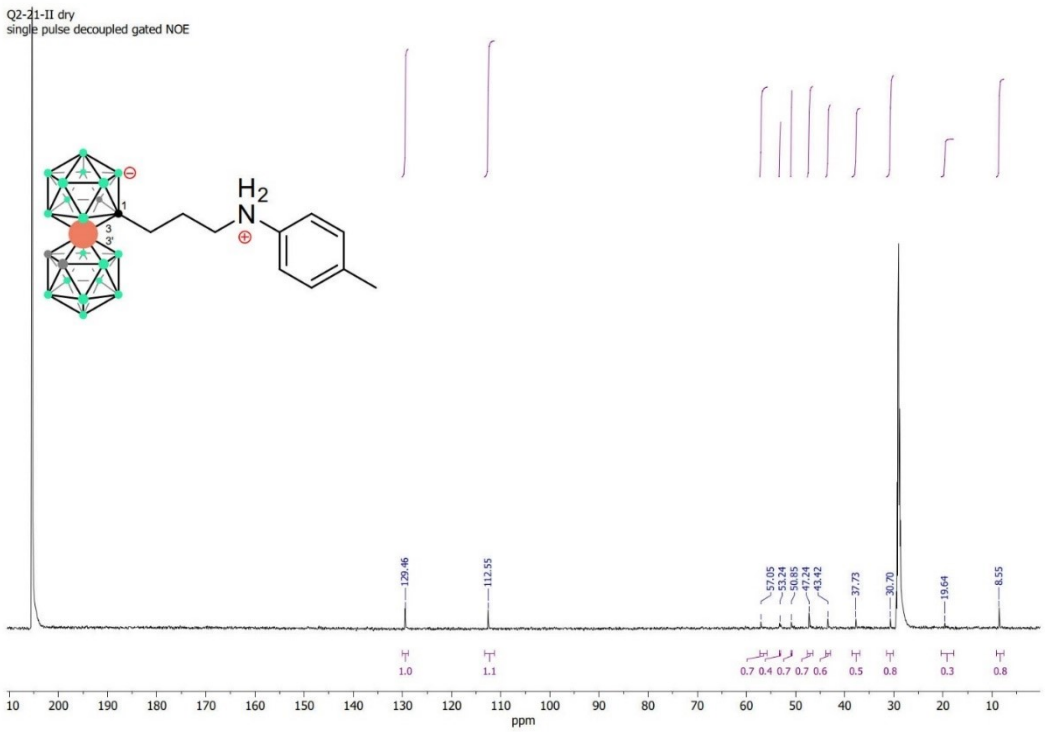

*Figure S44. ^{1}H NMR spectrum of **10**.*

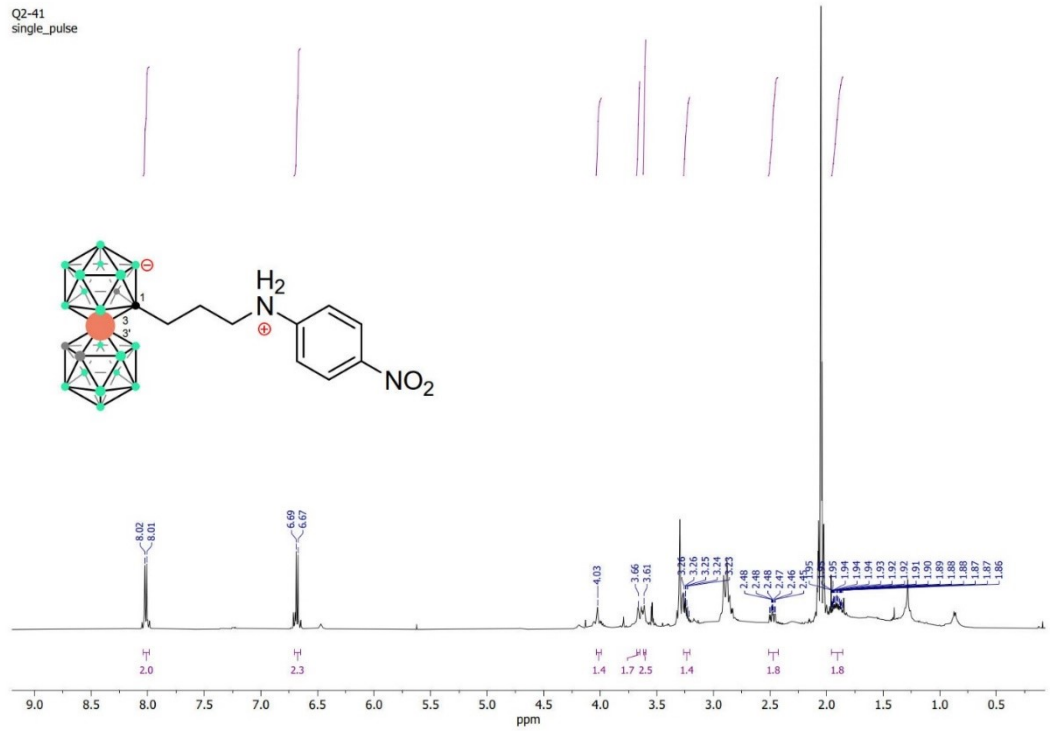

*Figure S45. $^{1}H\{^{11}B\}$ NMR spectrum of **10**.*

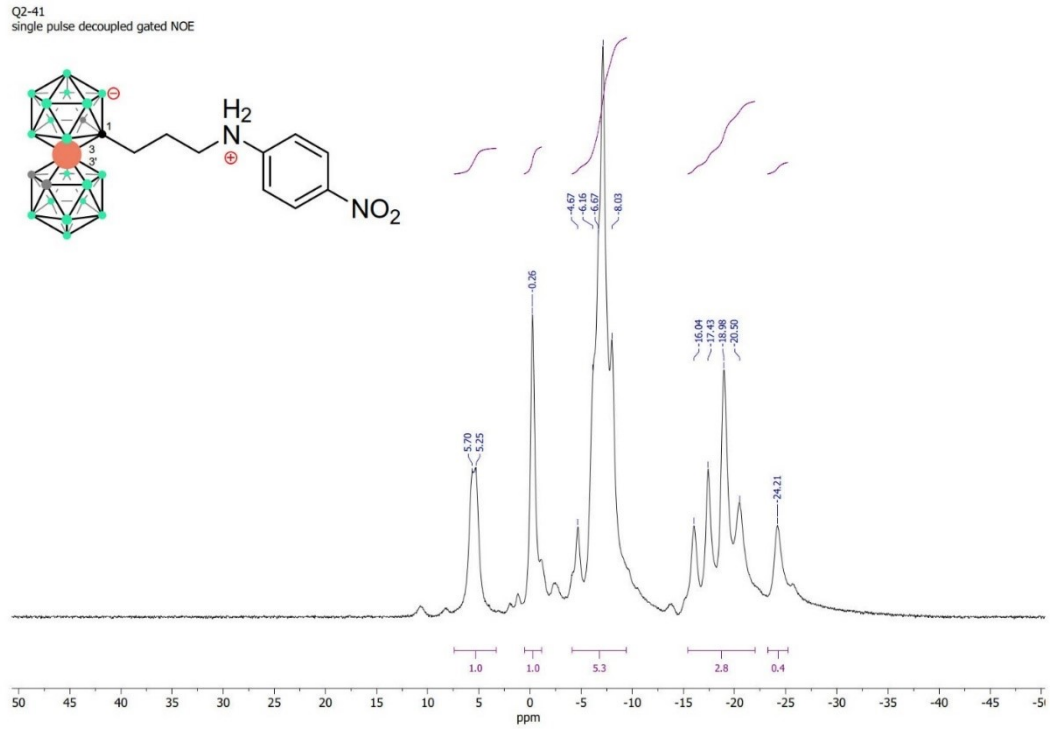

*Figure S46. ^{11}B NMR spectrum of **10**.*

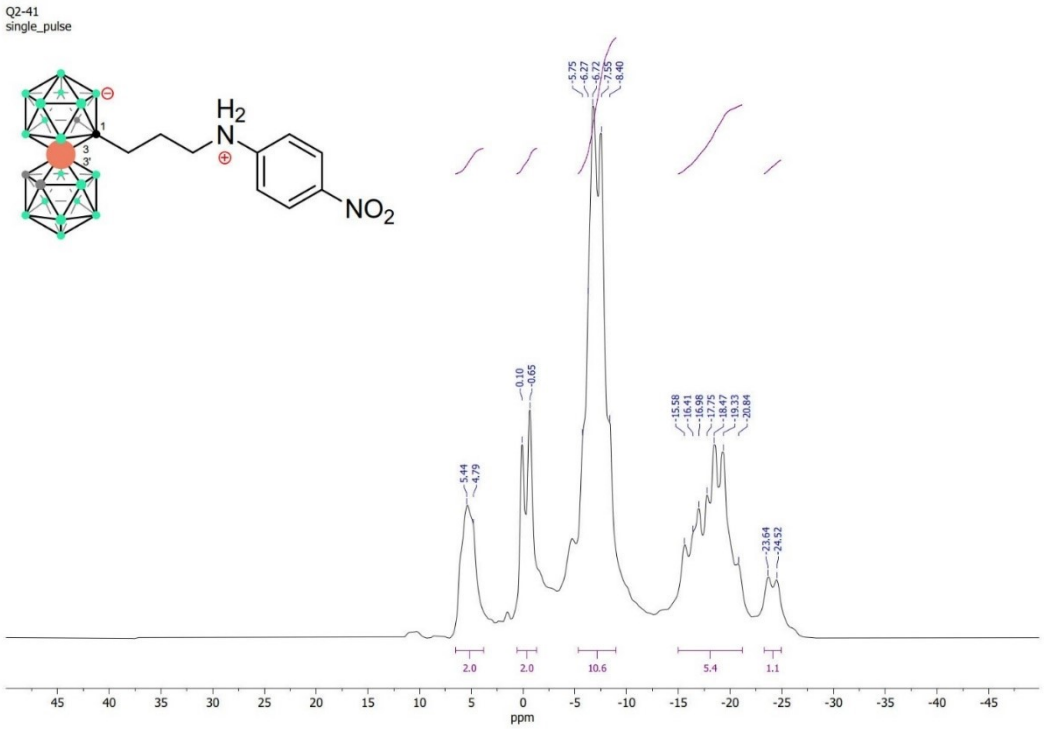

*Figure S47. ^{13}C NMR spectrum of **10**.*

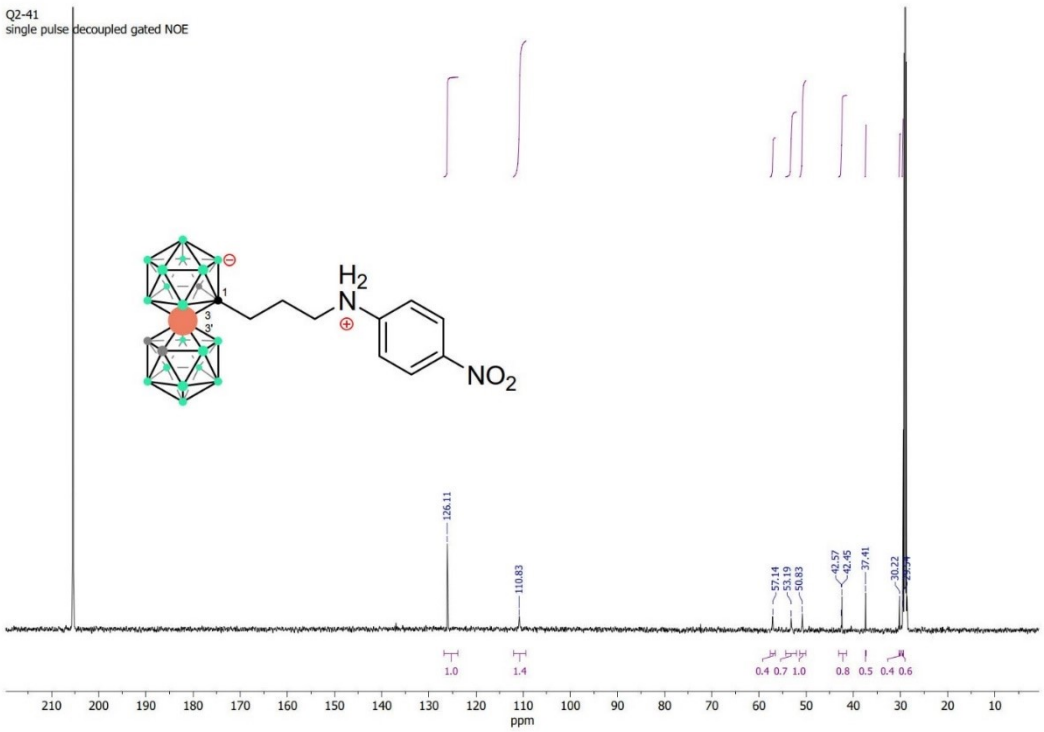

*Figure S48. ^{1}H NMR spectrum of **11**.*

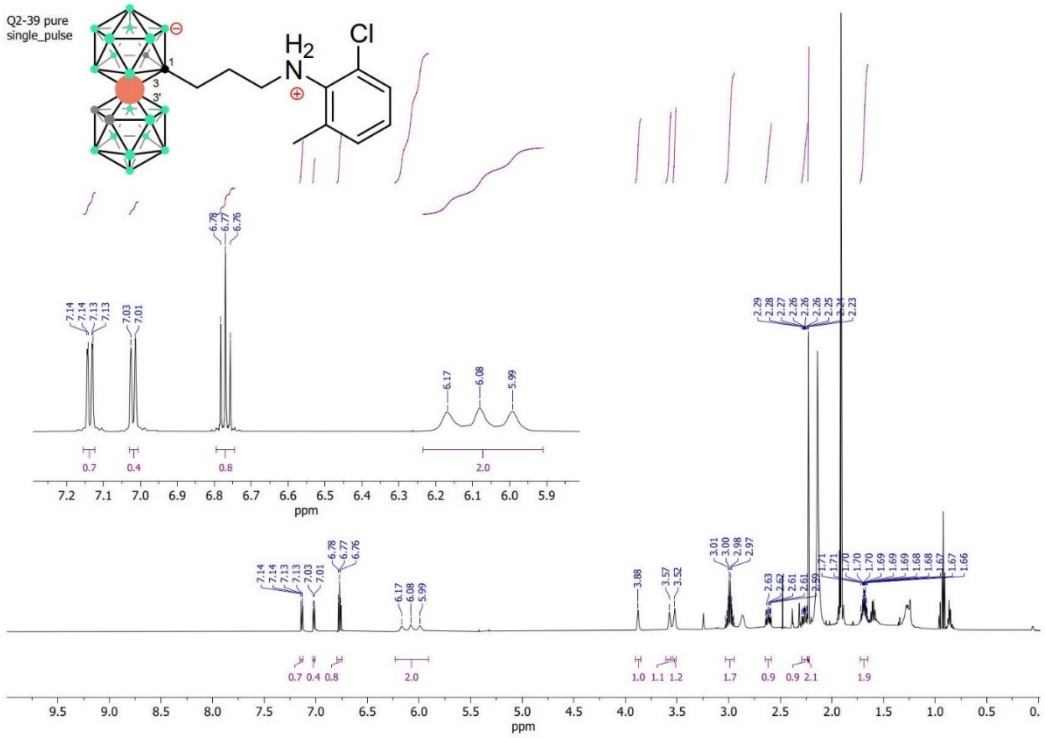

*Figure S49. $^{1}H\{^{11}B\}$ NMR spectrum of **11**.*

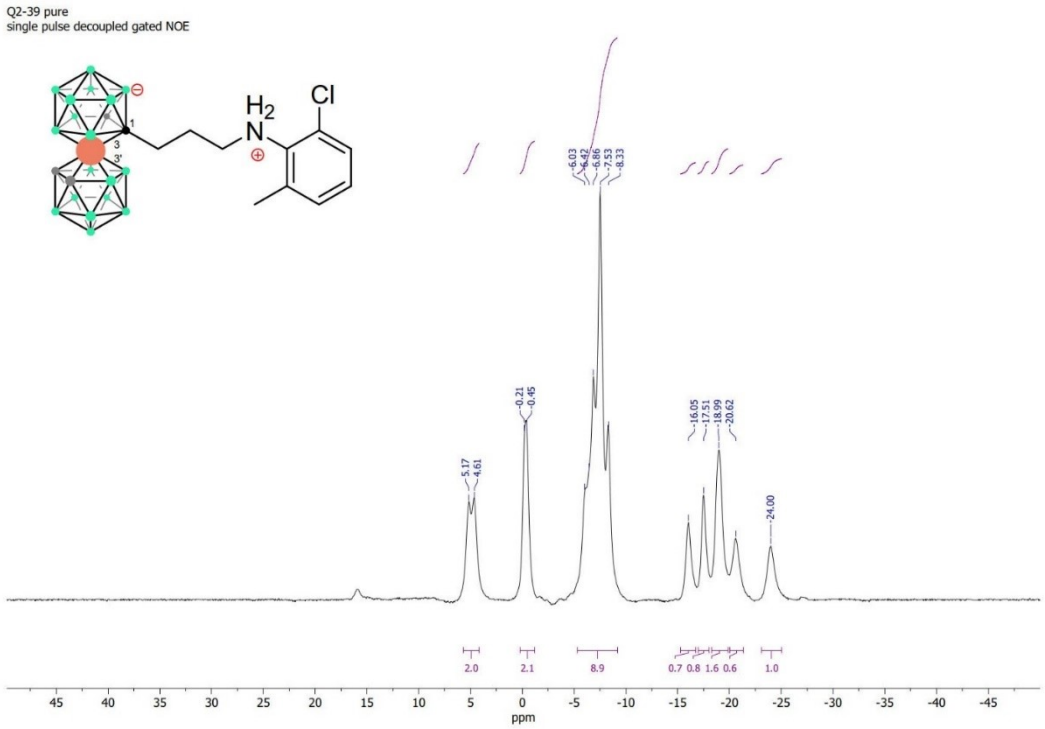

*Figure S50. [11]B NMR spectrum of **11**.*

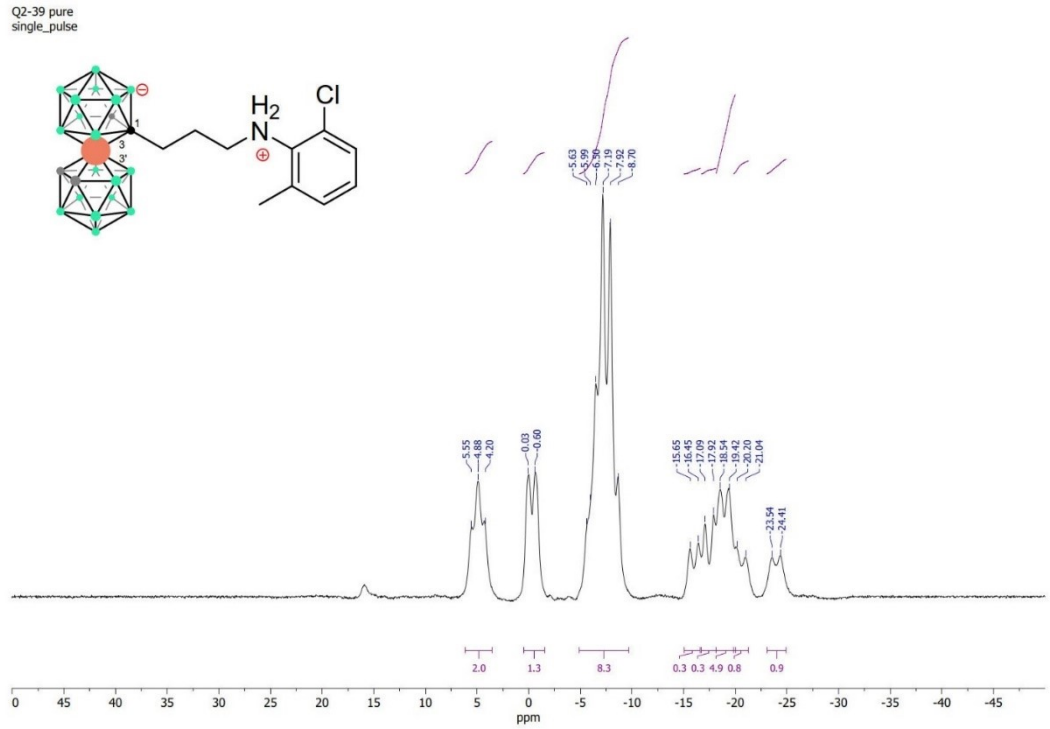

*Figure S51. [13]C NMR spectrum of **11**.*

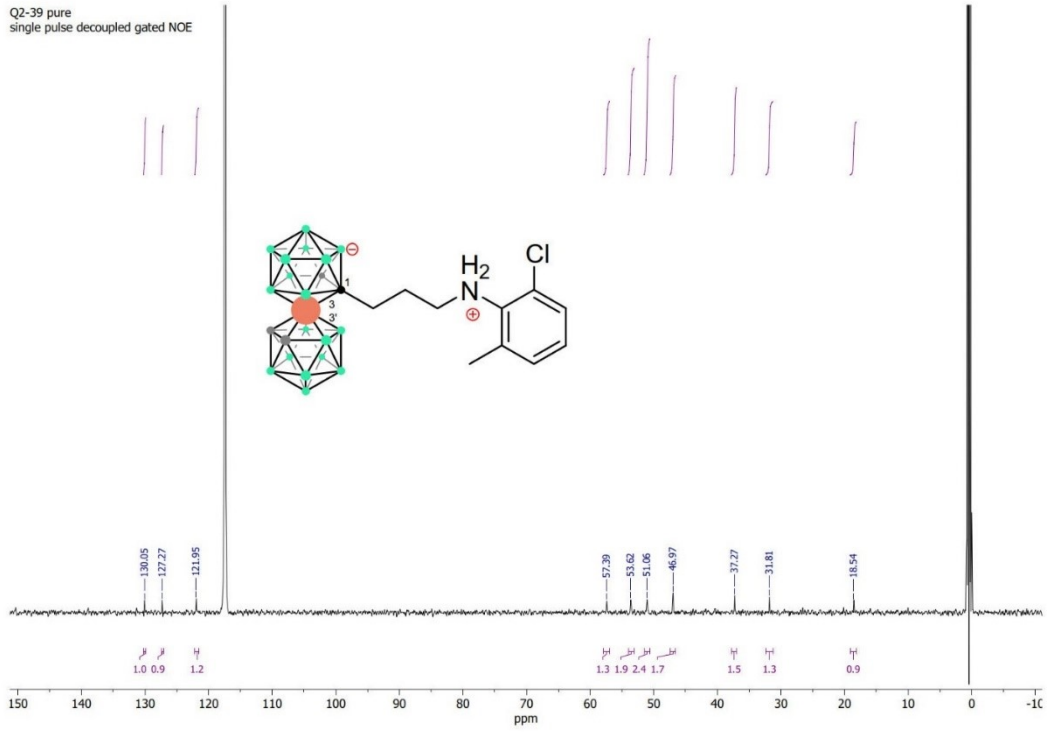

*Figure S52 ^{1}H NMR spectrum of Me_4N**15a**.*

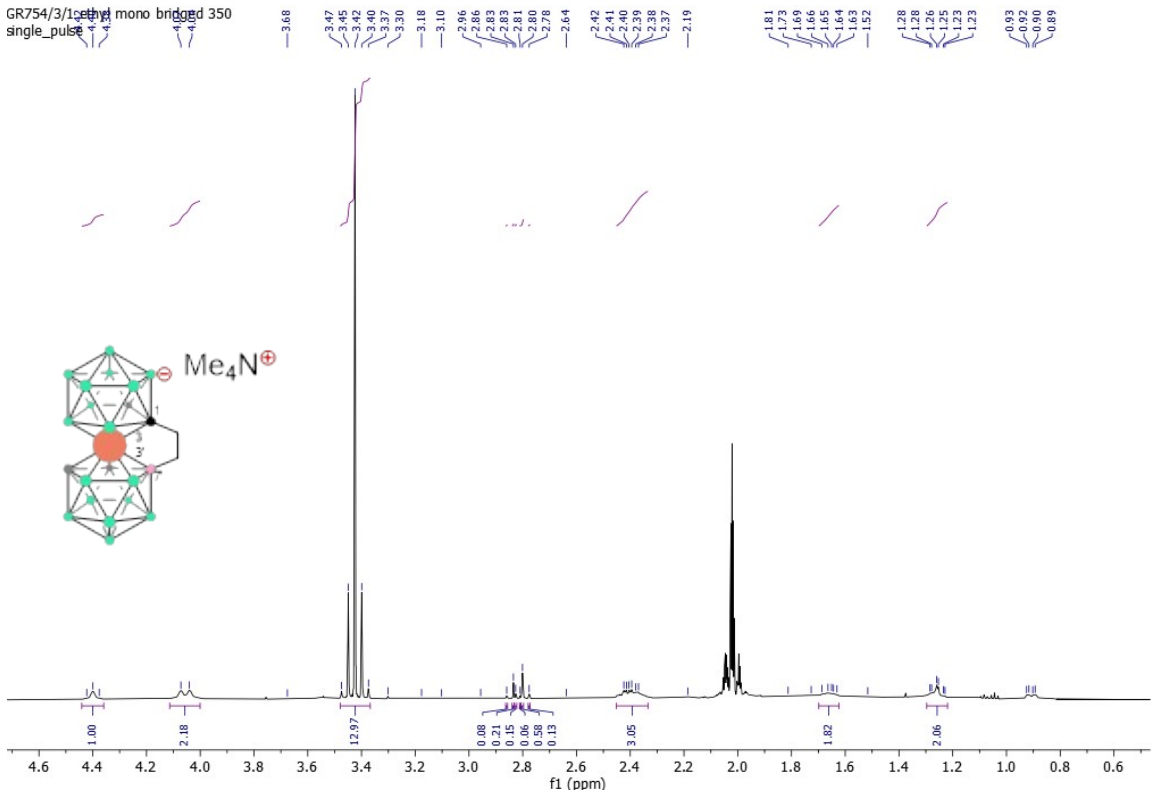

*Figure S53 $^{1}H\{^{11}B\}$ NMR spectrum of Me_4N**15a**.*

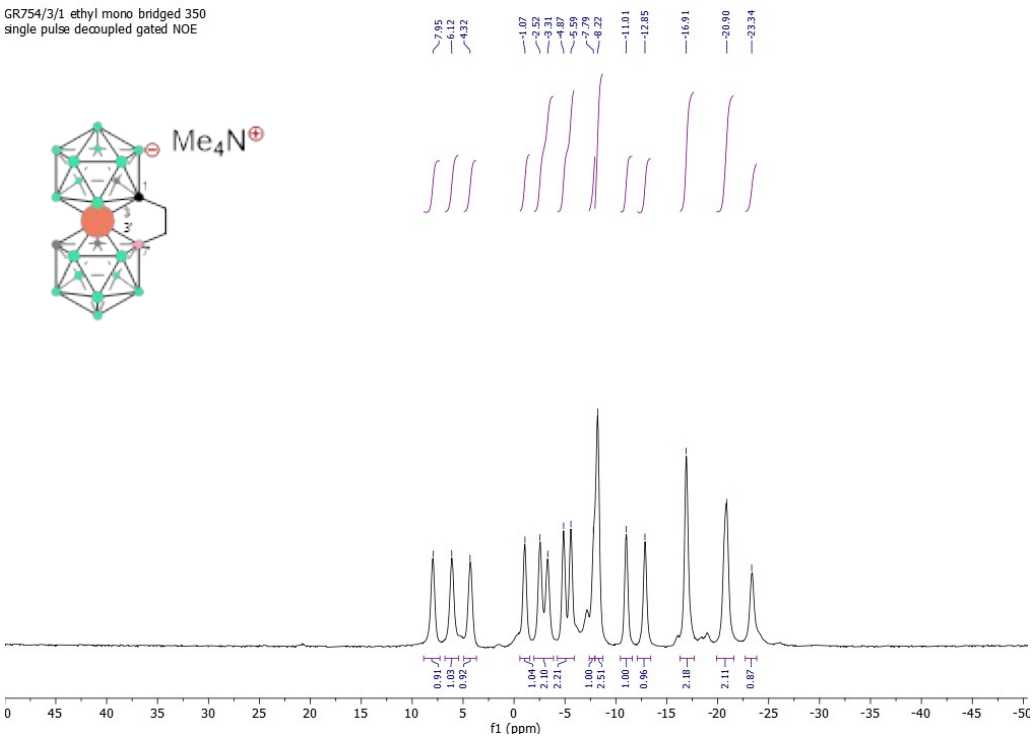

*Figure S54 ^{11}B NMR spectrum of Me_4N**15a**.*

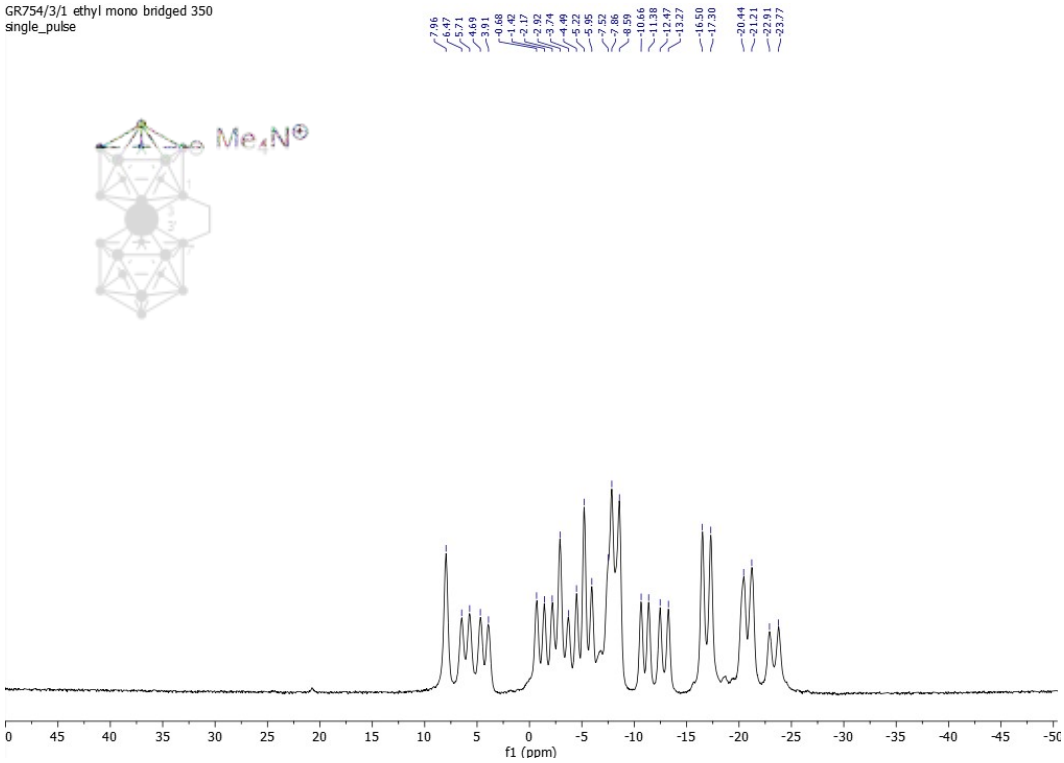

*Figure S55 ^{13}C NMR spectrum of Me_4N**15a**.*

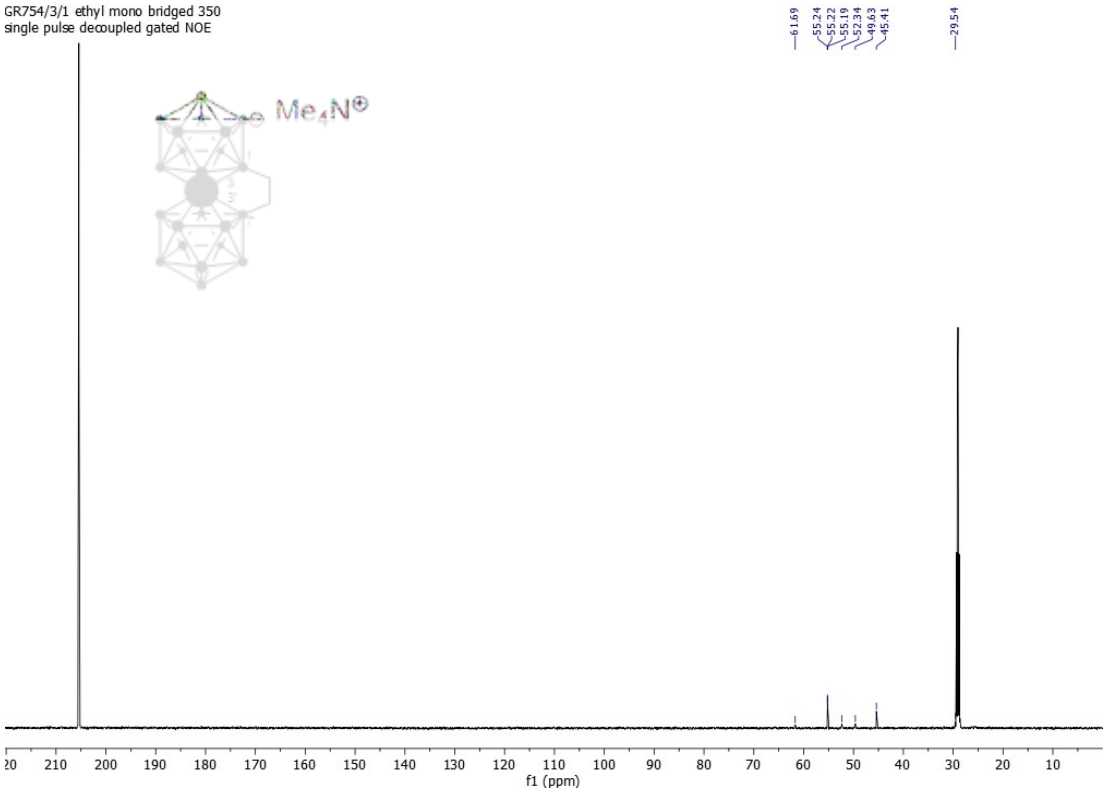

*Figure S56. ^{1}H NMR spectrum of Me_4N**15b**.*

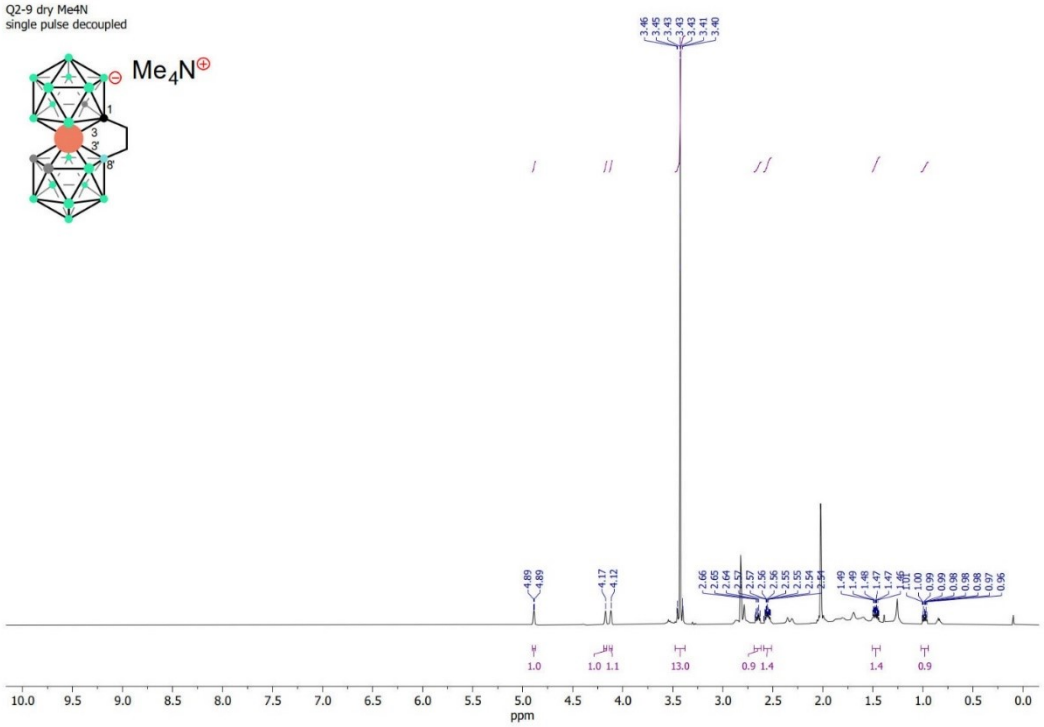

*Figure S57. $^{1}H\{^{11}B\}$ NMR spectrum of Me_4N**15b**.*

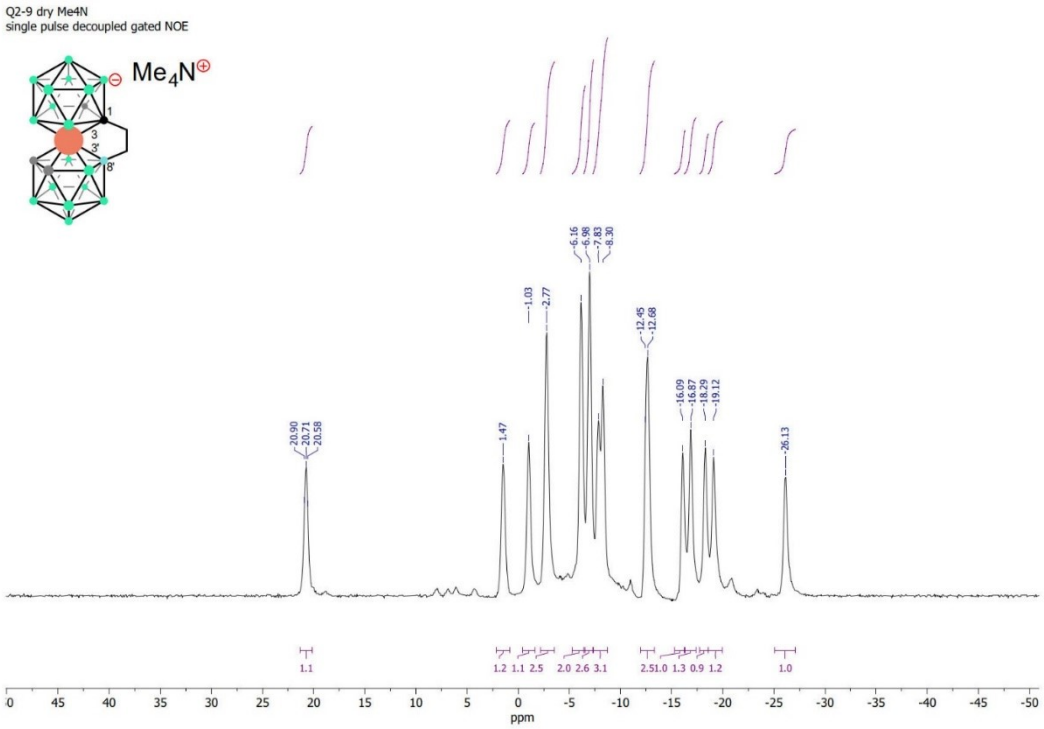

*Figure S58. ^{11}B NMR spectrum of Me_4N**15b**.*

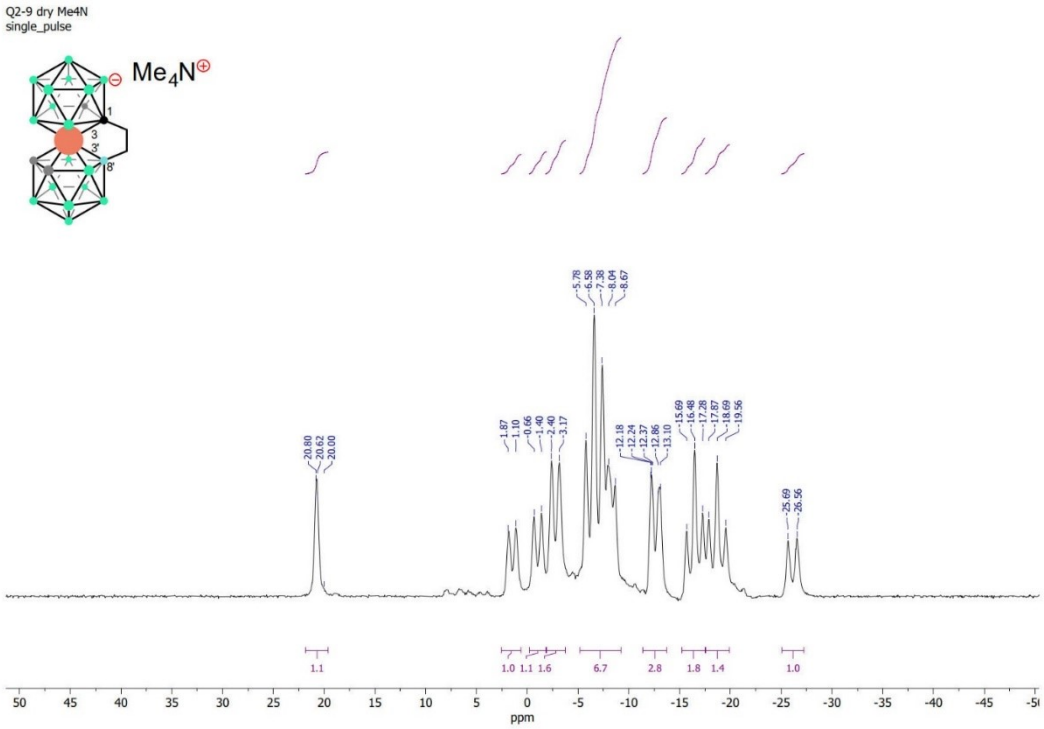

*Figure S59. ^{13}C NMR spectrum of Me_4N**15b**.*

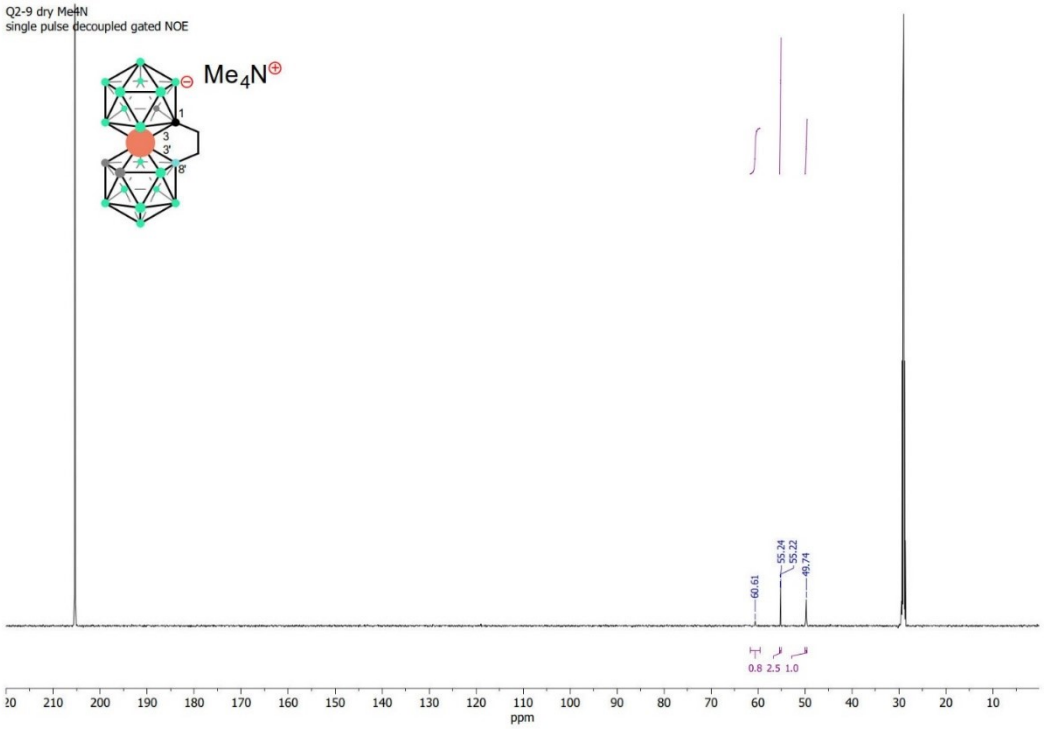

*Figure S60. ^{1}H NMR spectrum of **16**.*

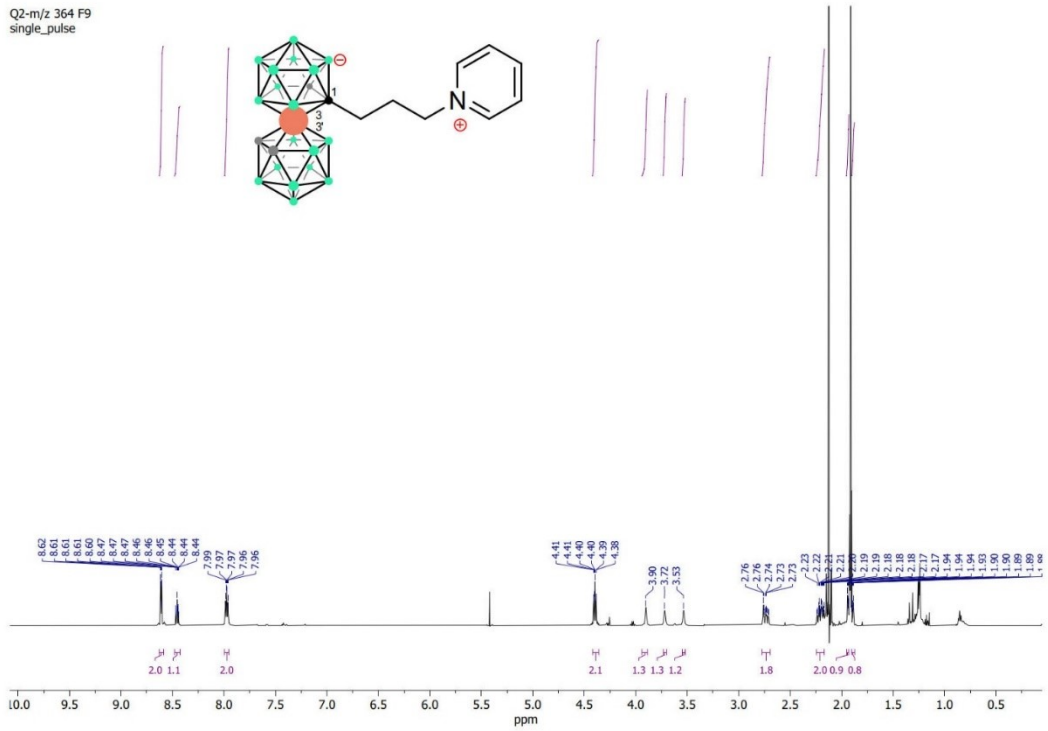

*Figure S61. $^{1}H\{^{11}B\}$ NMR spectrum of **16**.*

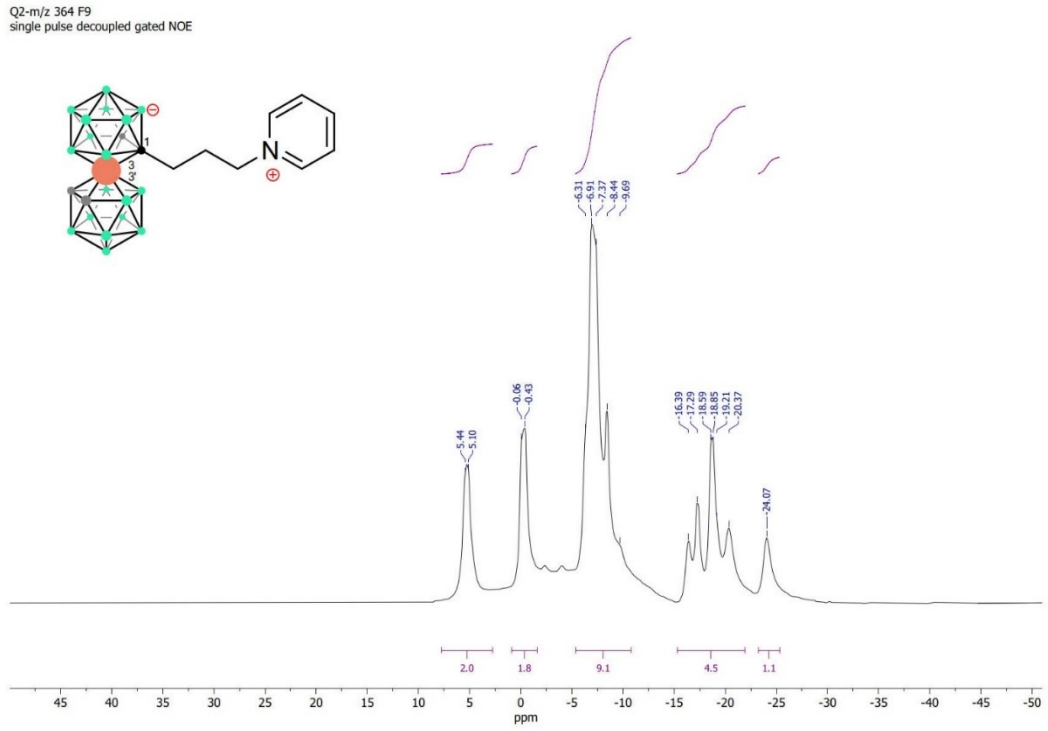

*Figure S62. ^{11}B NMR spectrum of **16**.*

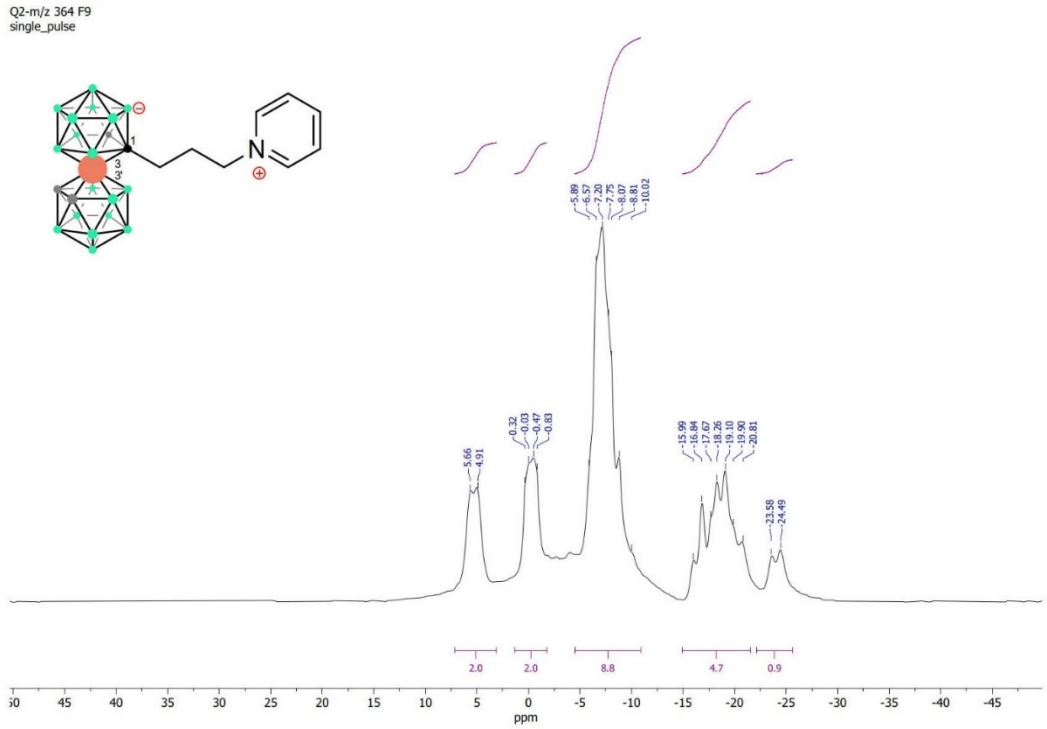

*Figure S63. ^{13}C NMR spectrum of **16**.*

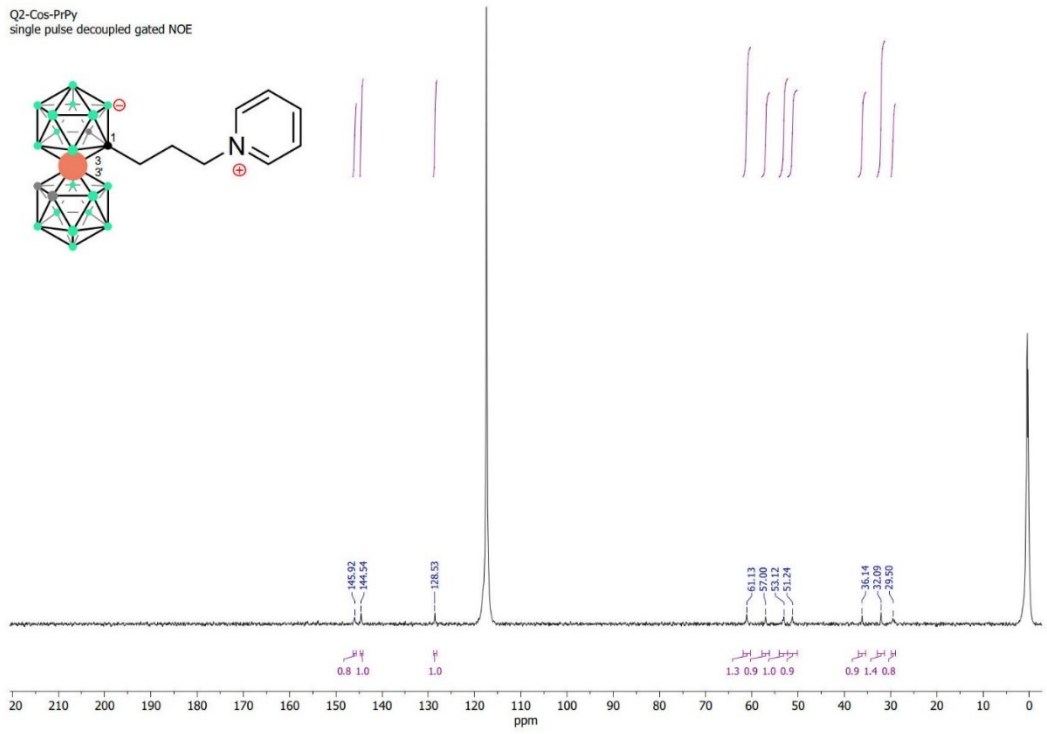

*Figure S64. ^{1}H NMR spectrum of **18**.*

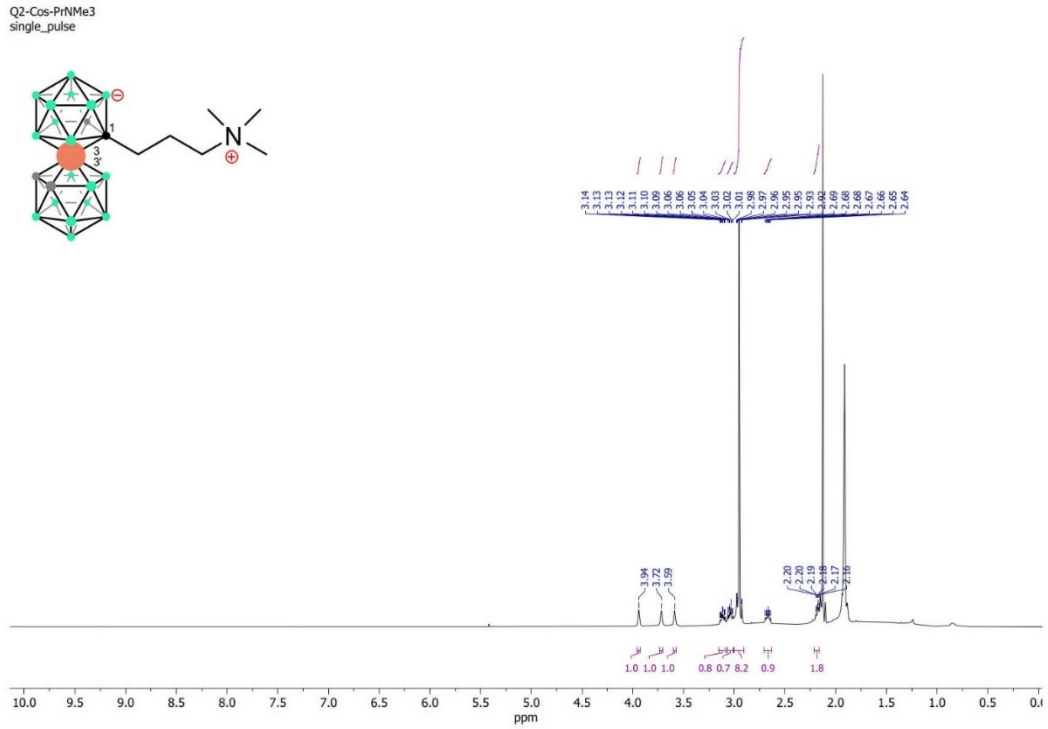

*Figure S65. $^{1}H\{^{11}B\}$ NMR spectrum of **18**.*

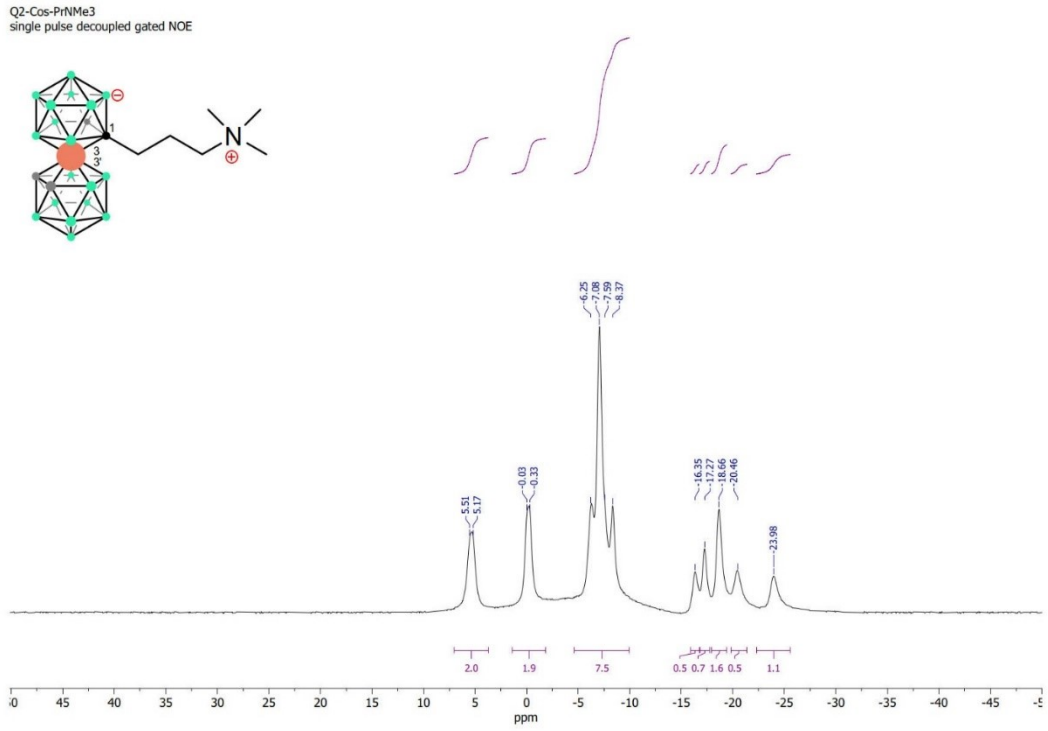

*Figure S66. ^{11}B NMR spectrum of **18**.*

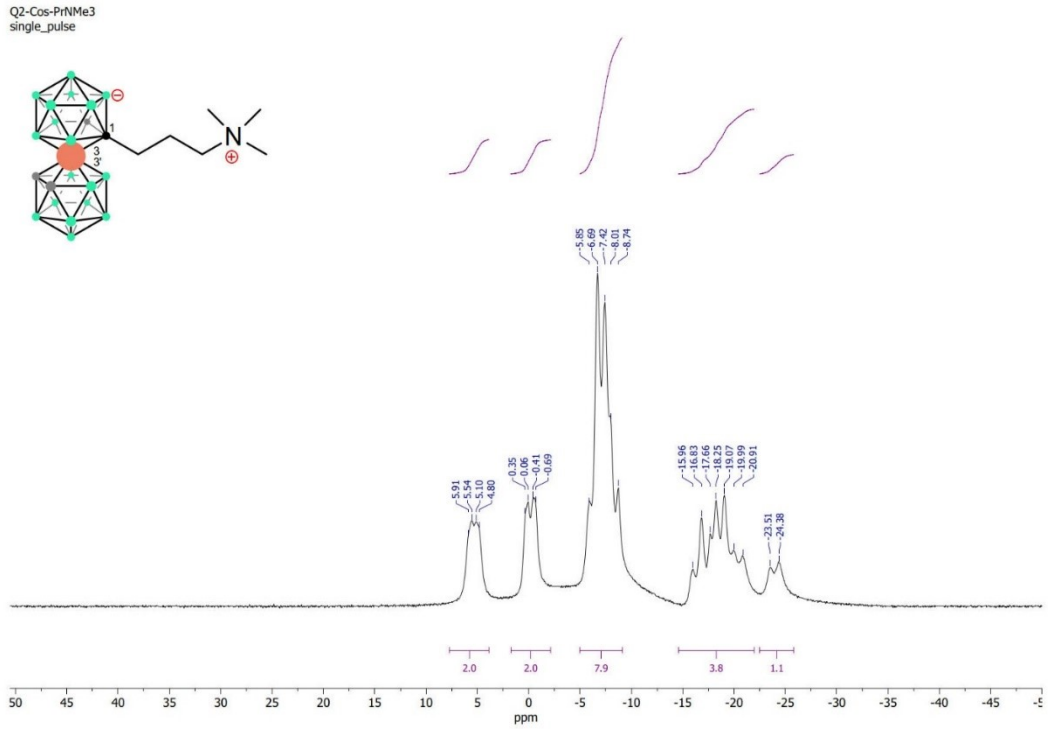

*Figure S67. ^{13}C NMR spectrum of **18**.*

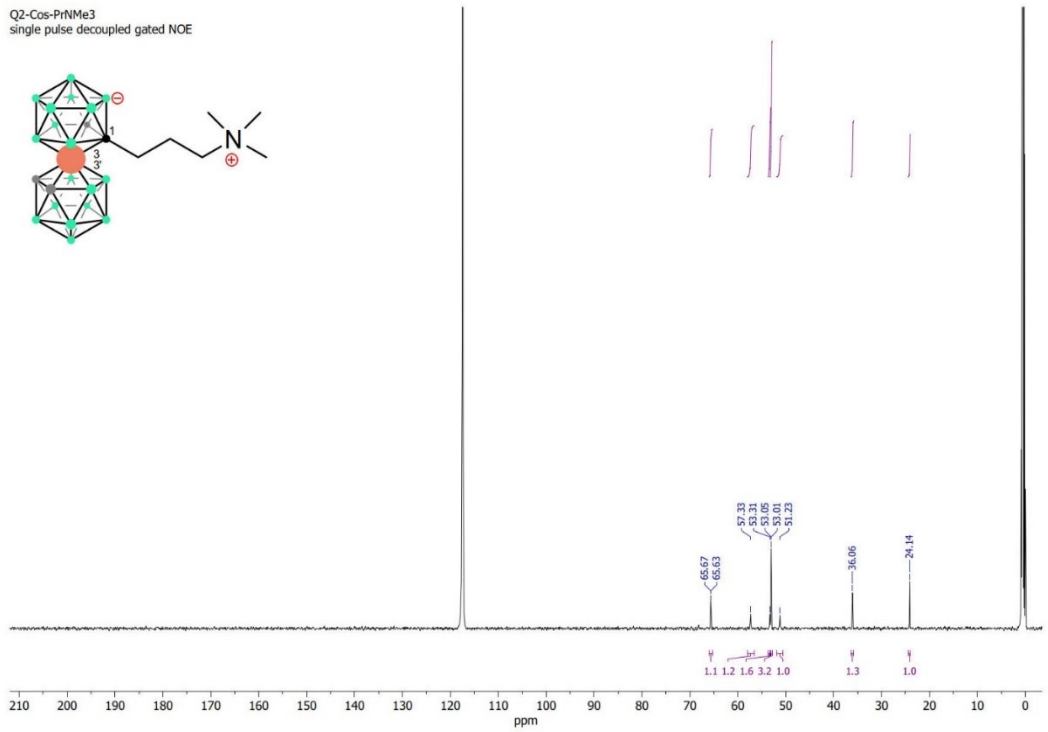

*Figure S68 ^{1}H NMR spectrum of **20a**.*

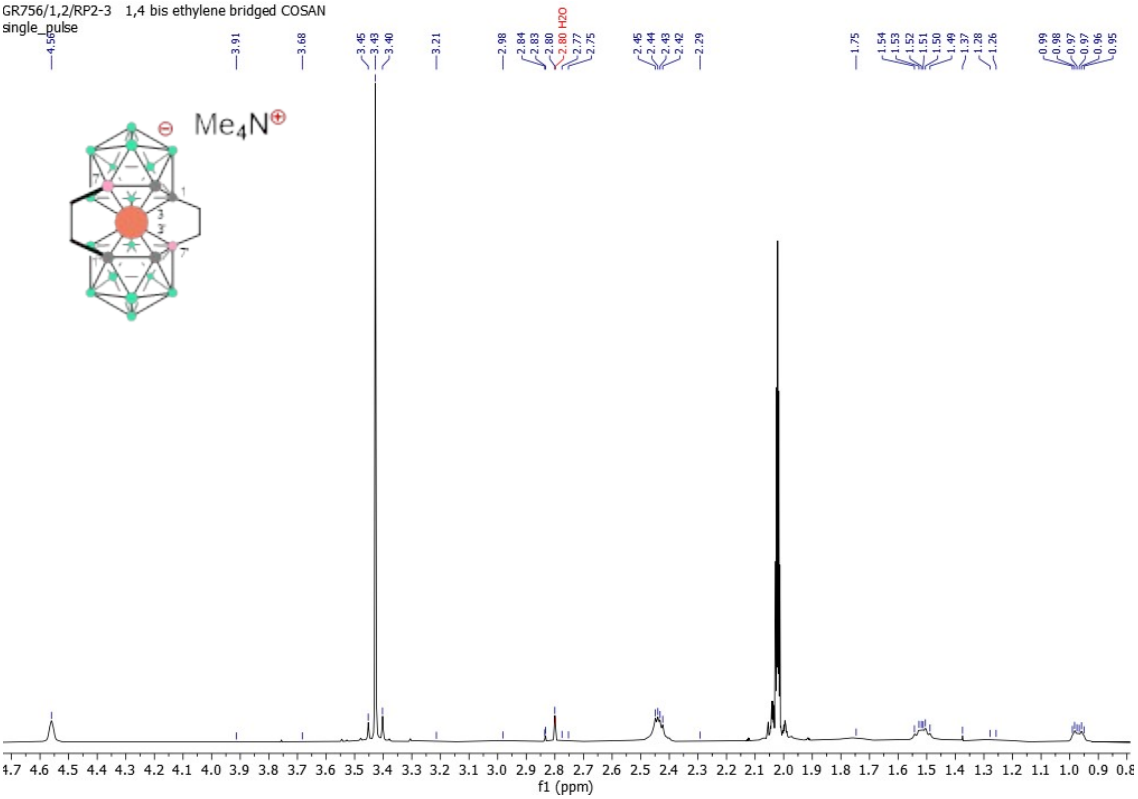

*Figure S69 $^{1}H\{^{11}B\}$ NMR spectrum of **20a**.*

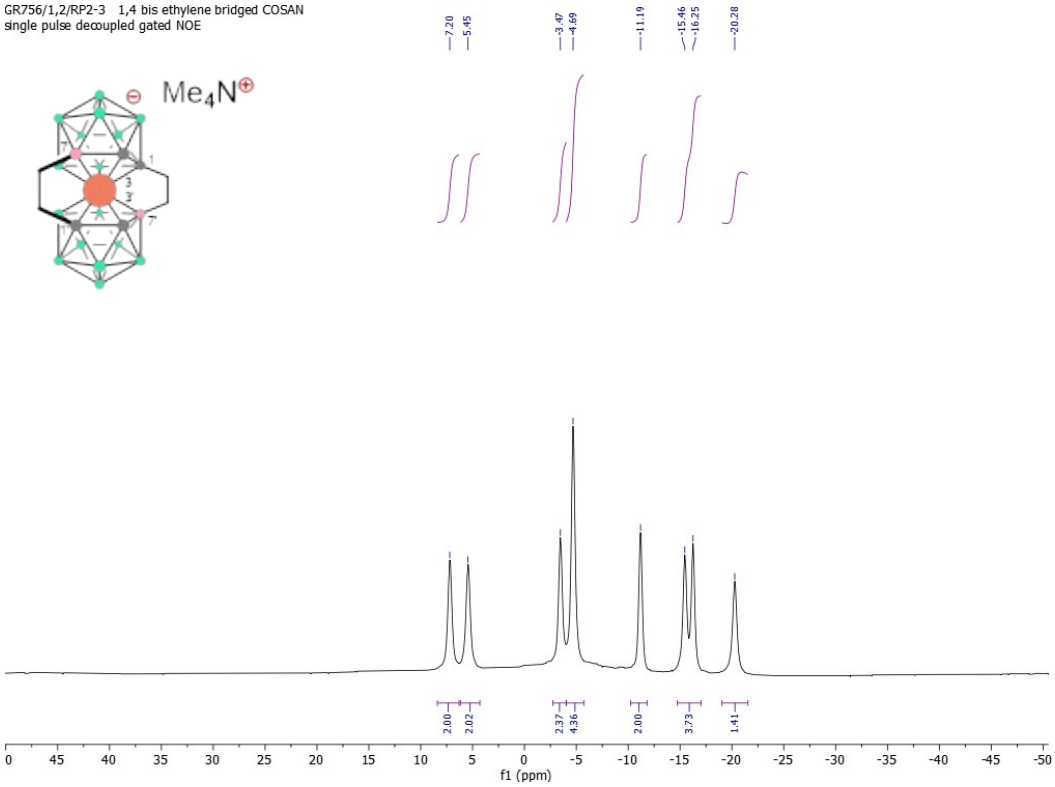

*Figure S70 [11]B NMR spectrum of **20a**.*

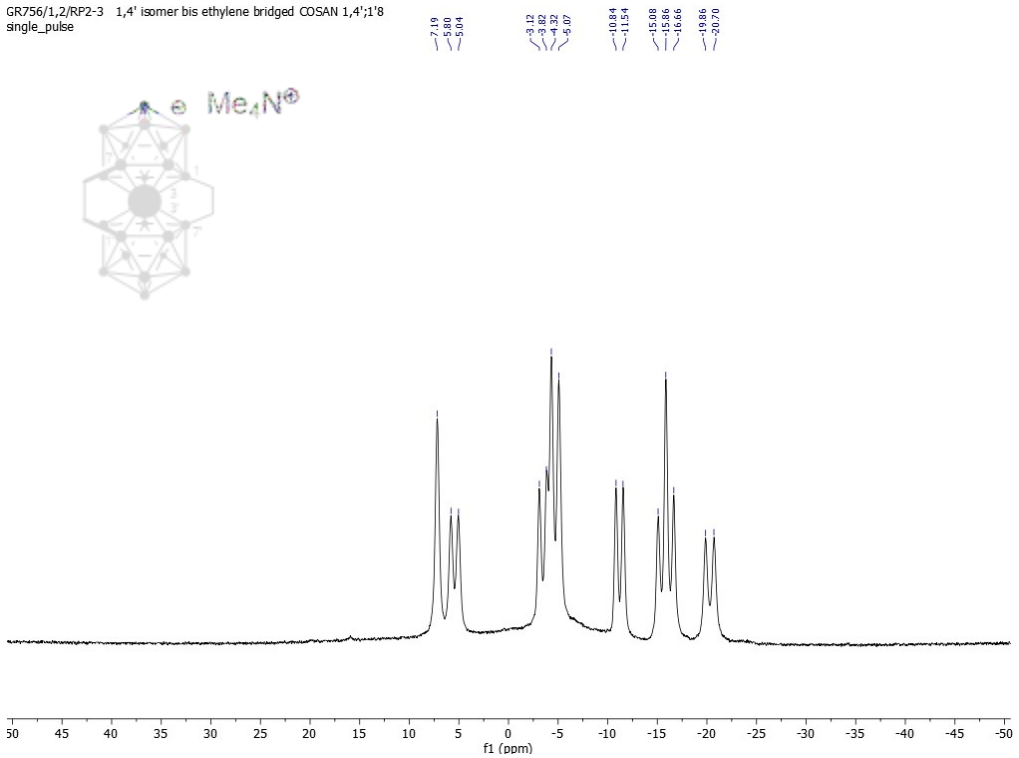

*Figure S71 [13]C NMR spectrum of **20a**.*

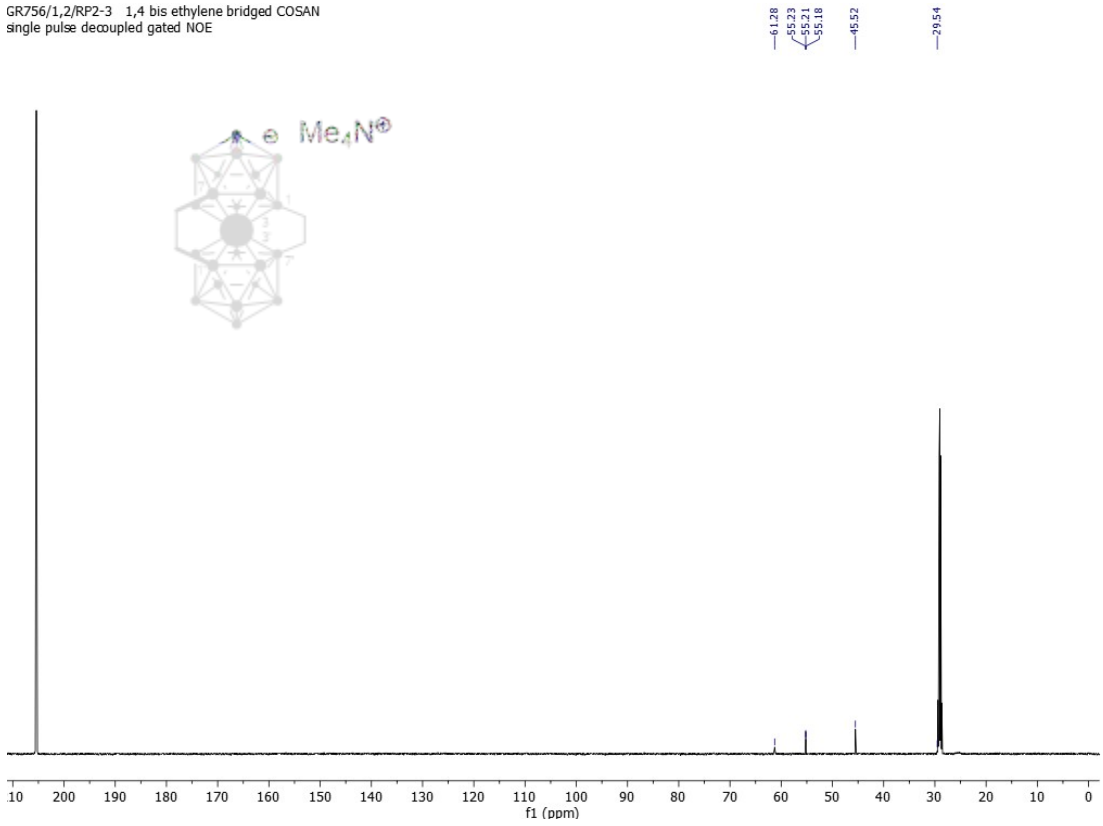

*Figure S72 ^{1}H NMR spectrum of **20b**.*

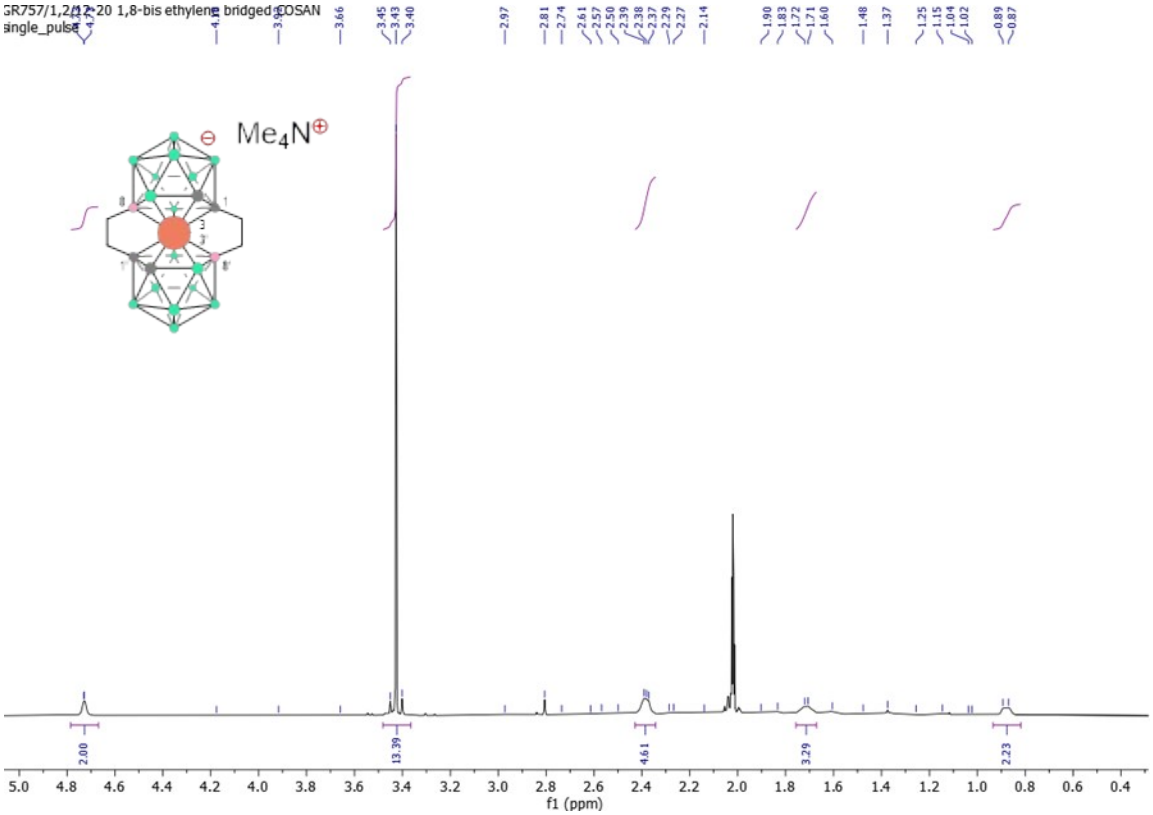

*Figure S73 $^{1}H\{^{11}B\}$ NMR spectrum of **20b**.*

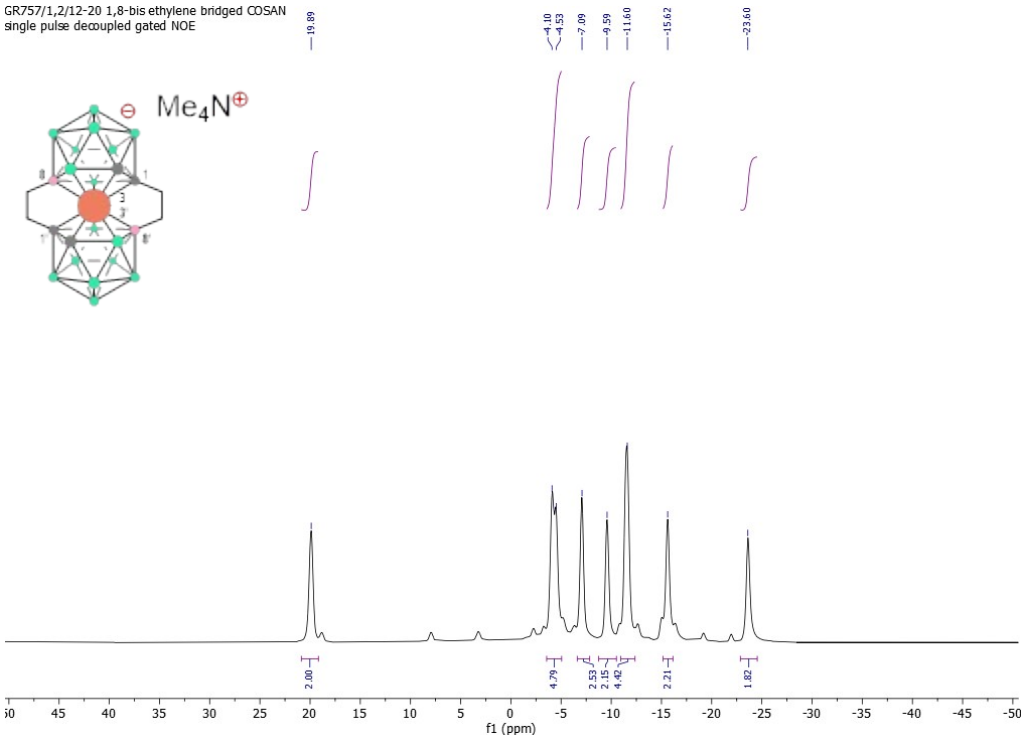

*Figure S74 ^{11}B NMR spectrum of **20b**.*

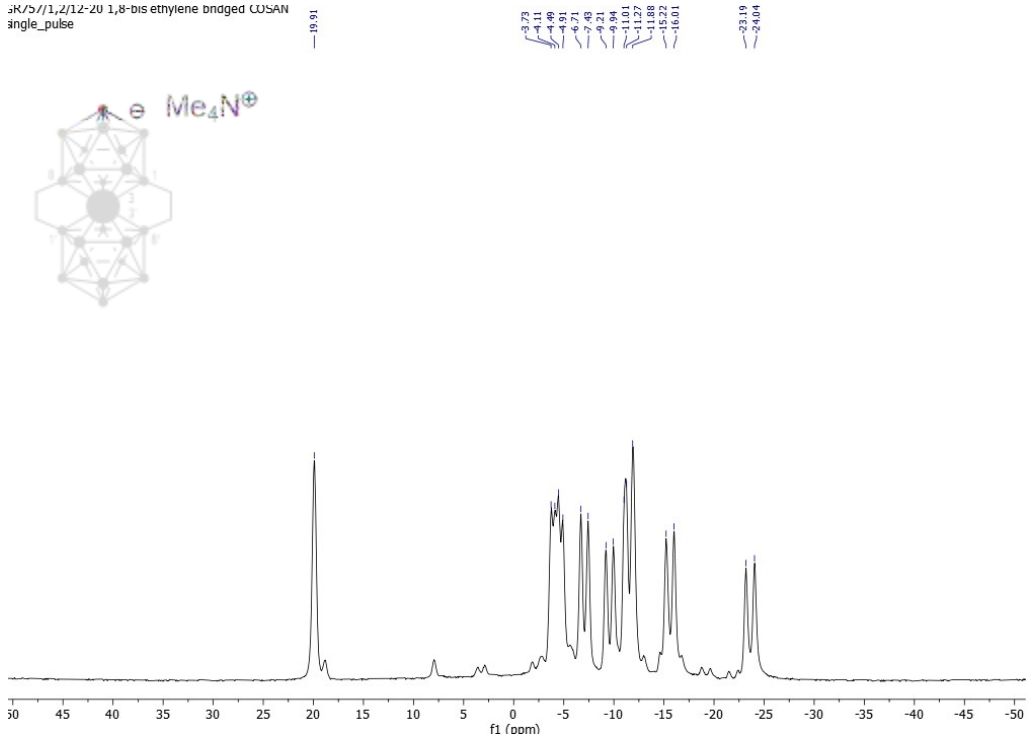

*Figure S75 ^{13}C NMR spectrum of **20b**.*

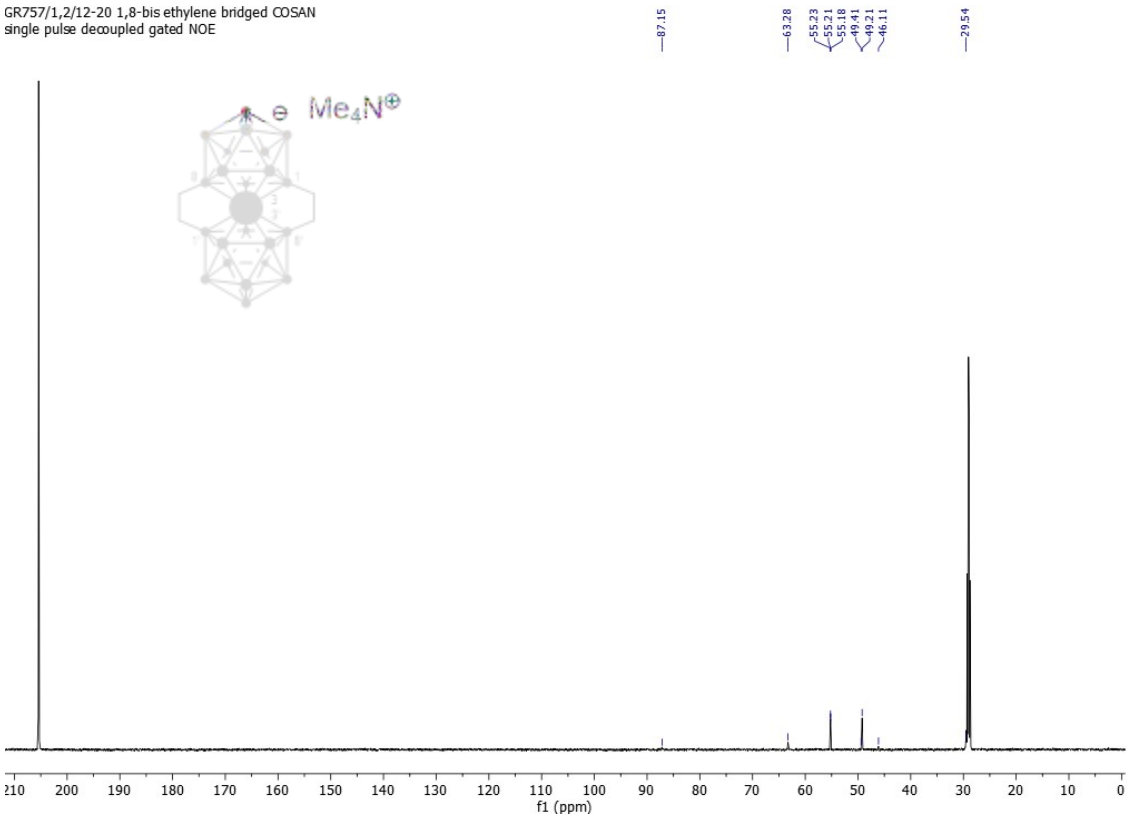

References

1. P. Řezáčová, J. Pokorná, J. Brynda, M. Kožíšek, P. Cígler, M. Lepšík, J. Fanfrlík, J. Řezáč, K. Grantz Šašková, I. Sieglová, J. Plešek, V. Šícha, B. Grüner, H. Oberwinkler, J. Sedláček, H.-G. Kräusslich, P. Hobza, V. Král and J. Konvalinka, *J. Med. Chem.*, 2009, **52**, 7132-7141.
2. J. Nekvinda, J. Švehla, I. Císařová and B. Grüner, *J. Organomet. Ch.*, 2015, **798**, 112-120.
3. Rigaku, *Journal*, 2022.
4. R. C. Clark and J. S. Reid, *Acta Crystallogr. A*, 1995, **51**, 887-897.
5. O. V. Dolomanov, L. J. Bourhis, R. J. Gildea, J. A. K. Howard and H. Puschmann, *J. Appl. Crystallogr.*, 2009, **42**, 339-341.
6. G. M. Sheldrick, *Acta Cryst. Sect. A*, 2015, **71**, 3-8.
7. G. M. Sheldrick, *Acta Crystallogr., Sect. C: Cryst. Struct. Commun.*, 2015, **71**, 3-8.
8. P. K. B. GbR, *Journal*, 2020.
9. L. Palatinus and G. Chapuis, *J. Appl. Crystallogr.*, 2007, **40**, 786-790.
10. V. Petříček, L. Palatinus, J. Plášil and M. Dušek, *Z. Kristallogr.*, 2023, DOI: doi:10.1515/zkri-2023-0005.
11. V. Petříček, P. Coppens and P. Becker, *Acta Crystallogr. A*, 1985, **41**, 478-483.
12. V. Schomaker and K. Trueblood, *Acta Crystallogr. B*, 1968, **24**, 63-76.
13. V. Petříček, V. Eigner, M. Dušek and A. Čejchan, *Z. Kristallogr.*, 2016, **231**, 301-312.
14. W. R. Busing and H. A. Levy, *Acta Crystallogr.*, 1957, **10**, 180-182.
15. V. N. Kalinin, E. G. Rys, A. A. Tyutyunov, A. Z. Starikova, A. A. Korlyukov, V. A. Ol'shevskaya, D. D. Sung, A. B. Ponomaryov, P. V. Petrovskii and E. Hey-Hawkins, *Dalton Trans.*, 2005, **5**, 903-908.